# Role of the Aryl Hydrocarbon Receptor in Disease Tolerance to *Staphylococcus aureus*

Andreea Damian

Department of Microbiology and Immunology

McGill University, Montreal

Submitted June 2017

A thesis submitted to McGill University in partial fulfillment of the requirements of the degree of Masters of Science

## Table of Contents

## Acknowledgments

I would like to thank Dr. Joaquin Madrenas for the opportunity to do research in his lab, and for all his support, mentorship, and guidance. I also thank my co-supervisor, Dr. Sylvie Fournier, for her feedback, encouragement, and support. I am grateful to my committee members Dr. Irah King and Dr. Samantha Gruenheid who provided me with useful advice, feedback, and experimental suggestions. I would also like to thank all the members of the Madrenas laboratory for their help and support, especially Dr. Benoit Levast for all the help in designing the infection model and troubleshooting the potential infection models. I would like to thank Ms. Camille Stegen for all the help with the cell sorting and flow cytometry data. I am thankful for Dr. Vladimir Andrey Gimenez Rivera and Mr. Adam Peres for lending a helping hand, and their useful discussions and experimental suggestions. Lastly, I would like to thank Dr. Frank Gonzalez for providing us with the AHR-deficient mice.

## List of abbreviations

| | |
|---|---|
| AD | Atopic dermatitis |
| AHR | Aryl Hydrocarbon Receptor |
| AHRR | AHR repressor |
| AMP | Antimicrobial peptide |
| APC | Antigen-presenting cells |
| ARNT | AHR nuclear translocator |
| bp | Base pairs |
| B2m | Beta-2 microglobulin |
| CA | Community acquired |
| CCL | C-C motif chemokine ligand |
| CCR | C-C motif chemokine receptor |
| CD | Cluster of Differentiation |
| CFU | Colony forming unit |
| CRAMP | Cathelicidins-related antimicrobial peptides |
| CXCL | C-X-C motif chemokine ligand |
| CYP | Cytochrome P450 |
| DC | Dendritic cell |
| DKO | Double knock out |
| DNA | Deoxyribonucleic acid |
| DNase | Deoxyribonuclease |
| dNTP | Deoxyribonucleotide triphosphate |
| EAE | Encephalomyelitis |

| | |
|---|---|
| ELISA | enzyme-linked immunosorbent assay |
| FACS | Fluorescence-activated cell sorting |
| FMO | Fluorescence minus one |
| FITC | 6-formylindolo[3,2-b]carbazole |
| Foxp3 | Forkhead box P3 |
| GATA3 | Trans-acting T-cell-specific transcription factor |
| GM-CSF | Granulocyte-macrophage colony-stimulating factor |
| H&E | Hematoxylin and eosin |
| HPRT | hypoxanthine-guanine phosphoribosyltransferase |
| Hsp | Heat shock protein |
| IFN | Interferon |
| Ig | Immunoglobulin |
| ILC | Innate lymphoid cell |
| IL | Interleukin |
| IP-10 | IFN-gamma-inducible protein 10 |
| IRAK | IL-1 receptor-associated kinase |
| Isd | Iron-regulated surface determinant protein |
| ITE | 2-(1′H-in- dole-3′- carbonyl)-thiazole-4-carboxylic acid methyl ester |
| IVIS | *In vivo* imaging system |
| KO | Knock out |
| LB | Luria Bertani |
| LN | Lymph node |
| LPS | Lipopolysaccharide |

| | |
|---|---|
| MAPK | Mitogen-activated protein kinases |
| MDP | Muramyl dipeptide |
| MHC | Major histocompatibility complex |
| mRNA | Messenger RNA |
| MRSA | Methicillin resistant *S. aureus* |
| MyD88 | Myeloid differentiation factor 88 |
| NF- κB | Nuclear factor kappa-light-chain-enhancer |
| NLR | NOD like receptor |
| NLRP3 | NOD-, LRR- and pyrin domain-containing 3 |
| NOD | nucleotide-binding oligomerization |
| OD | Optical density |
| PAMPs | Pathogen associated molecular pattern |
| PBS | Phosphate-buffered saline |
| PCR | Polymerase chain reaction |
| PFA | Paraformaldehyde |
| PGN | Peptidoglycan |
| pH | Potential of hydrogen |
| PMN | Polymorphonuclear neutrophils |
| PRR | Pathogen recognition receptor |
| R | Receptor |
| RAG1 | Recombination activating gene 1 |
| RNA | Ribonucleic acid |
| RNase | Ribonuclease |

| | |
|---|---|
| ROR | Retinoid-related orphan |
| ROS | Reactive oxygen species |
| rpm | Revolutions per minute |
| RPMI | Roswell Park Memorial Institute |
| RT-qPCR | Quantitative reverse transcription PCR |
| SEM | standard error of the mean |
| Stat | Signal transducer and activator of transcription |
| S8 | *S. aureus* strain 8 |
| TB | Tuberculosis |
| T-bet | T-box protein expressed in T cells |
| TBP | TATA-binding protein |
| TCDD | toxin 2,3,7,8– tetrachloro-dibenzo-para-dioxin |
| TCR | T cell receptor |
| $T_H$ | T helper |
| TIRAP | Toll-interleukin 1 receptor (TIR) domain-containing adapter protein |
| TLR | Toll-like receptor |
| $T_r1$ | Type 1 regulatory |
| $T_{reg}$ | Regulatory T cell |
| TSB | Tryptic soy broth |
| WT | Wild type |

## Abstract

*Staphylococcus aureus (S. aureus*) is a Gram-positive bacterium that commonly colonizes healthy human beings. However, *S. aureus* is also a frequent causative agent of serious diseases ranging from skin infections to sepsis and toxic shock syndrome. A protective immune response leading to the clearance of *S. aureus* includes the production of IL-17A, neutrophil recruitment, and a subsequent $T_H17$ immune response. Our laboratory has observed that staphylococcal peptidoglycan selectively down-regulates the expression of some genes in the aryl hydrocarbon receptor (AHR) gene battery in primary human monocytes and GM-CSF-derived macrophages. Current literature suggests AHR to be an important regulator of immune cells. However, the role of AHR in immune responses to *S. aureus* is unknown. We hypothesized that AHR is necessary for a protective immune response against a S. aureus cutaneous infection, and for the induction of a disease tolerant state to this microbe. Our data show that AHR knock out (KO) mice were able to clear *S. aureus* as effectively as wild type (WT) mice, but with a decreased inflammatory phenotype. Yet, *S. aureus* remained detectable in both strains of mice 21 days post infection. Remarkably, AHR KO mice were able to mount a proper neutrophil response at the site of infection while exhibiting decreased numbers of T cells, including γδ T cells. In addition, WT mice but not AHR KO mice had an expansion of IL-17A-producing γδ T cells after a primary infection and these cells remained at the site of infection for at least 21 days. Lastly, the expanded γδ T cell pool did not affect the bacterial burden upon rechallenge. Altogether, our data suggest that inhibiting AHR would not affect the ability to protect against *S. aureus* and would promote disease tolerance during an infection. Future experiments will look into disease tolerance to *S. aureus* in carriage states and in systemic infections to further elucidate the role of AHR.

## Résumé

*Staphylococcus aureus* (*S. aureus*) est une bactérie Gram-positive qui colonise généralement des êtres humains en bonne santé. Cependant, *S. aureus* peut aussi provoquer des maladies graves allant d'infections cutanées à la septicémie et au syndrome du choc toxique. L'élimination de *S. aureus* nécessite une réponse immunitaire protectrice qui mène à la production d'IL-17A, au recrutement de neutrophiles et à une réponse adaptative de type $T_H17$. Notre laboratoire a observé que, dans les monocytes primaires humains et les macrophages générés in vitro en présence de GM-CSF, le peptidoglycan de *S. aureus* affecte sélectivement l'expression de certains gènes régulés par le récepteur d'hydrocarbures aryl (AHR). La littérature scientifique suggère que AHR est un important régulateur des cellules immunitaires. Cependant, le rôle de AHR au cours de la réponse immunitaire contre *S. aureus* est inconnu. Nous avons émis l'hypothèse que AHR est nécessaire pour une réponse immunitaire protectrice contre une infection cutanée par *S. aureus* et pour l'induction d'un état de tolérance à la maladie induite par ce microbe. Notre étude montre que les souris déficientes dans l'expression de AHR (AHR KO) éliminent *S. aureus* aussi efficacement que les souris de type sauvage (WT), mais avec une réaction inflammatoire atténuée au site d'infection. Pourtant, *S. aureus* est détectable dans les deux souches de souris 21 jours après l'infection. De façon remarquable, les souris AHR KO recrutent de façon appropriée des neutrophiles au site d'infection mais ont un nombre réduit de cellules T, y compris les cellules T γδ. De plus, contrairement aux souris AHR KO, les souris WT ont une expansion de cellules T γδ qui secrètent de l'IL-17A après une infection primaire et ces cellules persistent au site d'infection pendant au moins 21 jours. Enfin, cette expansion persistante de cellules T γδ ne permet pas une élimination plus rapide des bactéries lors d'une infection secondaire. L'ensemble de nos données suggère que l'inhibition de AHR n'a pas d'incidence sur la capacité des souris à se protéger contre

une infection cutanée par *S. aureus* mais favoriserait plutôt d'un état de tolérance à la maladie induite au cours d'une infection. Afin d'élucider davantage le rôle de AHR dans la réponse immune contre *S. aureus*, les expériences futures porteront sur l'état de tolérance à la maladie lors de la colonisation par S. aureus et lors d'infections systémiques.

# 1. Introduction

*Staphylococcus aureus (S. aureus)* is a Gram-positive bacterium that frequently causes a variety of skin and soft tissue infections (1). If the microbe enters the blood stream and spreads systemically, it can ultimately lead to life-threatening infections such as bacteremia, and endocarditis (2). Treatment options for *S. aureus* infections involve the use of antibiotics, and are often limited by the increasing prevalence of methicillin-resistant *S. aureus* (MRSA) (3). Despite its pathogenicity, *S. aureus* commonly colonizes the anterior nares of at least a third of the population, and this colonization is clinically asymptomatic (4). The precise anti-inflammatory and pro-inflammatory mechanisms that promote *S. aureus* commensalism versus pathogenicity remain unidentified. An effective and protective immune response to *S. aureus* correlates with innate interleukin (IL)-17A production leading to neutrophil recruitment, abscess formation, and an adaptive T helper ($T_H$)-17 immune response (5, 6). On the other hand, an unregulated $T_H17$ immune response is commonly associated with chronic inflammatory skin conditions such as psoriasis (7). The determinants of whether *S. aureus* infection leads to chronic inflammation or resolution via anti-inflammatory mechanisms remain unclear.

Disease tolerance is the prevention of damage produced by inflammatory responses that emerge during infection. Some mechanisms of immune modulation by *S. aureus* may play a role in disease tolerance. The Madrenas lab has previously shown that *S. aureus* can modulate the host immune response in a multitude of ways. Observations suggest a link between the aryl hydrocarbon receptor (Ahr) and *S. aureus* since staphylococcal PGN decreases transcription of

some genes in the AHR gene battery in monocytes (8). AHR was originally discovered for its involvement in detoxification against environmental pollutants such as dioxins, but recently it has become a novel topic of study in immunology (9). Currently, research on AHR focuses on the link between AHR modulation and cellular differentiation since AHR is commonly expressed in various $CD4^+$ T cell lineages (10), and innate lymphocytes (11).

Based on previous literature, a paradox exists in the roles of AHR as it has been documented to act as both an inflammatory regulator and an anti-inflammatory regulator. For example, AHR expression is reported to be the most abundant in $T_H17$ cells, and is required for their full development and effector functions (12). Additionally, *in vivo* activation of AHR has been shown to increase the severity of experimental autoimmune encephalomyelitis (EAE) (12), and AHR is expressed higher in patients with inflammatory skin diseases (13). In stark contrast, AHR activation in the same manner has been found to reduce inflammation in a psoriasis model (14). Moreover, AHR activation by another ligand has been shown to suppress EAE through the induction of $Foxp3^+$ T regulatory ($T_{reg}$) cells (16). In regards to a worm or bacterial infection, AHR activation has been linked to the transdifferentiation of $T_H17$ cells into type 1 regulatory ($T_R1$) cells (17). Considering the current knowledge on AHR, our research aims to reveal and clarify the AHR pathway as a mechanism through which the host promotes *S. aureus* disease tolerance and potentially commensalism. This mechanism may provide an alternative target for novel anti-inflammatory therapeutics against *S. aureus* cutaneous infections.

### *1.1. S. aureus*

#### *1.1.1. S. aureus* characteristics, epidemiology, and pathology

*S. aureus* is a Gram-positive bacterium that was first isolated and identified from a surgical abscess in 1880 by Sir Alexander Ogston (18). The bacterium is a member of the Firmicutes family and is commonly known for its appearance as a cluster of golden cocci. Its characteristic golden color is due to the production of staphyloxanthin, a pigment and virulence factor produced to protect the bacterium from neutrophil and oxidant killing (19). In addition, the microbe is a facultative anaerobe that can modulate both its metabolic and replicative ability in response to a change in oxygen concentration (20). Microbiology characterization of this bacterium include catalase, coagulase, and ß-hemolysis activities (21).

*S. aureus* causes a wide range of human diseases (1). Most frequently *S. aureus* causes skin and soft tissue infections such as dermatitis, impetigo, and cellulitis (1). However upon a breach in the host's epithelial layer occurs, the microbe can ultimately lead to invasive infections such as bacteremia, endocarditis, and sepsis (2). Lastly, toxic shock syndrome can occur when *S. aureus* secretes pyrogenic-toxin superantigens that directly link invariant MHC class II molecules on antigen-presenting cells (APCs) with the variable regions of the T-cell-receptor (TCR) resulting in massive immune cell activation and the formation of a cytokine storm (2). Overall, infections by *S. aureus* cause high morbidity and mortality illustrated by over 500,000 hospitalizations per year in the United States of America and a mortality rate ranging from 15-67% (22).

Although infection by *S. aureus* is a serious health concern, treatment options are often limited due to the increasingly high prevalence of drug resistant *S. aureus* strains such as MRSA

(23). MRSA was first identified in 1961 (24), and by 1997 *S. aureus* had already developed resistance against the drug of last resort, vancomycin (25, 26). In the United States of America, MRSA is responsible for 20,000 deaths per year (3). MRSA was originally discovered as a nosocomial pathogen (24). However since then, more virulent MRSA strains began to be documented in otherwise healthy individuals (27-29). Community acquired (CA)-MRSA has rapidly spread through the industrialized nations and is currently a global threat (23).

In addition to diseases in which *S. aureus* is the main causative agent, there exist inflammatory diseases to which *S. aureus* has been linked. For example, it has been known since the early 1980s that *S. aureus* heavily colonizes patients suffering from AD, also known as eczema (30). Through microbiome studies, increased *S. aureus* abundance has been correlated with AD flares (31). In addition, a murine model of AD demonstrated that *S. aureus* directly causes the inflammation in eczematous dermatitis through an immunological pathway that is yet to be determined (32). These studies illustrate that *S. aureus* can have an active role in inflammatory skin diseases via its interaction with the host immune system.

Despite its pathogenicity, *S. aureus* commonly colonizes the anterior nares of at least a third of the general population, and this colonization is clinically asymptomatic and can be chronic (4). In fact, it has been suggested that all adults have been colonized by *S. aureus* at some point during their lives since immunoglobulin (Ig) G antibodies against *S. aureus* can often be found regardless of the history of infection with *S. aureus* (33). Moreover, persistent colonization has been linked to a higher risk of developing bacteremia with the colonizing staphylococcal strain being the main causative agent (34, 35). Given this increased risk, it is remarkable that patients

with bacteremia who had prior colonization with *S. aureus* have the best clinical outcomes (35). The precise mechanisms that promote *S. aureus* commensalism versus pathogenicity remain unidentified.

### *1.1.2.* Cutaneous immunity to *S. aureus*

The skin acts as both a physical and immunological barrier against *S. aureus* and other pathogens. It is comprised of an outer epidermal layer, and an inner dermal layer. Below these two layers is the subcutaneous layer and the muscle layer. The physical barrier is provided by the outermost epidermal layer, known as the corneal layer, that is composed of terminally differentiated keratinocytes that have migrated upward from the basal layer and will be shed during the final stage of the skin self-renewal process (36). Keratinocytes can sample the microbiota for pathogen-associated molecular patterns (PAMPs) through their pattern recognition receptors (PRRs) such as toll like receptors (TLRs) and nucleotide-binding oligomerization domain (NOD)-like receptors (NLRs) (36). Upon injury or infection, keratinocytes secrete pre-made IL-1α in order to initiate an autocrine activation loop through their IL-1 receptor (IL-1R) (1). Additionally, the corneal layer contains a variety of antimicrobial peptides (AMPs), the majority of which are secreted by keratinocytes in order to prevent the colonization of pathogens (1, 37). Some of the human AMPs that act against *S. aureus* include β-defensins, cathelicidins, lysozyme, psoriasin, and RNase 7 (37). Similarly, mice produce their own types of AMPs, such as the cathelicidins-related antimicrobial peptides (CRAMP) (38).

Furthermore, the skin microbiota can potentially promote or prevent the colonization of certain pathogens (39). A recent study has demonstrated that skin bacterial communities are

correlated to different infection outcomes and can themselves be altered by an infection (40). Overall the sites of skin on the body widely differ in temperature, moisture, osmolarity, and pH leading to distinctive ecosystems harbouring a variety of diverse microbial species (36). The four major phyla broadly comprising the human skin microbiota are Actinobacteria, Firmicutes, Bacteroidetes, and Proteobacteria (36, 40). Within these phyla, the most commonly studied resident genera are *Staphylococcus*, *Streptococcus*, *Corynebacterium*, *Propionibacterium*, and *Pseudomonas* (41). Several resident microbial species, such as *S. epidermidis,* have been negatively correlated with *S. aureus* carriage (42). This is in agreement with previous literature suggesting that pheromones produced by *S. epidermidis* have a strong inhibitory effect on *S. aureus* virulence factor expression (43, 44). Additionally, a recent study has illustrated that *S. epidermis* can secrete two phenol-soluble modulins that resemble host AMPs, and can have direct bactericidal effects on *S. aureus* and Group A *Streptococcus* (45). One of these two modulins was also shown to enhance the function of the innate immune response by cooperating with AMPs produced by the host (46). In summary, the microbiota can interfere with pathogen growth by occupying niches on the body and secreting molecules that inhibit the growth of other species.

Once *S. aureus* crosses the epithelial barrier, both keratinocytes and resident cutaneous innate immune cells can detect the bacterium and initiate a pro-inflammatory immune response. Resident epidermal immune cells that respond to *S. aureus* include Langerhans cells (a subset of dendritic cells (DCs)) and γδ T cells (only in mice) (1). The resident dermal immune cells include DCs, macrophages, mast cells, natural killer cells, γδ T cells, plasma cells, T and B cells, and fibroblasts (1). Keratinocytes and immune cells can detect various *S. aureus* PAMPs through PRRs (including TLRs and NLRs).

Extracellular *S. aureus* PAMPs can be detected by trans-membrane PRRs, such as TLRs. Most commonly, immune cells detect *S. aureus* lipopeptides and lipoteichoic acids through TLR2 (1). TLR2 activation occurs by dimerization with TLR1 or TLR6 and the subsequent recruitment of adaptor proteins (TIRAP, MyD88, IRAK 1 and 4) to initiate the NF-κB and mitogen-activated protein kinases (MAPKs) pro-inflammatory pathways (47). These signaling pathways lead to the production of numerous cytokines (including IL-1ß, IL-16, TNF, and IL-12p70) and chemokines (including CXCL1, CXCL2, CXCL8, CCL2 andCCL20) that ultimately activate and recruit more immunological cells to the site of infection (47). The pro-inflammatory cytokine IL-1ß is the result of inflammasome activation that leads to its processing and maturation prior to secretion (48). Furthermore, activation of the IL-1R has a synergistic effect as its signaling converges on the MyD88 and IRAK4 pathway to further enhance pro-inflammatory cytokine and chemokine secretions (1). Human deficiencies in either MyD88 (49) and IRAK4 (50, 51) have been associated with increased susceptibility to pyogenic bacterial infections, including *S. aureus* skin infections. Similarly, mice deficient in TLR2 or MyD88 show increased mortality during *S. aureus* bacteremia infections (52). However, only MyD88- and IL-1R-deficient mice, and not TLR2-deficient mice, have increased skin lesions and decreased neutrophil recruitment to the site of *S. aureus* infection (53). This discrepancy in the role of TLR2 illustrates how defining immunity to *S. aureus* is dependent on the site of infection.

*S. aureus* PAMPs can be detected within the cytoplasm of cells by NLRs. For example, NOD2 can detect muramyl dipeptide (MDP) ubiquitously expressed as part of bacterial PGN, including *S. aureus,* and induce a pro-inflammatory response through downstream NF-κB and

MAPK signaling (47). During a *S. aureus* infection, mice deficient in NOD2 have increased skin lesions, increased bacterial burden, and decreased IL-1ß production resulting in reduced bacterial killing by neutrophils (54). Lastly, multiple mechanisms including haemolysin pore formation, and PGN digestion and phagosome rupture have been suggested to activate the NLRP3 inflammasome important in the processing of the pro-inflammatory cytokine IL-1ß during a *S. aureus* cutaneous infection (1).

The next stages of an effective immune response to *S. aureus* correlates with a rapid burst of IL-1- and TLR2-dependent IL-17 production by innate immune cells leading to neutrophil recruitment, abscess formation, and a $T_H17$ adaptive immune response (5, 6). This response if graphically summarized below in Figure 1.1. A $T_H17$ type of immune response is not only required for the clearance of an infection but also for the clearance of nasal carriage (55). In a murine model, IL-17A and IL-17F production within 24 hours after *S. aureus* infection has been shown to be necessary for the clearance of the infection (5). Furthermore, the source of this early IL-17 was determined to be the epidermal $V\gamma5^+$ γδ T cells, and in the absence of γδ T cells there is a drastic reduction in neutrophil recruitment to the site of infection (5). Once secreted, the IL-17 cytokines have multiple functions to further promote the pro-inflammatory immune response. IL-17A and IL-17F can bind and activate IL-17 receptors (IL-17RA and IL-17RC) on keratinocytes to enhance production of AMPs, cytokines, chemokines, and adhesion molecules (1). More specifically, IL-17 mediates the recruitment of neutrophils to the site of infection by promoting the production of neutrophil chemoattractants and granulopoiesis factors (5). Although epidermal γδ T cells do not exist in the human epidermis, other cells in the skin, such as $T_H17$ or dermal γδ T cells, may have equivalent functions (1).

Neutrophils play an essential protective role against bacterial infections, and it has long been known that individuals with low neutrophil counts, such as patients with Chédiak-Higashi syndrome, commonly have recurrent skin and lung infections caused by *S. aureus* (56). Neutrophil recruitment due to chemoattractants such as CXCL2 occurs very early on during *S. aureus* infection. These cells kill the bacteria at the site of infection by phagocytosis, reactive oxygen species (ROS), AMPs, and by the production of neutrophil extracellular traps (57-60). More specifically, hypochloric acid and oxygen radicals produced by the neutrophils destroy engulfed bacteria (59). Extracellular bacteria are simultaneously targeted by extracellular traps, which are made up of DNA, AMPs, and various proteases that target virulence factors (60). Although neutrophils are needed to resolve *S. aureus* infections, in some instances enhanced neutrophil recruitment has been shown to increase *S. aureus* pathogenicity by allowing *S. aureus* to survive within the neutrophils (59, 61).

In addition to the neutrophil response, an adaptive $T_H17$ immune response to *S. aureus* is thought to be critical since a type of $T_H17$ cell deficiency results in an increase of staphylococcal abscesses and the development of the Hyper-IgE Syndrome (62). This syndrome is caused by a genetic mutation in *stat3* resulting in decreased levels of the $T_H17$ master regulator, retinoid-related orphan receptor (ROR) γt, a decrease in IL-17A production, and an increase in susceptibility to *S. aureus* infections (62). Infections in these patients preferentially occur in the skin and lungs because these epithelial cells require $T_H17$ cytokines (IL-17A and IL-22) to synergize with pro-inflammatory cytokines, such as IL-1ß, for optimal production of anti-staphyloccocal factors (63). Similarly, IL-17A- and IL-17F-deficient mice were more susceptible to *S. aureus* skin infections but their survival during bacteremia was not affected (64). However in direct contrast, other studies

have shown that single deficiencies in IL-17R signaling (65) or RORγt (66) in humans do not directly lead to increased susceptibility to *S. aureus*. These opposing results bring to question what is the important component in the $T_H17$ response for clearing *S. aureus* infections in humans, and for regulating the balance between commensalism and disease by this microbe.

One additional reason for $T_H17$ deficiency potentially leading to the susceptibly of *S. aureus* infections could be the deficiency of IL-22, a commonly overlooked $T_H17$-associated cytokine. Eighty to 100% of AD patients are colonized by *S. aureus*, and in these patients staphylococcal exotoxins induce IL-22 secretion, which may contribute to their chronic skin inflammation (67). IL-22 functions complementary to IL-17A to recruit neutrophils and promote additional antimicrobial peptides such as CRAMP (67). Additionally, the stimulatory effects of IL-22 are suppressed in *stat3* deficient conditions (68). In the context of nasal colonization, it has been recently reported that IL-22 produced by T cells and innate lymphoid cells 3 (ILC3s) regulates the production of antimicrobial peptides and keratinocyte differentiation to promote *S. aureus* decolonization (69). However, a well-defined role of IL-22 during the innate immune response to *S. aureus* remains elusive.

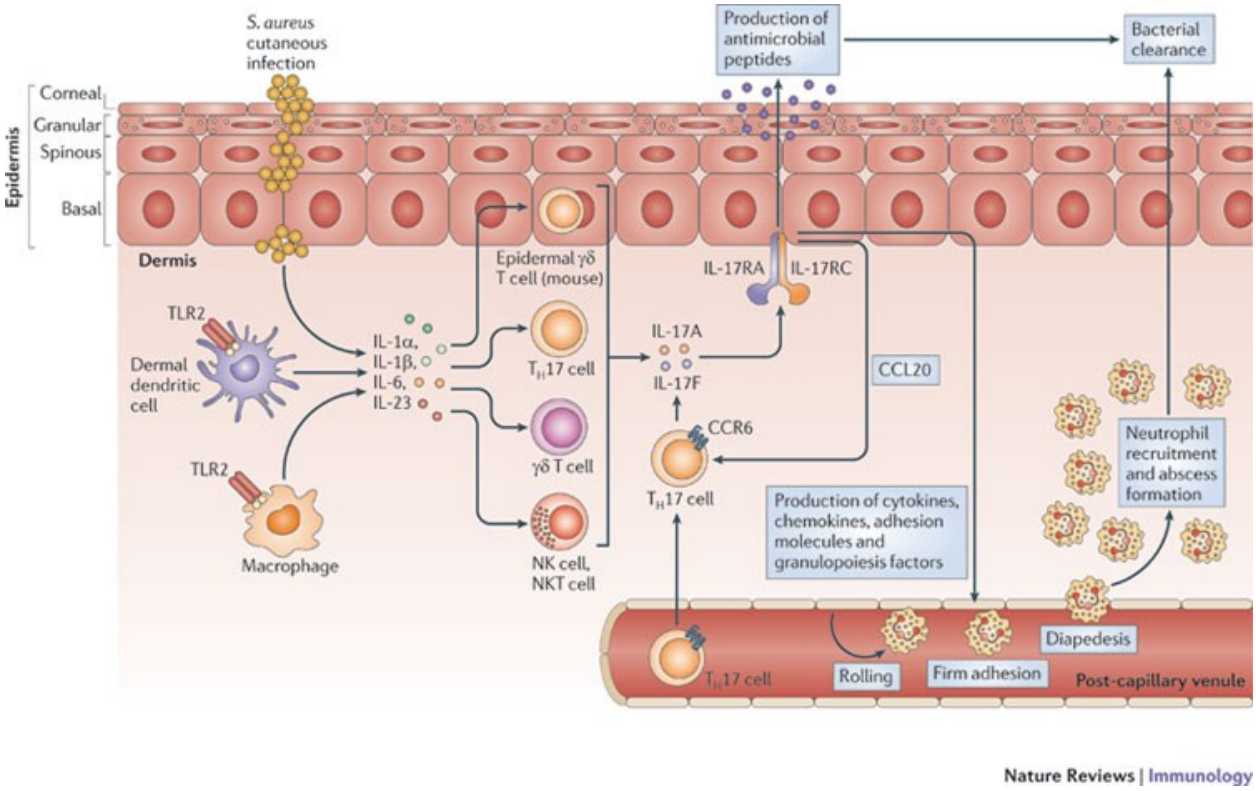


**Figure 1.1. Overview of the cutaneous immune response to *S. aureus*.** This schematic representation summarizes the key immunological mechanisms required for clearing a *S. aureus* skin infection in both humans and mice (1). Permission included in thesis appendices.

### *1.1.3.* Immunological memory to *S. aureus*

Immunity and immunological memory to *S. aureus* are still incompletely understood making any progress in vaccine development challenging. This challenge is further complicated because immune correlates depend on a variety of factors including the site of infection, the host (mouse versus human), and the type of infection that is caused by *S. aureus*. As discussed in section 1.1.2, cutaneous immunity is normally attributed to the $T_H17$ immune response (1) while systemic immunity is more commonly associated with T helper 1 ($T_H1$) immunity (70) and the production of serum IgG (33). Serum IgG antibodies have been shown to naturally target 20 extracellular proteins, of which 7 are conserved and contained within the core genome of *S. aureus* (33). These antibodies enhance intracellular killing of *S. aureus* by promoting opsonization by granulocytes (71). Although specific immune responses have been correlated with protection, memory is not thought to develop naturally since a primary *S. aureus* infection has not been documented as protective against recurrent infections (72).

Despite the incomplete understanding of immunological memory to *S. aureus*, several immunoglobulin therapies (passive immunization) and vaccines (active immunization) have been evaluated to clinical trials (73). Unfortunately, none of these therapeutic agents have proven to be effective in these trials. Most recently, the V710 vaccine (Merk Sharp & Dohme Corp) targeting the conserved *S. aureus* iron surface determinant B (IsdB) was developed. In murine models, IsdB immunization was effective in protecting from *S. aureus* bacteremia via the $T_H17$/IL-17A pathway (74) and the production of anti-IsdB antibodies (75). However, clinical trials with this vaccine were halted because of increased mortality observed in patients who had received the V710 vaccine and developed postoperative *S. aureus* infections (76). In fact, data analysis indicated that patients

who had developed *S. aureus* infections and after receiving the V710 vaccine were five times more likely to die than the placebo group (73). This study suggests that "immune-priming" to *S. aureus* may be more detrimental than protective to the host (73). A recent murine model supports this speculation, by illustrating that vaccination can induce $CD4^+$ T cell mediated mortality upon a systemic *S. aureus* infection (77). Therefore, mechanisms of disease tolerance should be considered during the development of future vaccines.

### *1.1.4.* Disease tolerance to *S. aureus*

Although important for clearing *S. aureus* infections, an exacerbated $T_H1/T_H17$ immune response can additionally lead to chronic inflammatory skin conditions such as psoriasis (7). Moreover, "immune-priming" can potentially lead to increased multiple organ failure and mortality during *S. aureus* infection (73). Disease tolerance is the prevention of damage produced by the inflammatory responses that emerge during infection without changing the microbial load (78, 79). It is distinct from immunological tolerance (inability of an antigen to induce an immune response), and mechanisms of immune evasion and resistance to infection (80). Typically, exposure to *S. aureus* can result in disease and/or clearance due to inflammation and pro-inflammatory immune responses. However, *S. aureus* exposure can also lead to disease tolerance and/or colonization via anti-inflammatory mechanisms. The determinants for either outcome during exposure to *S. aureus* are unknown. However, some mechanisms of immune modulation by *S. aureus* have potential roles in disease tolerance.

Using systems biology to investigate differentially regulated genes during exposure to *Staphylococcal* cell wall components, our group has shown that *S. aureus* can modulate the host

immune response in a multitude of ways. For example, *S. aureus* can down-regulate T cell activation through its PGN layer in a mouse model of toxic shock syndrome (81). In addition, the immune response to *S. aureus* can be imprinted by a profile of anti-inflammatory cytokine production characterized by the production of high levels of IL-10 from monocytes or macrophages (82). Furthermore, this anti-inflammatory response is mechanistically uncoupled from the pro-inflammatory response to the microbe (83). However, this anti-inflammatory response can dampen the inflammatory response by downregulating the production of IFN-gamma-inducible protein (IP-10) and the recruitment of $T_H1$ cells (84). Recently, our research group has reported that AHR may have an immunological role during a *S. aureus* infection since *Staphylococcal* PGN decreases transcription of some the AHR gene battery in human primary monocytes (8). Therefore, our research intends to uncover if AHR has a role in mediating an anti-inflammatory response against a *S. aureus* cutaneous infection, and if it is involved in a mechanism of disease tolerance.

## *1.2.* The aryl hydrocarbon receptor (AHR)

### *1.2.1.* The physiological roles of AHR

AHR is a ligand-activated transcription factor that is part of the basic-helix-loop-helix-PER-ARNT-SIM transcription factor family (85, 86). AHR was originally discovered for its involvement in detoxification against environmental pollutants such as dioxins, but recently it has become an intense focus of study in immunology because of its role in T cell differentiation (9). Ligands of AHR are typically planar, aromatic, and hydrophobic molecules, such as the toxin 2,3,7,8–tetrachloro-dibenzo-para-dioxin (TCDD), more commonly known as a by-product in the synthesis of Agent Orange (9, 87). However, AHR can also bind endogenous ligands such as

kyneurines, catabolites of tryptophan (88). Once AHR is bound by a ligand, it dissociates from its cytoplasmic complex containing heat-shock protein (Hsp) 90, and heterodimerizes with the AHR nuclear translocator (ARNT) (87, 89). Upon entering the nucleus, AHR targets dioxin responsive elements in the DNA to initiate the transcription of the AHR gene battery. The AHR gene battery includes the AHR repressor (AHRR) and the cytochrome P450 enzymes (CYP1A1, CYP1A2, and CYP1B1), which function to metabolize AHR ligands (eliminate the environmental toxins) (9, 87). AHR has been broadly implicated in numerous cellular and physiological processes including reproduction and embryogenesis (90), growth and development (91), and tumorigenesis (92). AHR-deficient mice commonly suffer from increased neo-natal death, stunted growth, decreased fertility, liver abnormalities (size and function), and decreased lymphocyte and splenocyte numbers (91, 93).

### *1.2.2.* The immunological roles of AHR

AHR has been recently shown to play a role in regulating the immune response to bacterial antigens. Gram-negative lipopolysaccharide (LPS) can activate AHR leading to an endotoxin-tolerant state that prevents immunopathology against both Gram-positive and Gram-negative bacteria (94). Similarly, AHR-deficient mice show hypersensitivity to LPS resulting in LPS-induced septic shock (95). Mechanistically, AHR in LPS-stimulated macrophages forms a DNA-bound complex with Stat1 and NF-κB in order to inhibit the transcription of pro-inflammatory cytokines (96). This inhibition is reported to occur regardless of IL-10 production by macrophages (96), suggesting that AHR can contribute to disease tolerance through IL-10-independent mechanisms.

Furthermore, AHR has been suggested to be an intracellular PRR that regulates the expression of cytokines such as IL-12 and IL-6, and chemokines (CXCL1 and CXCL5) (97). The rationale behind its role as a PRR is that AHR can bind bacterial pigments such as phenazines from *Pseudomonas aeruginosa*, and napthoquinone phthiocol from *Mycobacterium tuberculosis (M. tuberculosis) (97)*. Additionally, AHR has been reported to be critical for the immunity to these pathogens and AHR-deficient mice have decreased survival rates (97). Lastly, tryptophan metabolites produced by the microbiota can directly activate AHR to promote the transcription of IL-22 and enhance the mucosal protection against pathogens and inflammation (98). It is tempting to speculate that AHR might recognize the pigment of *S. aureus*, staphyloxanthin, or part of its PGN layer. However, no research has addressed this yet.

It has been known since 1995 that AHR-deficient mice have decreased lymphocytes in the periphery (99). An area of active research on AHR is focused on the link between AHR modulation and T cell differentiation. AHR is commonly expressed in various $CD4^+$ T cell lineages such as $T_H17$ (12), $T_{reg}$ (10), $T_{reg}17$ (100), $T_r1$ (101), and $T_H9$ (102). AHR expression is reported to be the greatest in $T_H17$ cells (103) and is thought to be controlled by Stat3 (104). AHR is required for their development by inhibiting Stat1 and Stat5, which normally function to prevent $T_H17$ differentiation (105). Murine $T_H17$ effector functions, such as optimal production of IL-17A and IL-22, are also AHR-dependent (12). However, activation of AHR in human $CD4^+$ T cells only leads to an increase in IL-22 production, and not IL-17A (106). This difference in the role of AHR in human lymphocytes may be explained by the different activity reported in the human AHR compared to the mouse AHR (87).

Additionally, AHR is important for the development of anit-inflammatory Foxp3$^+$ $T_{reg}$ (10) and $T_R1$ cells (101). The differentiation into $T_H17$ or $T_{reg}$ cells has been proposed to be reciprocally regulated by AHR-dependent epigenetic modifications (107). More specifically, AHR activation leads to the demethylation and methylation of CpG islands of IL-17 and Foxp3 promoters respectively (107). Similarly, a murine mouse model of *S. aureus* bacteremia illustrated that activation of AHR can also induce trans-differentiation of $T_H17$ cells into $T_r1$ cells (17). There are no other reports on the regulatory role of AHR during *S. aureus* infections, especially *S. aureus* skin infections.

AHR is commonly expressed in innate-like T cells, including γδ T cells (11) and ILCs (108). Murine cutaneous γδ T cells require AHR for their survival and proliferation (109). However, the extent of AHR function and necessity for survival is not the same in all γδ T cells and is suggested to be dependent on the γδ T cell subset (characterized by the Vγ chain) (103). Unlike $T_H17$ cells, γδ T cells and ILC3s do not require AHR to produce IL-17A but they do require AHR for their production of IL-22 (11, 108). In lymphocytes containing both RORγt and AHR, it is speculated that RORγt promotes AHR recruitment and transcription of AHR-regulated genes (110). This has been well described in ILC3s, where RORγt is recruited and cooperates with AHR on the *Il22* locus in order to promote the production of IL-22 and ultimately provide protection to *Citrobacter rodentium* (*C. rodentium*) infections (108). Resident cutaneous γδ T cells play a critical role in clearing *S. aureus* infections (5). However, the role of AHR in these cells during *S. aureus* infections is not documented.

Although AHR has a major role in regulating $T_H17$ cytokines, not all $T_H17$-like cytokines are AHR-dependent and the dependency changes depending on the cell type. In contrast to the variant dependency seen with IL-17A, most lymphocytes expressing AHR regulate IL-22 production in an AHR-dependent mechanism. However, novel sources of IL-22 production that are independent of AHR are starting to emerge. For example, IL-22 can be produced by a subset of natural killer cells in the lung after an influenza virus infection (111). In addition, there have been a couple of publications claiming that IL-22 production and secretion can come from neutrophils (112, 113). All these results suggest that there might be additional sources of IL-22 that are independent of AHR and are present in multiple models of viral and bacterial infections.

### *1.2.3.* The role of AHR in disease

Through the production of IL-17A and IL-22 both $T_H17$ and γδ T cells can promote pathogen clearance at the site of infection by recruiting neutrophils (114, 115). As mentioned above, neutrophils are essential for *S. aureus* clearance (60) but they can also be detrimental to the host at high numbers by promoting inflammatory skin conditions (115). A few studies have reported a potential role of AHR in regulating various neutrophil responses (116-118). Recent studies illustrate that AHR activation in keratinocytes with a high affinity ligand, FICZ, in an imiquimod-induced skin inflammation model of psoriasis ultimately leads to both a decrease in neutrophil infiltration and mRNA levels of inflammatory cytokines (14). In the opposite case, AHR-deficient mice display an exacerbation of skin inflammation due to increased level of IL-17A production by γδ T cells (11, 14). This is reminiscent of inflammatory skin conditions, such as psoriasis, where inflammation is attributed to the IL-17A production by dermal γδ T cells (115). These findings

suggest that depending on the scenario, AHR-expressing cells can differentially regulate inflammation and potentially promote disease tolerance.

Yet, a paradox exists in the roles of AHR because it has been documented to play both a pro-inflammatory role as well as an anti-inflammatory role depending on the clinical condition. For example, *in vivo* activation of AHR with 6-formylindolo[3,2-b]carbazole (FICZ) has been shown to increase the severity of EAE (12). Similarly, a pilot study has shown that skin lesions of patients with chronic inflammatory skin conditions, such as psoriasis or AD, show increased expression of AHR (13). But in stark contrast to the EAE model, AHR activation by FICZ has been found to reduce inflammation in a murine model of psoriasis (14). Moreover, AHR activation by an endogenous ligand, 2-(1′H-in- dole-3′- carbonyl)-thiazole-4-carboxylic acid methyl ester (ITE), has been shown to suppress EAE through the induction of $Foxp3^+$ $T_{reg}$ cells (16). Specifically with regards to helminth or bacterial infections, AHR activation has been linked to the transdifferentiation of $T_H17$ cells into $T_R1$ cells (17). It has recently been suggested that $T_H17$ have the potential to reprogram their transcriptional profile to differentiate into either $T_H1$-like cells or $T_R1$ cells (17). The trans-differentiation of $T_H17$ in $T_H1$-like cells is correlated with EAE pathology, and conversely the transdifferentiation into $T_R1$ promotes disease tolerance (17). All in all, the immunological role of AHR during inflammatory diseases and the resolution of infections is still unclear.

# 2. Project overview

## 2.1. Rationale and hypothesis

In order for a *S. aureus* cutaneous infection to be effectively cleared, a $T_H17$/IL-17 inflammatory response has to occur (1). However, this inflammatory response is commonly associated with chronic inflammatory skin diseases (119). The Madrenas group has proposed that *S. aureus* colonization, or disease tolerance, may occur through $T_{reg}$/IL-10 anti-inflammatory mechanisms (120). AHR has been reported to regulate both $T_H17$/IL-17 and $T_{reg}$/IL-10 immune responses (103). Since the role of AHR during *S. aureus* skin infections is currently unknown, and that AHR has been shown to be an important regulator of the $T_H17$-mediated immunity, we propose to study the role of AHR in this context. We hypothesize that AHR is necessary for a protective immune response against a *S. aureus* cutaneous infection, and for the induction of a disease tolerance to this microbe (Figure 2.1).

The Madrenas group has shown that the *S. aureus* PGN layer can modulate the host's immune response to promote of disease tolerance (120). Our recent observation that *S. aureus* down-regulates transcription of some of the AHR gene battery (83), suggests that *S. aureus* may promote disease tolerance through the AHR pathway. Our objective is to reveal and clarify the AHR pathway as a mechanism through which the host promotes *S. aureus* disease tolerance and potentially commensalism. Identification of the AHR pathway as a mechanism of disease tolerance may provide an alternative to antibiotics by serving as a template for the development of anti-inflammatory therapies against *S. aureus* infections

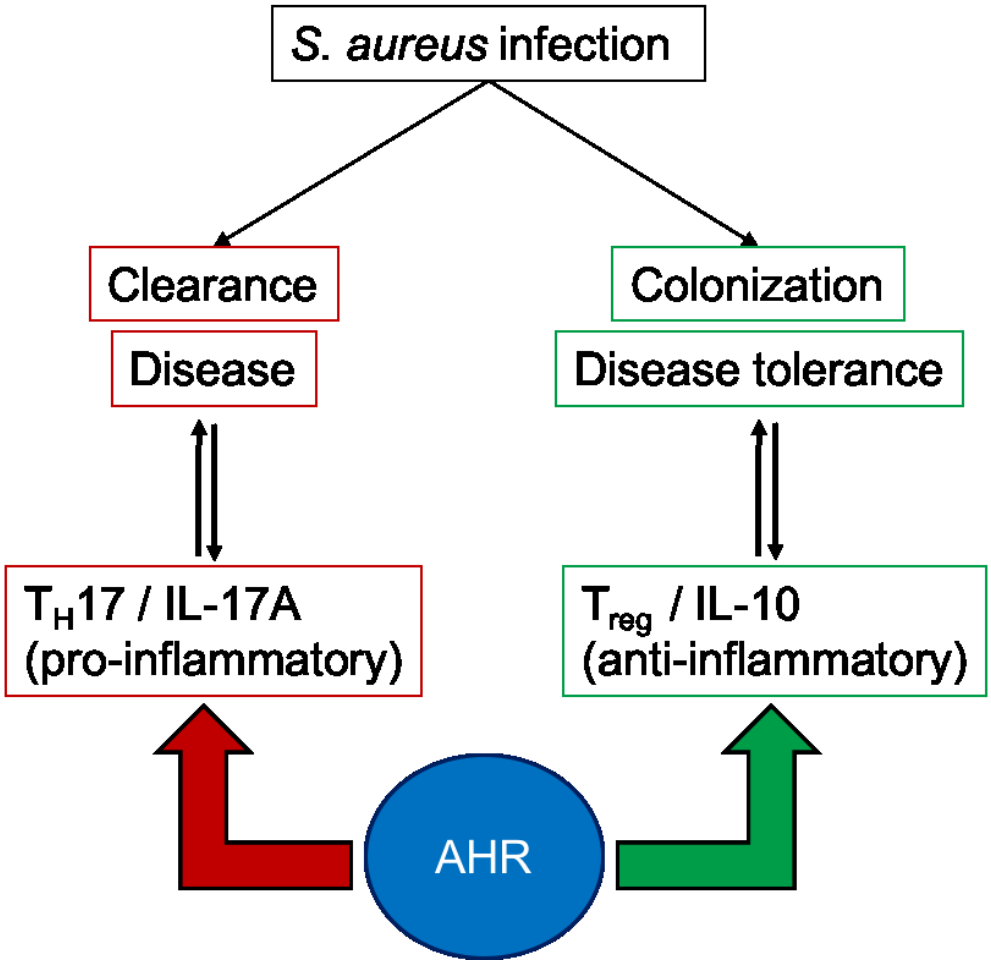


**Figure 2.1. AHR may be necessary for both protection and disease tolerance to *S. aureus*.** A *S. aureus* skin infection can either lead to clearance/disease or colonization/disease tolerance. AHR has been reported to play an important role in immune responses that lead to each outcome. We hypothesize that AHR is necessary for clearance of a *S. aureus* cutaneous infection and for disease tolerance to this microbe.

## 2.2. Specific aims

To test this hypothesis, we will address the following three specific aims:

I. Determine if AHR is necessary for *S. aureus* clearance during a cutaneous infection;

II. Establish the cellular response to *S. aureus* infection in the presence and absence of AHR expression;

III. Investigate whether AHR contributes to the generation of immunological memory to *S. aureus*

These aims will be addressed by studying AHR-competent and AHR-deficient mice in a mouse model of cutaneous infection by *S. aureus*.

# 3. Materials and methods

## 3.1. Mouse strains and housing conditions

Wild type (WT) C57BL/6 mice were obtained from The Jackson Laboratory. AHR knock out (KO) mice on the C57BL/6 background strain were obtained from Dr. Frank Gonzalez at the National Institutes of Health (Bethesda, MD) (99). RAG KO mice were obtained from Dr. Irah King at McGill University and were bred with AHR KO mice to generate double knock out (DKO) mice. All mice were bred and maintained in the Lyman Duff Animal Facility at McGill University. Experiments were all done on male and female mice between six to twelve weeks of age. The McGill University Animal Care and Use Committee approved all protocols that were used in these studies. Ear thickness was measured by using a Mitutoyo thickness gauge while mice were anesthetized with isoflurane.

## 3.2. *Ahr* and *Rag1* genotyping

Ear nudges were obtained from the mice at the time of weaning and DNA isolation was performed using the GeneJet Genomic DNA Purification Kit (ThermoFisher Scientific). PCR was performed for the AHR gene with the AHR primers (forward, 5'-GGCTAGCGTGCGGGTTTC TC-3'; reverse, 5'-CTAGAACGGCACTAGGTAGGTCAG-3') and the REDExtract-N-Amp PCR ReadyMix$^{TM}$ (Sigma-Aldrich). The PCR program was carried out on a PTC-100 Peltier Thermal Cycler (Bio-Rad) and is as follows: i) 3 minutes predenaturation at 94°C, ii) 1 minute denaturation at 94°C, iii) 1 minute annealing at 60°C, iv) 2.5 minutes extension at 72°C, and v) repeat steps ii-iv for 30 cycles. The PCR products were ran on a 2% agarose gel and visualized with ethidium bromide. A 450 bp band indicates the presence of the WT *Ahr* gene whereas a 1.45 kbp band

indicates the presence of the insert mutation in the *Ahr* gene present in the AHR KO mice. Real time polymerase chain reaction (RT)-PCR, also known as quantitative PCR (qPCR), was performed for RAG1 (forward WT, 5'-TCTGGACTTGCCTCCTCTGT-3'; forward KO, 5'-TGGATGTGGAATGTGTGCGAG-3'; common reverse, 5'-TGGATGTGGAATGTGTGCGAG -3') with the SsoAdvanced Universal SYBR Green Supermix (Bio-Rad). The qPCR program was carried out on a CFX96 Touch™ Real-Time PCR Detection System and is as follows: i) 2 minutes predenaturation at 94°C, ii) 20 seconds denaturation at 94°C, iii) 15 seconds annealing at 65°C, iv) 10 seconds 68°C, v) repeat ii-iv for 10 cycles (each cycle the annealing temperature is decreased by 0.5°C), vi) 15 seconds denaturation at 94°C, vii) 15 seconds annealing at 60°C, viii) 10 seconds extension at 72°C, ix) Repeat vi-viii for 28 cycles, and x) 2 minutes long extension at 72°C. The *Rag1* genotype was determined by the melt curve peaks (WT RAG1: one peak at 83.5°C; heterozygous for RAG1: one peak at 83.5°C and another at 88°C; KO RAG1: one peak at 88°C).

### 3.3. *S. aureus* cultures

The *S. aureus* 8 (S8) strain is a community isolate from a nasal swab of an individual undergoing nasal surgery. A frozen stock of this microbe or a colony from an agar plate of S8 was grown over night in 5 ml of Tryptic Soy Broth (TSB) at 37°C with shaking (250 rpm). Following overnight growth, 100 µl was aliquoted into 5 ml TSB and incubated for an additional three hours. 2ml of the exponential culture was washed with 1 ml PBS and spun for 10 minutes at 6000g for a total of 3 washes. After the final wash, the bacterial pellet was resuspended in a final volume of 1 ml PBS. Bacterial concentrations were quantified by measuring the optical density (OD) at 600 nm by a spectrophotometer. The correlation between the OD-600 nm value and CFU was determined by plating and counting *S. aureus* CFUs at several OD-600 nm values. For the infection model, the

concentration of bacteria was adjusted with PBS so that each mouse received $5x10^6$ colony forming units (CFUs) in an intradermal ear injection of 15 µl. An aliquot of the injection mixture was diluted and plated on Luria Bertani (LB) agar in order to count CFUs and verify the bacterial load delivered after each injection day.

### 3.4. Mouse model of *S. aureus* cutaneous infections

Mice were anesthetized during all injections with isoflurane. Naïve mice received a single exposure to *S. aureus* through an intradermal ear injection of 15 µl containing $5x10^6$ CFUs. However, since no differences were observed between the WT and AHR KO mice, we decided to increase the exposure time to 3 days. When naïve mice were administered a daily injection of $5x10^6$ CFUs *S. aureus* for 3 days the mice were labelled as receiving a "prolonged exposure". Mice were monitored for up to 21 days. Secondary prolonged exposures to *S. aureus* were initiated in primed mice who received an initial prolonged exposure to *S. aureus* 40 days prior. Age matched naïve mice were subjected to a primary prolonged exposure in parallel to the primed mice. All mice were euthanized prior to the experimental end point (Day 46).

### 3.5. Organ harvest and digestion

#### 3.5.1. Ear harvest and digestion

The injected ear was cut off at its base. Each ear was separated into two pieces: the dorsal and ventral side. The ear was manually cut into pieces smaller than 2 mm pieces using fine scissors in 500 µL of PBS. A 30 µL aliquot of the mixture was kept for CFU counts. The remaining mixture was centrifuged at 1600 rpm for 10 minutes, and the supernatant was discarded or stored at -20°C for ELISA analysis. After the wash, 500 µl of R10 media containing 1 µg/ml Golgi Plug (BD),

50U/ml DNAse I (Sigma-Aldrich), and 250 μg/ml collagenase Type XI (Sigma-Aldrich) was added. The digestion mixture was incubated for two hours at 37°C while shaking at 1200 rpm. The mixture was flushed with a 1 ml pipette four to six times and then transferred to the filter cap of 5 ml FACS tubes (Falcon). The cells were washed with 1 ml PBS and the tubes were centrifuged at 1600 rpm for five minutes. The cells were resuspended in PBS for cell staining and cell counting with CountBright™ Absolute Counting Beads (Life Technologies).

#### 3.5.2. Lymph node and spleen harvest

Lymph nodes or spleens were mechanically homogenized in 500 μl PBS and filtered through the filter caps of 5 ml FACS tubes (Falcon). The cells were washed with 1 ml PBS and spun at 1600 rpm for 10 minutes. Spleen cells were subjected to an additional red blood cell lysis step using 0.2% sodium chloride solution and 1.6% sodium chloride solution. All cells were resuspended in R10 media and are counted using Trypan Blue (Gibco) or alternatively resuspended in PBS for cell staining and cell counting with CountBright™ Absolute Counting Beads (Life Technologies).

### 3.6. Bacterial load determination by CFU counts

The aliquoted mixture of the ear was diluted by 10-fold serial dilutions and plated on LB agar. The plates were incubated at 37°C for 18 hours and colonies were counted to calculate CFUs. *S. aureus* colonies are characterized as small, round, opaque, and cream-colored on the LB agar. Colony identification of *S. aureus* was verified by PCR.

### 3.7. PCR confirmation of *S. aureus* CFUs

Isolated colonies were picked from the LB agar plates and grown overnight in 5 ml of TSB at 37°C

with shaking (250 rpm). DNA isolation was done with the GeneJet Genomic DNA Purification Kit (ThermoFisher Scientific). PCR was performed using a PCR mix containing 20 U/µl *Taq* DNA Polymerase (ThermoFisher Scientific), 1X *Taq* Buffer (ThermoFisher Scientific), 0.67 mM $MgCl_2$, 5 mM deoxyribonucleotide triphosphate (dNTP) (Bio Basic), 16s RNA primers (forward, 5'-AGAGTTTGATCATGGCTCAG-3'; reverse, 5'-GGACTACCAGGGTATCTAA T-3'), and *S. aureus* nuclease (nuc) primers (forward, 5'-GCGATTGATGGTGATACGGTT-3'; reverse, 5'-ACGCAAGCCTTGACGAACTAAAGC-3'). The PCR program was carried out on a PTC-100 Peltier Thermal Cycler (Bio-Rad) and is as follows: i) 5 minutes predenaturation at 95°C, ii) 30 seconds denaturation at 95°C, iii) 30 seconds annealing at 55°C, iv) 30 seconds extension at 72°C, v) repeat steps ii-iv for a total of 30 cycles, and vi) 8 minutes final extension at 72°C. The PCR products were ran on a 2% agarose gel and visualized with ethidium bromide. A 279 bp band and a 796 bp band indicates the presence of the *16S* rRNA and *S. aureus nuc* gene respectively.

3.8. Bacterial load quantification by IVIS

Mice were transferred to the Goodman Cancer Center animal facility for *in vivo* imaging. Mice were anesthetized during the dye injection and imaging with isoflurane. Bacterial load was determined with the Xenolight Bacterial Detection Probe 750 (PerkinElmer). Each mouse received 10 µl of the respective dye administered intradermally at the base of the ear (below the site of infection). The bioluminescence of each probe was measured by IVIS spectrum with the filters set for excitation at 745nm and emission at 800nm.

3.9. Hematoxylin-Eosin histology evaluation of the pinna

Tissues were fixed for 24 hours in 4% PFA. Tissues were then transferred into cassettes and stored in 70% ethanol. Tissue processing, embedding, sectioning, and staining was performed by the McGill University Histology Core. Hematoxylin-Eosin (H&E) stained slides were sent to Charles River and scored blindly for inflammation and other microscopic changes by the pathologist, Dr. Theresa Albers.

### 3.10. Cell recruitment determined by flow cytometry staining

#### 3.10.1. Intracellular cytokine straining

Cells obtained from tissue digestions were washed once with PBS and were stained for viability by incubation with Zombie Aqua™ (Biolegend) for 20 minutes at 4°C. All incubations were done in the dark. Cells were washed once with FACS buffer, and cell surface staining for different molecules was done by incubation with anti-mouse CD16/CD32 (clone: 2.4G2, mouse BD Fc Block), and antibodies for Ly6G-FITC (clone: 1A8; eBioscience), CD11b-APC (clone: M1/70; BD), CD3-BUV395 (clone: 145-2C11; BD), CD4-PerCP-Cy5.5 (clone: RM4-5; BD), γδ TCR-BV605 (clone: GL3; Biolegend), CD45.2-Alexa Flour® 700 (clone: 104; Biolegend), F4/80-PE-Cy7 (clone: BM8 ; eBioscience), CD103-Alexa Flour 647(2E7; Biolegend), and CD44-APC-eFlour780 (clone: IM7; eBioscience) for 20 minutes at 4°C. Cells were washed once with FACS buffer. Cells were permeabilized with 200 µl of Cytofix/Cytoperm (BD) for 45 minutes at 4°C, and washed twice afterwards with Perm/Wash buffer (BD). Intracellular staining was done by incubating the samples with antibodies for IL-17A-BV421 (clone: TC11-18H10.1; Biolegend), IL-22-PE (clone: 1H8PWSR; eBioscience), and IFNγ-PE-eFluor610 (clone: XMG1.2; eBioscience) for 45 minutes at 4°C. The IFNγ antibody was only used in the absence of CD103 staining. Afterwards, cells were resuspended in 300 µl PBS containing CountBright™ Absolute

Counting Beads (Molecular Probes), and flow cytometry was performed using a BD LSRFortessa$^{TM}$ and BD FACSDIVA software. Data analysis was performed using FlowJo. Total cells were gated on first, and then single cells were gated on twice. Lastly, viable CD45$^{+}$ cells were gated from the single cells. The gating for the rest of the analysis was based on the staining and the populations of interest.

3.10.2. Intracellular staining for transcription factors

Viability and extracellular staining was done as mentioned above. Cell lineages were analyzed with the following antibodies: Ly6G-Pe-Cy7 (clone: 1A8; Biolegend), γδ TCR-BV605 (clone: GL3; Biolegend), CD3-BUV395 (clone: 145-2C11; BD), CD4-BUV737 (clone: GK1.5; BD), CD11b-BUV661 (clone: M1/70; BD), CD45.2-Alexa Flour® 700 (clone: 104; Biolegend), CD8-FITC (clone: 53-6.7; eBioscience) , CD103-Alexa Flour 647(2E7; Biolegend), and CD44-APC-eFlour780 (clone: IM7; eBioscience). The cells were fixed for 50 minutes at 4°C and stained Intracellularly for another 50 minutes at 4°C using the Transcription Factor Buffer Set (BD). All incubations were done in the dark. The intracellular antibodies used were RORγt-BV786 (clone: Q31-378; BD), Foxp3-PE-eFlour610 (clone: FJK-16s; eBioscience), GATA3-Alexa Flour® 647 (clone: 16E10A23; Biolegend), and T-bet-BV421 (clone: 4B10; Biolegend). The rest of the protocol was done as mentioned above in the intracellular staining and flow cytometry analysis.

3.11. Sorting of γδ T cells

Viability and extracellular staining was done as mentioned above on cells isolated from the ear or lymph nodes of mice 10 days after infection with *S. aureus*. The extracellular antibodies used were CD45.2-Alexa Flour® 700 (clone: 104; Biolegend), CD3-FITC (clone: 145-2C11; eBioscience),

and γδ TCR-BV605 (clone: GL3; Biolegend). Cells were resuspended in 300 µl of PBS. Single live cells were gated on, and the $CD45.2^+$, $CD3^+$, and γδ $TCR^+$ cells were sorted into Fetal Bovine Serum (FBS) using a BD FACSAria™ III. Sorted cells were centrifuged at 1600 rpm for 10 minutes and resuspended in R10 media.

### 3.12. Generation of heat-killed *S. aureus*

An overnight culture of *S. aureus* was made as described above. The following day, 1 mL of the overnight culture was transferred into an Eppendorf tube and three washes with PBS were performed as described above. Next, the pellet was suspended in 1 ml of PBS and the CFU concentration was determined by measuring the OD-600 nm. The bacteria were incubated at 100°C for 60 minutes. Following the heat-killing, the tube was spun once more at 9335 g for 15 minutes. The supernatant was discarded and the pellet was resuspended in PBS at a concentration of $10^9$ CFU/ml. Heat-killed bacteria were stored at 4°C until use.

### 3.13. *In vitro* stimulation of sorted γδ T cells

Spleen cells ($2x10^6$ cells/ml) from a naïve mouse were incubated with R10 media, heat killed $5x10^6$ CFU *S. aureus*, or heat-killed $5x10^6$ CFU *M. tuberculosis* (BD™ Difco™) for 2 hours at 37°C, 5% $CO_2$. Heat-killed *M. tuberculosis* was resuspended at a concentration of 4 mg/ml, and stored at 4°C. Isolated γδ T cells ($2x10^4$ cells/ml) were added to the spleen cells and were incubated for 72 hours at 37°C, 5% $CO_2$. Afterwards, the supernatant was removed and stored at -20°C for ELISA analysis.

### 3.14. RNA isolation and RT-qPCR

RNA was extracted from homogenized ear samples or sorted γδ T cells by using an RNA Miniprep Super Kit (Bio Basics). The RNA concentration obtained was quantified using Nanodrop. Normalized levels of RNA (100 ng) underwent reverse transcription into cDNA by using a High Capacity cDNA Reverse Transcription Kit (AB Applied Biosystems™). The RT program was run on a PCR Thermocycler and the steps are as follows: 10 minutes at 25°C, 120 minutes at 37°C, and 10 minutes at 85°C. The generated cDNA underwent a threefold dilution and was stored at -20°C. Afterwards, 2 µl of cDNA was used as a template for real-time PCR using the SsoAdvanced Universal SYBR Green Supermix (Bio-Rad). RT-qPCR was performed on a CFX96 Touch™ Real-Time PCR Detection System (Bio-Rad) and the protocol is as follows: i) three minutes denaturation at 95°C, ii) 15 seconds at 95°C, iii) 30 seconds at 60°C, iv) plate read, v) repeat steps i-iv 39 times, and vi) melting curve analysis from 55°C to 95°C reading the plate every 0.5°C. The reference genes used are *B2m* (forward, 5'- ACCCGCCTCACATTGAAATCC-3'; reverse, 5'-CGATCCCAGTAGACGGTCTTG-3'), *Tbp* (forward, 5'-AACAGCCTTCCACCTTATGC-3'; reverse, 5'-TGCTGCTGCTGTCTTTGTTG-3'), and *Hprt* (forward, 5'-AGTCCCAGCGTCGT GATTAG-3'; reverse, 5'-CAGAGGGCCACAATGTGATG-3'). The best reference genes for each cell type were chosen after analysis using geNorm. Cytokines measured by qPCR were *Il17a* (forward, 5'-TTTAACTCCCTTGGCGCAAAA-3'; reverse, 5'-CTTTCCCTCCGCATTGA CAC-3'), *ifnγ* (forward, 5'-TGGCTTTGCAGCTCTTCCTC-3'; reverse, 5'-GCCAGTTCCTCCA GATATCC-3'), and *Il10* (forward, 5'-AGAAGCATGGCCCAGAAATC-3'; reverse, 5'-ATGGCCT TGTAGACA CCTTG-3'). Chemokines measured by qPCR were *cxcl2* (forward, 5'-CACCAACCACCAGGCTACAG-3'; reverse, 5'CGCCCTTGAGAGTGGCTATG-3'), *ccl2* (forward, 5'TCACCTGCTGCTACTCATTC-3'; reverse, 5'-TCTGGACCCATTCCTTCTTG-3'), and *cxcl9* (forward, 5'-CCCTCAAAGACCTCAAACAG-3'; reverse, 5'-TCTTCACATTT

GCCGAGTCC-3'). Additionally, the antimicrobial *cramp* (forward, 5'-AGTCCCTAGAC ACCAATCTC-3'; reverse, 5'-TGCCACATACAGTCTCCTTC-3') was measured by qPCR. Lastly, the Vγ chains measured by qPCR were *Vγ1.1* (forward, 5'-TTCTGCTGCCTCTGG GTTTTT-3'; reverse, 5'-TCCCTCCTAAGGGTCGTTGAT-3'), *Vγ2* (forward, 5'-TTGGTACCGGCAAAAAACAAATCA-3'; reverse, 5'-CAATACACCCTTATGACATCG-3'), *Vγ3* (forward, 5'-TTGCAAGCTCTCTGGGGTTC-3'; reverse, 5'-GGCACAGTAGTA CGTGGCTT-3'), *Vγ4* (forward, 5'-GGAAGCAGTCTCACGTCACC-3'; reverse, 5'-CTGCCA TGTCCTTGCCTCATA-3'), and *Vγ5* (forward, 5'-GATCCAACTTCGTCAGTTCCACAAC-3'; reverse, 5'-AAGGAGA CAAAGGTAGGTCCCAGC-3').

3.15. Cytokine determination by enzyme-linked immunosorbent assay (ELISA)

Cytokine levels in culture supernatants of re-stimulated sorted γδ T cells were determined with the use of the IL-17A Ready-Set-Go!® ELISA kit (eBioscience). Plates were read on a 680 microplate reader (Bio-Rad) at 450 nm with the use of 570 nm as a reference wavelength.

3.16. Statistics

Statistical analysis was done using the software GraphPad Prism. Two-way analysis of variance (ANOVA) and multiple Student's t test were used to measure significance between the experimental groups. Statistical significance was set at $p < 0.05$, where * signifies $p < 0.05$, ** signifies $p < 0.01$, and *** signifies $p < 0.001$. Cytokine levels measured by ELISA and cell populations measured by flow were expressed as means and standard error of the mean (SEM). Ear thickness is graphed as interleaved box and whiskers. Each dot on the dot plots represents the value for each individual mouse.

# 4. Results

## 4.1. Aim 1: Determine if AHR is necessary for *S. aureus* clearance during a cutaneous infection

### 4.1.1. AHR is not needed for the clearance of *S. aureus* after a single exposure

To begin identifying whether AHR is required for protection against *S. aureus* cutaneous infection, we first studied a single low dose *S. aureus* infection murine model. We choose the isolate S8 for our model, because of its strong pro-inflammatory and anti-inflammatory properties (83). WT and AHR KO mice were administered S8 on day 0 and monitored until day 8 post infection. There was no observed difference in ear swelling between the mice (Figure 4.1 a). The bacterial burden was determined as described in section 3.6. The CFU counts illustrated that the bacterial burden of both mouse strains steadily decreased at an identical rate (Figure 4.1 b). Interestingly, *S. aureus* CFUs could still be detected from both mouse strains on day 8.

Since *S. aureus* CFUs were still detected on day 8, we next tested whether the bacteria would be eventually cleared or not. In order to test whether colonization was occuring, we administered $5x10^6$ CFUs of S8 to both WT and AHR KO mice and monitored them until day 21 post infection. Mice were euthanized on day 21 and the supernatant of the homogenized ears was cultured overnight on LB agar. Cultured CFUs from the supernatants of both S8 and PBS treated mice appeared large, yellow, and filamentous (Figure. 4.2 a). In addition, the WT mice had more of these bacteria present on their skin (Figure 4.2 b). To confirm that these CFUs were not *S. aureus*, we performed *16s* and *S. aureus nuclease* (*nuc*) PCR amplification on the colonies. As a positive control, we also did PCR amplification of the S8 strain used during the injections. PCR

amplification of a 796 bp *16s* product is indicative of bacterial origin, and amplification of a 165 bp *nuc* product is indicative of *S. aureus*. All of the PCR products contained a large *16s* band (Figure 4.2 c). However, the colonies grown on day 21 did not have detectible *nuc* as indicated by the lack of a second smaller band. As expected, the PCR products of the S8 strain contained the second smaller *nuc* band. Therefore, these results suggest that both WT and AHR KO mice are able to clear a single low dose *S. aureus* infection equally well.

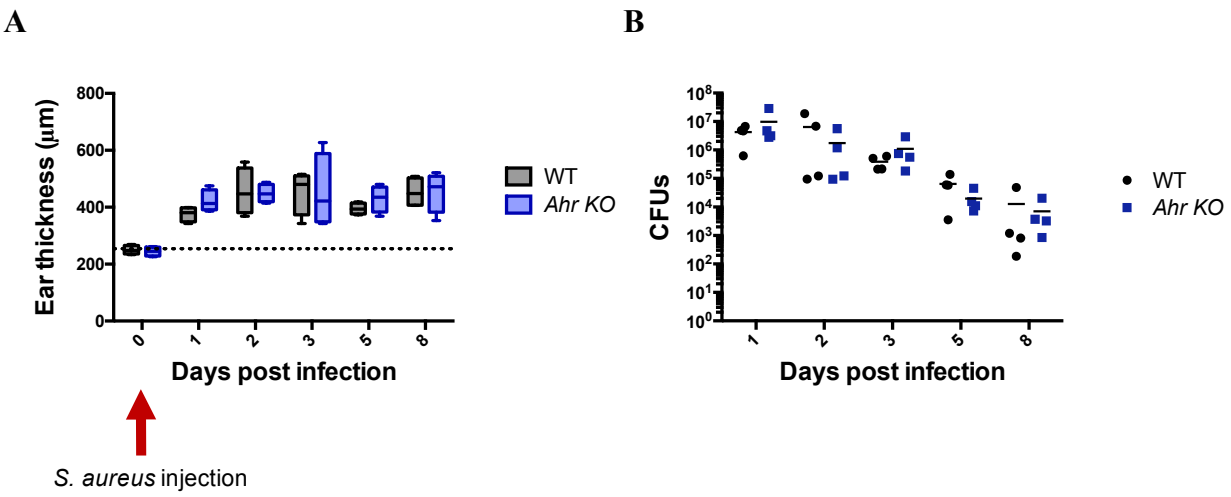


**Figure 4.1: Ear thickness and bacterial burden after the administration of a single low *S. aureus* dose.** Mice were administered 5x$10^6$ CFUs of S8 intradermally on day 0 (red arrow) and monitored until day 8 post infection. A) Ear thickness of S8 injected mice was measured on day 0, 1, 2, 3, 5, and 8 (n = 4). The dotted line represents the line of best fit for the ear thickness of the PBS injected mice (n = 5). Whiskers represent the maximum and minimum values. B) *S. aureus* CFUs (small, round, opaque, and cream-colored colonies) cultured overnight on LB agar from ear supernatants at day 1, 2, 3, 5, and 8 post infection. No colonies were cultured from the supernatants of PBS injected mice. The data shown are representative of two independent experiments.

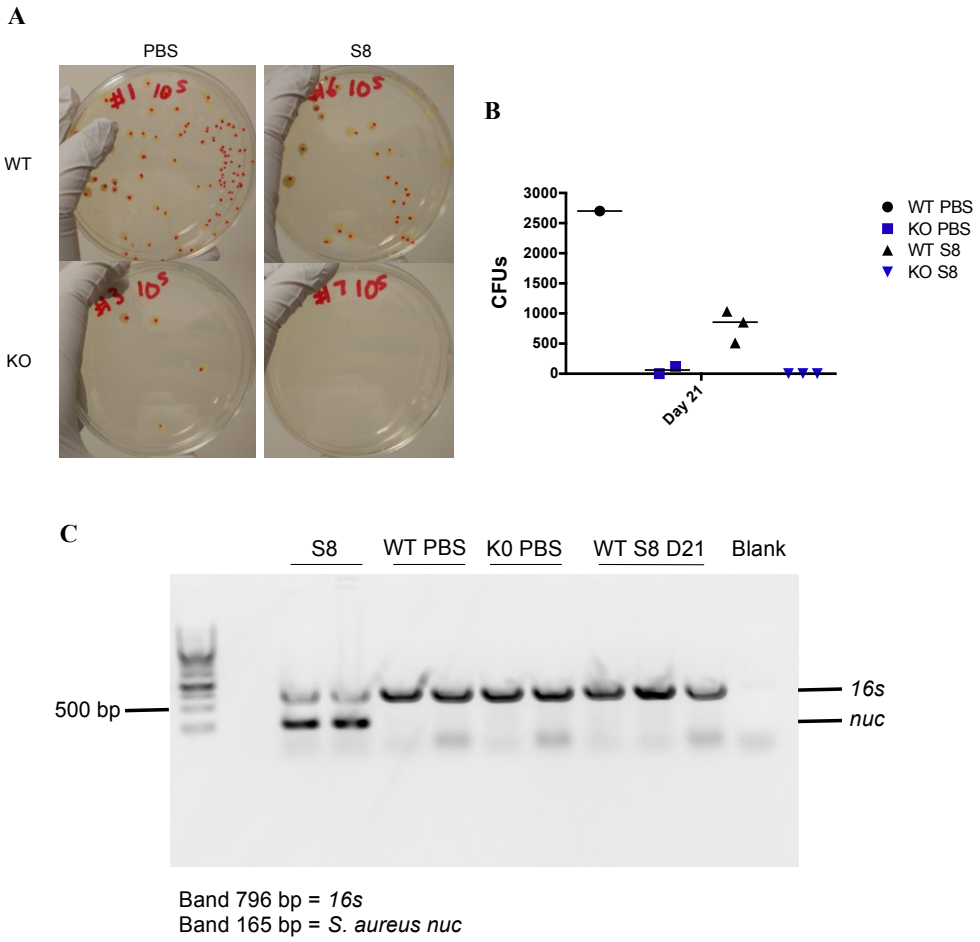


**Figure 4.2: Bacteria cultured 21 days post administration of a single low *S. aureus* dose.** Mice were administered 5x$10^6$ CFUs of S8 intradermally on day 0 and monitored until day 21. A) Large, yellow, and filamentous CFUs were cultured overnight on LB agar from ear supernatants at day 21. B) Total CFU counts on day 21 post infection from the supernatant of WT mice treated with PBS (n = 1) and S8 (n = 3), and AHR KO mice treated with PBS (n = 2) and S8 (n = 3). C) S8 and colonies from panel A were grown overnight and used for *16s* and *nuc* PCR amplification. PCR products were run on a 2% agarose gel and visualized with ethidium bromide. The presence of a 796 bp *16s* band is indicative of bacterial species. The presence of a 165 bp *nuc* band is indicative of *S. aureus*. The data shown are representative of a single independent experiment.

### 4.1.2. AHR is not needed for the clearance of *S. aureus* after prolonged exposure

In our single and low dose model, only minor ear swelling was observed and the bacterial burden started decreasing as early as day 2. Additionally, there was no significant difference between the WT and AHR KO mice. Therefore, we wanted to test if AHR would be protective under increased and prolonged *S. aureus* exposure. In order to test this, we administered $5x10^6$ CFUs of S8 intradermally on days 0, 1, and 2 to both WT and AHR KO mice. Bacterial burden was measured in parallel on day 3 by In Vivo Imaging Systems (IVIS) and CFU counts. Isoflurane anesthetized mice were administered a bacterial probe below the ear. Mice were imaged, and both WT and AHR KO mice had the same level of fluorescence detected (Figure 4.3 a and b). Mice were then euthanized and the supernatant of the homogenized ear samples was cultured overnight on LB agar. Again, no difference was observed in the *S. aureus* CFU counts between WT and AHR KO mice on day 3 (Figure 4.3 c).

In order to test if the level of clearance would be different among WT and AHR KO mice, both strains were administered $5x10^6$ CFUs of S8 intradermally on days 0, 1, and 2. Mice were euthanized on day 0, 1, 2, 3, 5, 9, and 21 in order to culture the supernatant from the homogenized ears (Figure 4.4 a). Prior to S8 administration (day 0), no *S. aureus* CFUs were detected, confirming that these mice are not natural reservoirs of *S. aureus*. Once S8 was administered, the bacterial burden remained relatively constant for about 5 days (Figure 4.4 a). After day 5, the bacterial burden started to decrease at an identical rate between both WT and AHR KO mice. However, at day 21 *S. aureus* could still be detected in half of the WT and AHR KO mice by CFU counting (Figure 4.4 a). The presence of *S. aureus* was confirmed by PCR performed on the cultured CFUs (Figure 4.4 b and c).

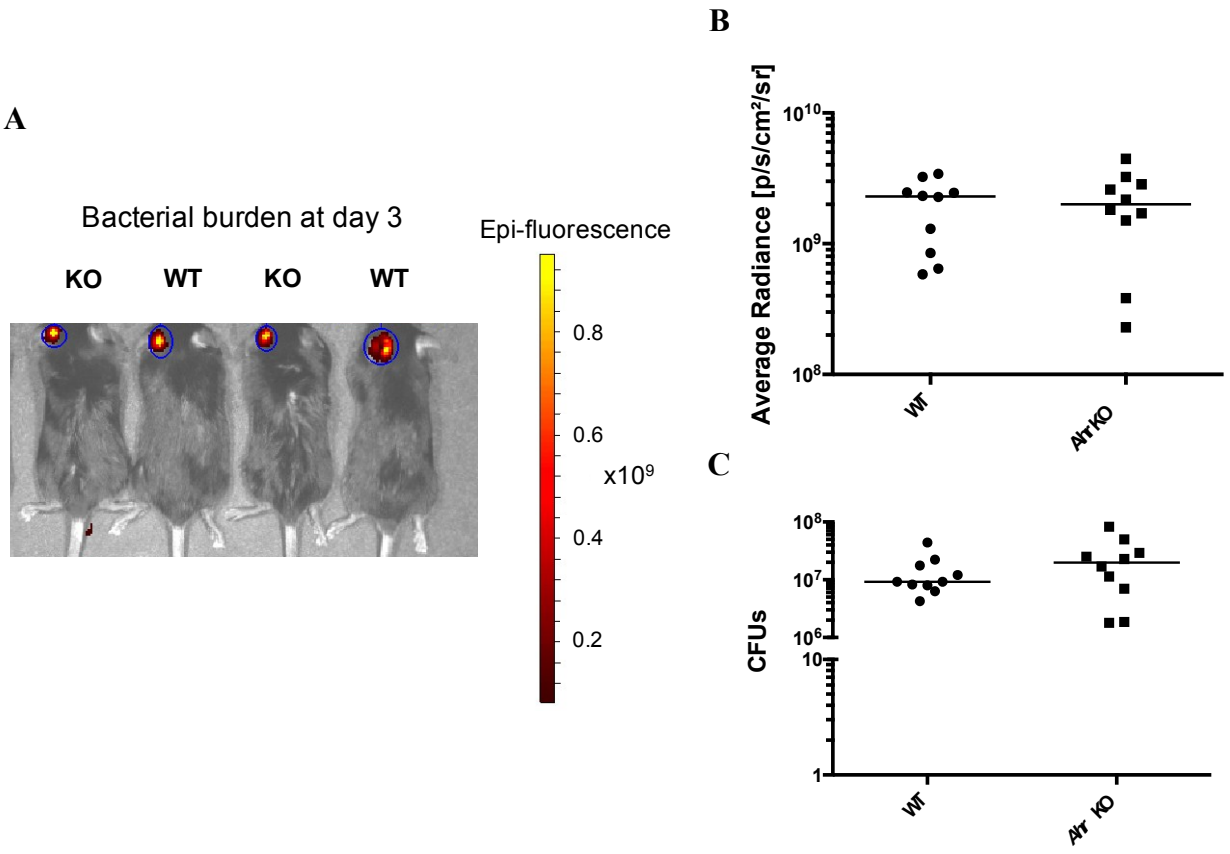


**Figure 4.3: Bacteria burden at day 3 post prolonged *S. aureus* exposure.** Mice were administered 5x10$^6$ CFUs of S8 intradermally on days 0, 1, and 2. A) Fluorescence of Xenolight Bacterial Detection Probe 750 (PerkinElmer) at 800 nm was measured 5-10 minutes after administration. C) The fluorescence intensity was measured as the average radiance for both mouse strains (n = 10). D) Ear supernatant was cultured overnight on LB Agar and *S. aureus* CFUs were counted the next day (n = 10). The data shown are representative of three independent experiments.

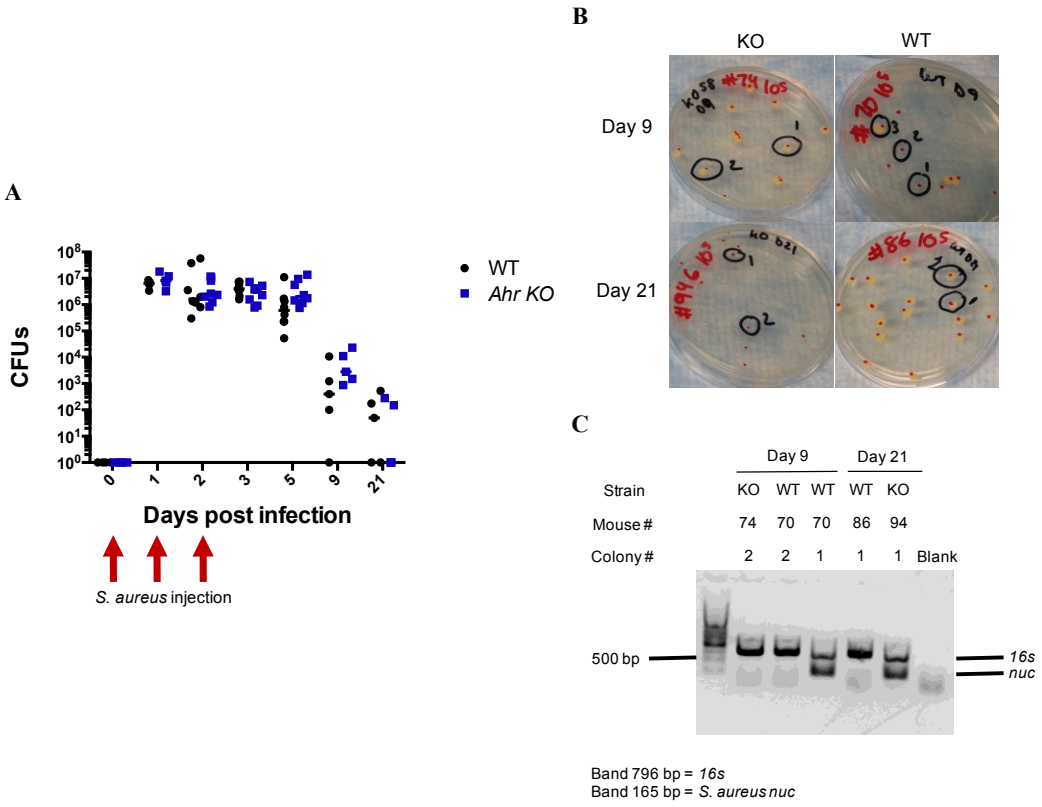


**Figure 4.4: Bacteria burden during prolonged *S. aureus* exposure.** Mice were administered 5x10$^6$ CFUs of S8 intradermally on days 0, 1, and 2 (red arrows). A) *S. aureus* CFUs cultured overnight on LB agar from ear supernatants on day 0 (n = 4), 1 (n = 5), 2 (n = 8), 3 (n = 8), 5 (n = 8), 9 (n = 5), 21 (n = 5) post infection. Day 0 samples were obtained prior to the administration of S8. No *S. aureus* colonies were detected on day 0 prior to an injection (n = 4), and on day 21 PBS injected mice (n = 4). B) Both *S. aureus* CFUs and unknown large, yellow, and filamentous CFUs were cultured overnight on LB agar from ear supernatants at day 9 (n = 5) and 21 (n = 5). C) Colonies grown from the supernatants on day 9 and 21 were used for *16s* and *nuc* PCR amplification. PCR products were run on a 2% agarose gel and visualized with ethidium bromide. The presence of a 796 bp *16s* band is indicative of a bacterial species, and a 165 bp *nuc* band is indicative of *S. aureus*. The data shown are representative of two independent experiments.

### *4.1.3.* AHR-deficient mice have decreased acute inflammation after prolonged exposure to *S. aureus*

Although AHR-deficiency did not affect the clearance rate of *S. aureus*, we wanted to test if AHR was required for disease tolerance to *S. aureus*, as defined by less inflammation documented by ear swelling and redness. Again, we administered $5x10^6$ CFUs of S8 intrademally on days 0, 1, and 2 to both WT and AHR KO mice. Ear redness and swelling (two signs of acute inflammation) were monitored for 21 days. The ears of WT mice had increased redness and morphological changes (crusting of the ear) compared to AHR KO mice (Figure 4.5 a-c). However, representative H&E stains of cross sections of WT and AHR KO show no microscopic differences between the two mouse strains on day 3 (Figure 4.5 d and e). Additionally, independent blind pathology scoring of the H&E slides (5 per group) indicated no significant differences in the severity of the microscopic lesions on day 3 (Table 4.1). Nevertheless, during the course of *S. aureus* infection WT mice had significantly ($p>0.001$) increased ear thickness compared to AHR KO mice on days 1, 2, 3, 5, and 9 as measured by a micrometer gauge (Figure 4.5 f). In conclusion, AHR is not needed for the clearance of *S. aureus* but may be involved in preventing disease tolerance to this microbe.

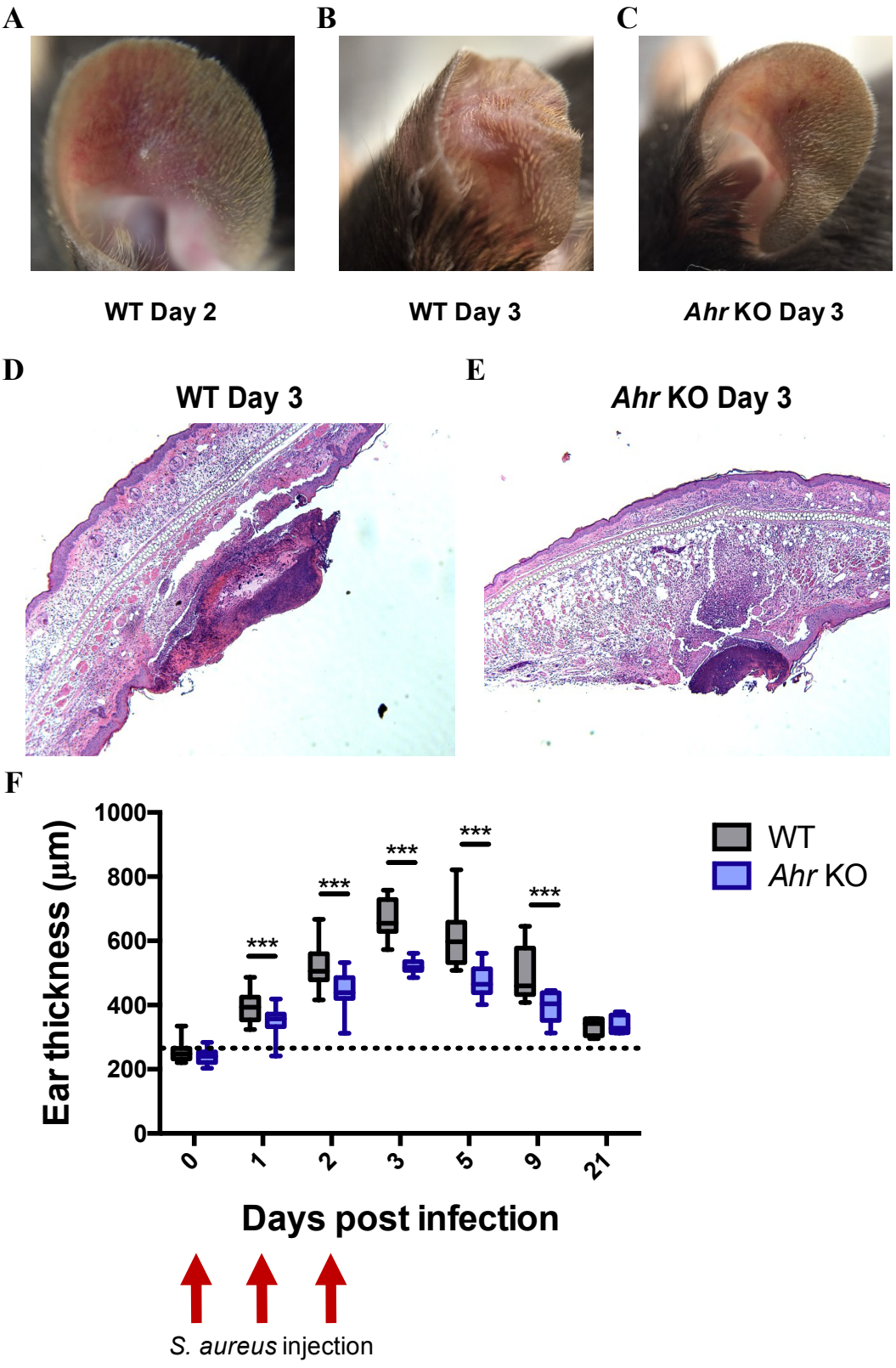
A
B
C
WT Day 2
WT Day 3
*Ahr* KO Day 3
D
WT Day 3
E
*Ahr* KO Day 3
F
Ear thickness (µm)
1000
800
600
400
200
0
***
***
***
***
***
0
1
2
3
5
9
21
Days post infection
WT
*Ahr* KO
*S. aureus* injection

**Figure 4.5: Ear redness, histology, and swelling post prolonged *S. aureus* exposure.** Mice were administered $5x10^6$ CFUs of S8 intradermally on days 0, 1, and 2 (red arrows). A) Representative image of a WT ear on day 2. B) Representative image of a WT ear on day 3. C) Representative image of a AHR KO ear on day 3. D) Representative H&E stains of cross sections of WT and AHR KO ears on day 3. F) Ear swelling of S8 infected mice was measured on days 0 (n = 42), 1 (n = 38), 2 (n = 33), 3 (n = 8), 5 (n = 8), 9 (n = 5), and 21 (n = 5). Ear swelling of the PBS injected group was measured on days 0, 1, 2 and 21 (n = 4). The dotted line represents the line of best of the ear thickness of PBS treated mice. The data shown are representative of two independent experiments. The whiskers represent the maximum and minimum values, $P<0.001$ = ***.

**Table 4.1: Ear pathology scores at day 3 of a *S. aureus* cutaneous infection.** Blind scoring of representative H&E stains of cross sections of WT and AHR KO mice on day 3 after prolonged exposure to *S. aureus* (n = 5 pooled from 2 independent experiments). All microscopic changes were graded for severity on a scale of 0-4.

| Pathology ID | 1 | 2 | 3 | 4 | 5 | 6 | 7 | 8 | 9 | 10 |
|---|---|---|---|---|---|---|---|---|---|---|
| Strain | C56Bl/6 | C56Bl/6 | C56Bl/6 | AHR -/- | AHR -/- | AHR -/- | C56Bl/6 | C56Bl/6 | AHR -/- | AHR -/- |
| Age (weeks) | 6 | 6 | 6 | 6 | 6 | 6 | 7 | 7 | 9 | 9 |
| Sex | Female | Female | Female | Female | Female | Female | Female | Female | Female | Female |
| Pinna-Microscopic changes | | | | | | | | | | |
| Extent of pinnal lesion | 3 | 2 | 2 | 2 | 2 | 3 | 3 | 3 | 2 | 2 |
| Thickness of pinna (mm) | 0.75 | 1.0 | 0.95 | 0.65 | 0.90 | 0.9 | 0.9 | 0.6 | 0.75 | 0.55 |
| Neutrophilic inflammation | 3 | 3 | 3 | 3 | 3 | 3 | 3 | 3 | 3 | 3 |
| Abscess, dermal | 1 | 2 | 3 | 2 | 2 | 2 | 3 | 3 | 2 | 1 |
| Ulcer | 3 | 3 | 3 | 3 | 3 | 4 | 2 | 3 | 3 | 1* |
| Edema | 2 | 3 | 3 | 3 | 3 | 4 | 2 | 2 | 3 | 3 |
| Bacteria | + | + | + | + | + | + | + | + | + | + |

Key: Extent of pinna lesion: 0 = no lesion, 1 = 1/3 pinna affected; 2 = 2/3 pinna affected; 3 = entire pinna affected.
*= thinning of epithelium with serocellular crusting, but no frank ulceration. 1 = minimal, 2 = mild, 3= moderate, 4= marked severity.

## 4.2. Aim 2: Establish the cellular response to *S. aureus* infection in the presence and absence of AHR expression

### *4.2.1.* AHR-deficient mice have reduced cutaneous T cells

AHR KO mice have already been reported to have immune cell impairment (99). Therefore, before investigating the cutaneous immune response of these mice we needed to identify the differences in the resident immune cells of naïve WT and AHR KO mice. Ears of naïve WT and AHR KO mice were enzymatically digested and analyzed by flow cytometry. The only cellular difference observed between the two mouse strains was a drastic decrease in the frequency of resident $CD3^+$ T cells in AHR KO mice (Figure 4.6 a). When analyzing the subset T cell populations, the γδ $TCR^+$ cells accounted for the majority of these cells in WT mice. Additionally, the AHR KO mice had reduced frequencies of γδ $TCR^+$ cells, in particular the γδ $TCR^{hi}$ population (~20% AHR KO vs ~60% WT) (Figure 4.6). It is important to note that the γδ $TCR^{int}$ is heavily comprised of dermal γδ T cells mainly responsible for the production of IL-17A, while γδ $TCR^{hi}$ is comprised of mostly epidermal γδ T cells (121).

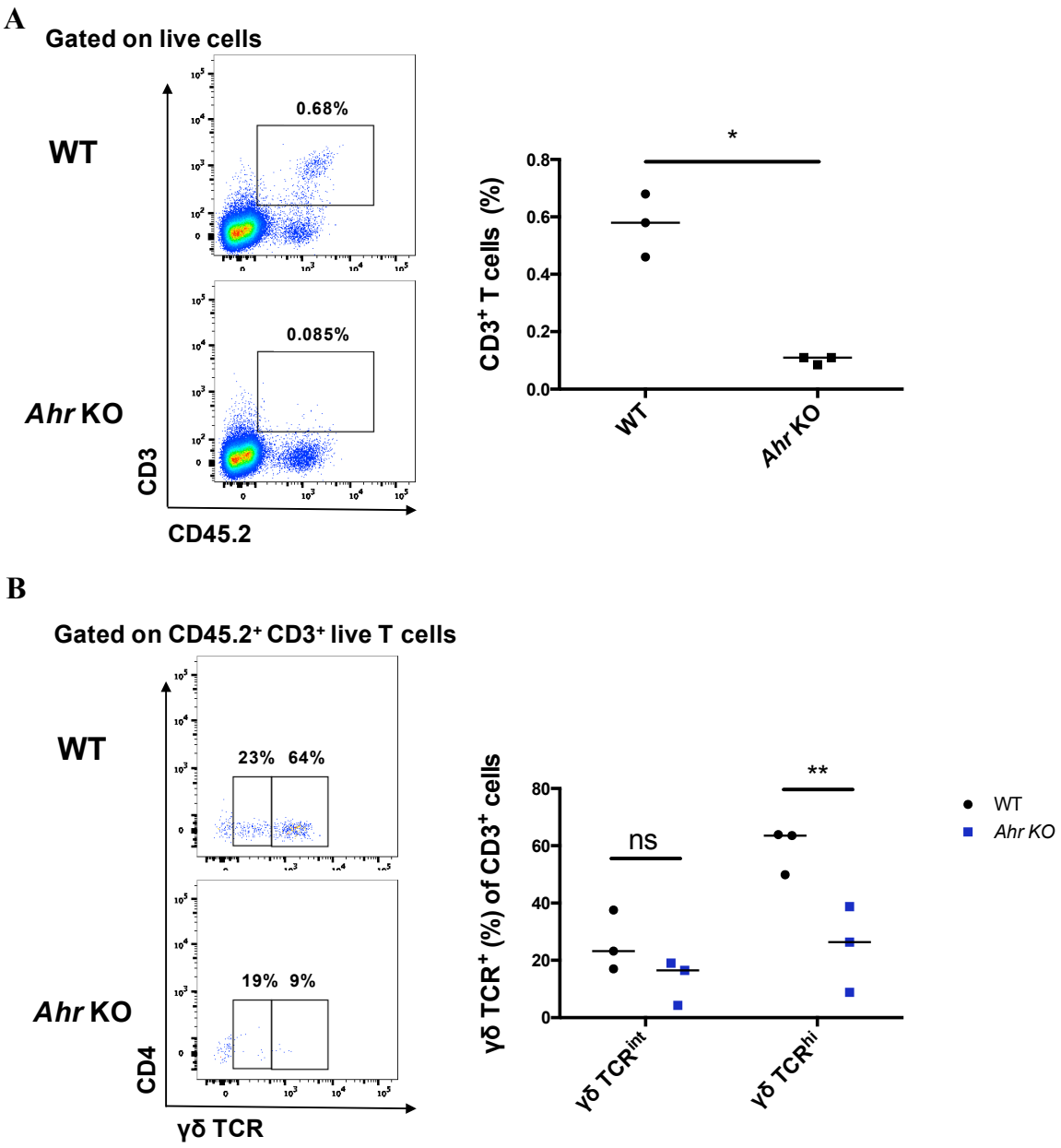


**Figure 4.6: Local T cells in the ear of naïve WT and AHR KO mice.** T cell populations localized in the ear of non-infected mice were analyzed by flow cytometry. A) Frequency of $CD3^+$ T cells in WT and AHR KO mice. B) Frequency of γδ $TCR^+$ within the $CD3^+$ T cell population of WT and AHR KO mice. The data shown are representative of a single independent experiment. $P<0.05$ = *, and $P<0.01$ = **.

### 4.2.2. AHR-deficient mice have preserved neutrophil recruitment

In order to test the cutaneous immune response to *S. aureus* in AHR-deficient mice, both WT and AHR KO mice were administered $5x10^6$ CFUs of S8 intradermally on days 0, 1, and 2. Ears were harvested and enzymatically digested on days 0, 1, 2, 3, 5, 9, and 21 in order to analyze the infiltrating cells by flow cytometry. As expected, neutrophils, identified as $Ly6G^+$ and $CD11b^+$, accounted for about 50% of the infiltrating cells during the first 3 days of infection and started to decrease afterwards (Figure 4.7 a). Similarly, macrophage ($CD11b^+$ and $F4/80^+$) numbers also increased during the first 3 days of infection (up to $5x10^4$ cells per ear) and then decreased (Figure 4.7 b). There were no significant differences in the neutrophil frequencies or absolute numbers recruited to the site of infection between WT mice and AHR KO mice. Although the macrophage frequency was slightly higher in the AHR KO mice during the infection, the absolute macrophage numbers between the mice strains were very similar, with the exception of day 3 where WT mice transiently had a higher number of macrophages. Therefore, these data indicate that the granulocyte recruitment at the site of infection is occuring properly in the AHR-deficient mice.

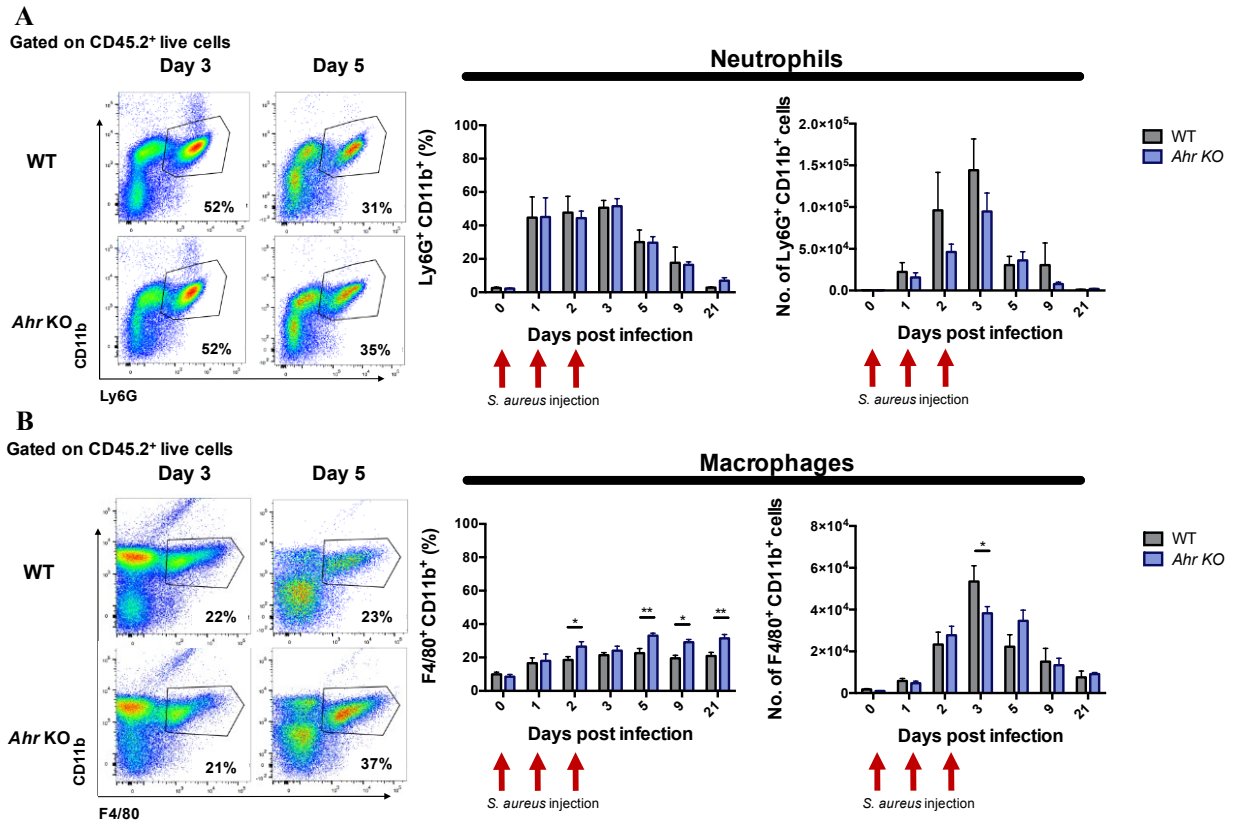


**Figure 4.7: Neutrophil and macrophage recruitment at the site of *S. aureus* infection.** Mice were administered 5x10$^6$ CFUs of S8 intradermally on days 0, 1, and 2 (red arrows). Cell infiltration was analyzed by flow cytometry on days 0 (n = 4), 1 (n = 5), 2 (n = 8), 3 (n = 8), 5 (n = 8), 9 (n = 5), and 21 (n = 5). A) Graphical representation of the CD45.2$^+$ CD11b$^+$ Ly6G$^+$ population at day 3 (left), the summarized frequencies (middle) and absolute neutrophil numbers (right). B) Graphical representation of the CD45.2$^+$ CD11b$^+$ F4/80$^+$ population at day 3 (left), the summarized frequencies (middle) and absolute macrophage numbers (right). Data are representative of two independent experiments. Error bars represent the SEM, P<0.05 = *, and P<0.01 = **.

### 4.2.3. AHR-deficient mice have impaired γδ T cell expansion

Since there was a difference in the cutaneous T cell populations of WT and AHR KO mice under basal conditions, we next analyzed these populations during an *S. aureus* infection. WT and AHR KO mice were administered $5x10^6$ CFUs of S8 intradermally on days 0, 1, and 2. Ears were harvested and enzymatically digested on days 0, 1, 2, 3, 5, 9, and 21 in order to analyze the T cell populations by flow cytometry. CD3, CD4, γδ TCR fluorescence minus ones (FMOs) were used to determine the proper gating strategy (Figure 4.8 a and b). On day 3, there was a slight decrease in the proportion T cells in the AHR KO mice (~6% AHR KO vs ~11% WT), and by day 9 this difference became more significant (~17% AHR KO vs ~30% WT) (Figure 4.8 c). Similarly, the proportion of γδ T cells in AHR KO mice was significantly lower than in WT mice on day 9 (Figure 4.8 d). During the infection, the absolute numbers of T cells drastically increased in WT mice at day 3, and remained high until the experimental end point, day 21 (Figure 4.8 e). This increase in T cells was absent in the AHR KO mice. When looking into the different T cell populations, the CD4 T cell number was transiently higher in WT mice on days 3 and 9 (Figure 4. 8 f). However, the γδ T cell population in the WT mice started to increase from ~5% on day 2 to ~25% on day 5, mimicking the increase seen in the overall T cell population (Figure 4.8 g). The increased γδ T cell numbers were maintained until day 21 and were absent in the AHR KO mice.

To further characterize the role of the increased T cells, we examined the production of cytokines by intracellular staining and flow cytometry. IL-17A and IL-22 FMOs were used to determine the proper gating strategy (Figure 4.9 a). The γδ $TCR^{int}$ population were positive for IL-17A, and the proportion of these cells increased from day 3 to day 9 (Figure 4.9 b). Overall, there

were 3 to 5 times more IL-17A$^{+}$ γδ T cells in the WT mice than the AHR KO mice, and these cells increased from 5x10$^{2}$ cells per ear on day 5 to 1.25x10$^{3}$ cells per ear on day 9 during the infection (Figure 4.9 d). In contrast, the IL-22$^{+}$ γδ T cells in the WT mice peaked at day 3 and decreased afterwards (Figure 4.9 c and d). There was no significant difference in IL-22$^{+}$ CD4 and IL- 17$^{+}$ CD4 T cell populations between WT and AHR KO mice (Figure 4.9 e).

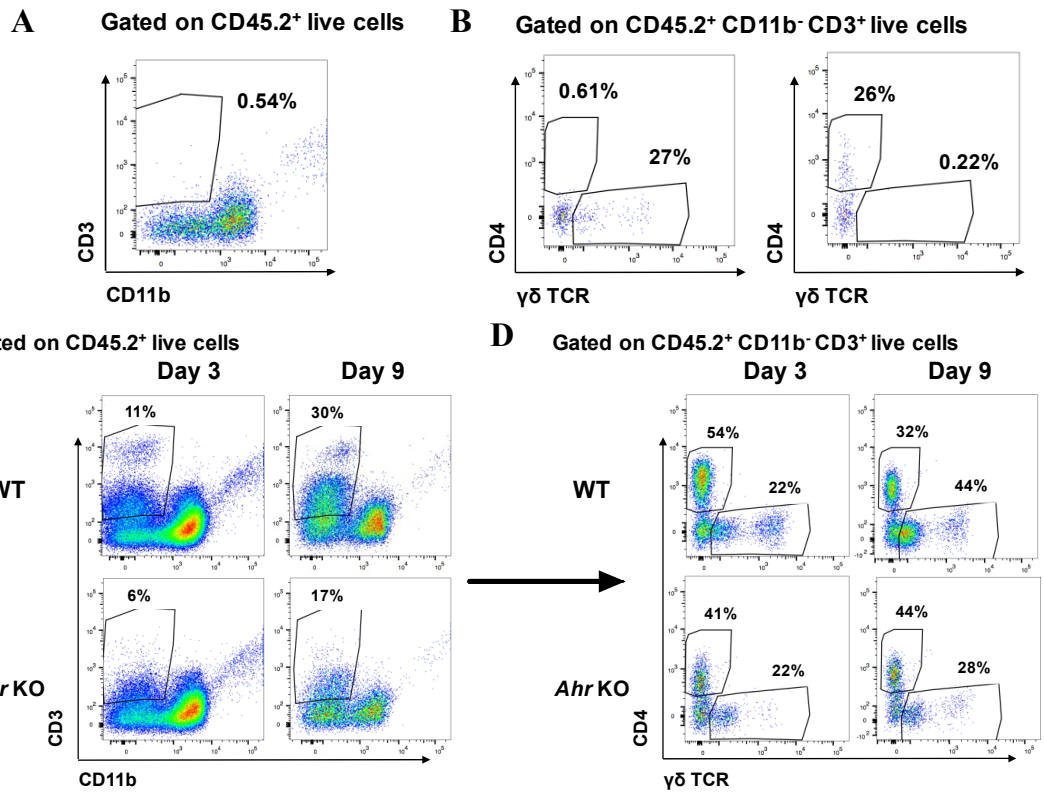
A
Gated on CD45.2+ live cells
0.54%
CD3
CD11b
B
Gated on CD45.2+ CD11b- CD3+ live cells
0.61%
27%
26%
0.22%
CD4
γδ TCR
C
Gated on CD45.2+ live cells
Day 3
Day 9
WT
Ahr KO
11%
30%
6%
17%
CD3
CD11b
D
Gated on CD45.2+ CD11b- CD3+ live cells
Day 3
Day 9
WT
Ahr KO
54%
22%
32%
44%
41%
22%
44%
28%
CD4
γδ TCR

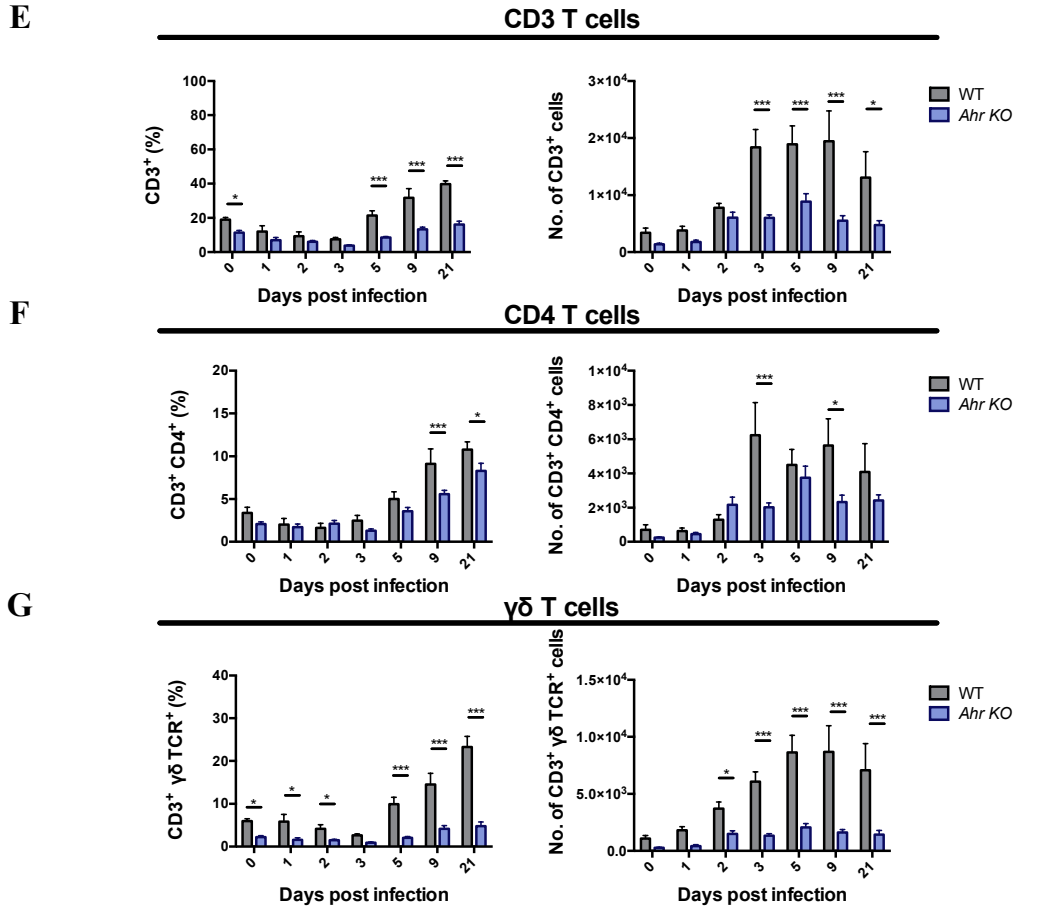
E
CD3 T cells
CD3+ (%)
No. of CD3+ cells
Days post infection
WT
Ahr KO
F
CD4 T cells
CD3+ CD4+ (%)
No. of CD3+ CD4+ cells
Days post infection
WT
Ahr KO
G
γδ T cells
CD3+ γδ TCR+ (%)
No. of CD3+ γδ TCR+ cells
Days post infection
WT
Ahr KO

**Figure 4.8: T cell recruitment at the site of *S. aureus* infection**. Mice were administered $5x10^6$ CFUs of S8 intradermally on days 0, 1, and 2 (red arrows). Flow cytometry was used to analyze the T cell populations in the ear of WT and AHR KO mice on days 0 (n = 4), 1 (n = 5), 2 (n = 8), 3 (n = 8), 5 (n = 8), 9 (n = 5), and 21 (n = 5). A) Graphical representation of the $CD45.2^+$ $CD3^+$ $CD11b^-$ cells in the CD3 FMO control. B) Graphical representation of the γδ $TCR^+$ $CD4^-$ and γδ $TCR^-$ $CD4^+$ populations in CD4 FMO (left) and γδ TCR FMO (right) controls. C) Graphical representation of the $CD45.2^+$ $CD3^+$ $CD11b^-$ cells in the ear at day 3 and 9. D) Graphical representation of the γδ $TCR^+$ $CD4^-$ and γδ $TCR^-$ $CD4^+$ populations at day 3 and 9. E) Summarized frequencies of the $CD45.2^+$ $CD3^+$ $CD11b^-$ cells are on the left, and the absolute CD3 T cell numbers are on the right. F) Summarized frequencies of the $CD45.2^+$ $CD3^+$ $CD11b^-$ γδ $TCR^-$ $CD4^+$ cells are on the left, and the absolute γδ T cell numbers are on the right. G) Summarized frequencies of the $CD45.2^+$ $CD3^+$ $CD11b^-$ γδ $TCR^+$ $CD4^-$ cells are on the left, and the absolute CD4 T cell numbers are on the right. The data shown are representative of two independent experiments. Error bars represent the SEM, $P<0.05$ = *, $P<0.01$ = **, and $P<0.001$ = ***.

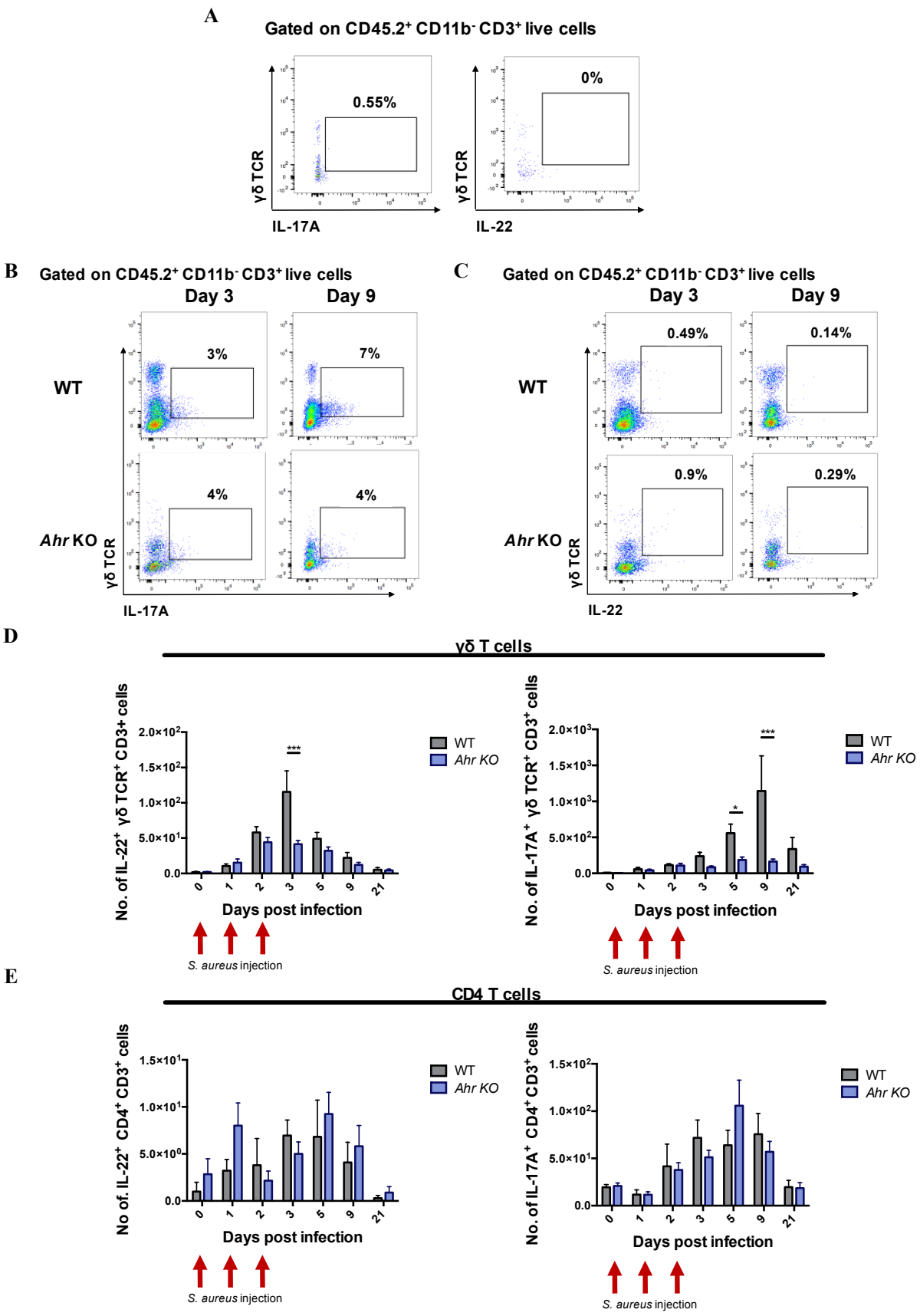
A
Gated on CD45.2+ CD11b- CD3+ live cells
0.55%
0%
γδ TCR
IL-17A
IL-22
B
Gated on CD45.2+ CD11b- CD3+ live cells
Day 3
Day 9
WT
Ahr KO
3%
7%
4%
4%
γδ TCR
IL-17A
C
Gated on CD45.2+ CD11b- CD3+ live cells
Day 3
Day 9
WT
Ahr KO
0.49%
0.14%
0.9%
0.29%
γδ TCR
IL-22
D
γδ T cells
No. of IL-22+ γδ TCR+ CD3+ cells
No. of IL-17A+ γδ TCR+ CD3+ cells
WT
Ahr KO
Days post infection
S. aureus injection
E
CD4 T cells
No of. IL-22+ CD4+ CD3+ cells
No. of IL-17A+ CD4+ CD3+ cells
WT
Ahr KO
Days post infection
S. aureus injection

**Figure 4.9: T cell production of IL-17A and IL-22 during a *S. aureus* infection.** Mice were administered $5x10^6$ CFUs of S8 intradermally on days 0, 1, and 2 (red arrows). Flow cytometry was used to analyze intracellular cytokines in the ear of WT and AHR KO mice on days 0 (n = 4), 1 (n = 5), 2 (n = 8), 3 (n = 8), 5 (n = 8), 9 (n = 5), and 21 (n = 5). A) Graphical representation of the the $CD45.2^+$ $CD3^+$ $CD11b^-$ γδ $TCR^+$ $CD4^-$ $IL\text{-}17A^+$ population in the IL-17A FMO (left) and $CD45.2^+$ $CD3^+$ $CD11b^-$ γδ $TCR^+$ $CD4^-$ $IL\text{-}22^+$ population in the IL-22 FMO (right). B) Graphical representation of the the $CD45.2^+$ $CD3^+$ $CD11b^-$ γδ $TCR^+$ $CD4^-$ $IL\text{-}17A^+$ population in the ear at day 3 and 9. C) Graphical representation of the the $CD45.2^+$ $CD3^+$ $CD11b^-$ γδ $TCR^+$ $CD4^-$ $IL\text{-}22^+$ population in the ear at day 3 and 9. D) The absolute number of $IL\text{-}22^+$ γδ T cells are on the left and absolute number of $IL\text{-}17A^+$ γδ T cells are on the right. E) The absolute number of $IL\text{-}22^+$ CD4 T cells are on the left and the absolute number $IL\text{-}17A^+$ CD4 T cells are on the right. The data shown are representative of two independent experiments. Error bars represent the SEM, $P<0.05$ = *, $P<0.01$ = **, and $P<0.001$ = ***.

The lack of γδ T cells at the site of infection could have been due to a defect in the production of pro-inflammatory cytokines and chemokines or an intrinsic defect in the γδ T cell population. To distinguish between these options, we performed RT-qPCR on cells isolated from enzymatically digested ears on days 0, 1, 2, 3, 5, 9, and 21 after infection (Figure 4. 10). The expression of a neutrophil chemoattractant, CXCL2, peaked early on at day 2 and then decreased afterwards. CXCL2 expression levels in WT mice were similar to AHR KO mice, except for the transient increase in WT mice on day 2. Both mouse strains also had relatively similar low expression levels of a monocyte chemoattractant, CCL2, and an antimicrobial peptide, CRAMP. However, a transient increase in the expression of CCL2 and CRAMP was observed in the AHR KO mice during the early stages of infection. Additionally, a T cell chemoattractant, CXCL9, was produced at relatively similar expression levels throughout the infection by both strains of mice. However, CXCL9 was transiently higher by the AHR KO mice on days 2 and 5. Furthermore, mRNA expression levels of multiple cytokines were analyzed in this experiment. IL-10, IL-17A, and IFNγ were overall expressed at similar levels among the WT and AHR KO mice. However, IFNγ and IL-17A was transiently higher in WT mice during the later stages of infection. The similar IL-17A mRNA levels in the WT and AHR KO mice suggests that another cell population might be compensating for the decreased IL-17A$^+$ γδ T cells. These data suggest that there is proper production of pro-inflammatory chemokines, cytokines, and antimicrobial peptides by the AHR KO mice.

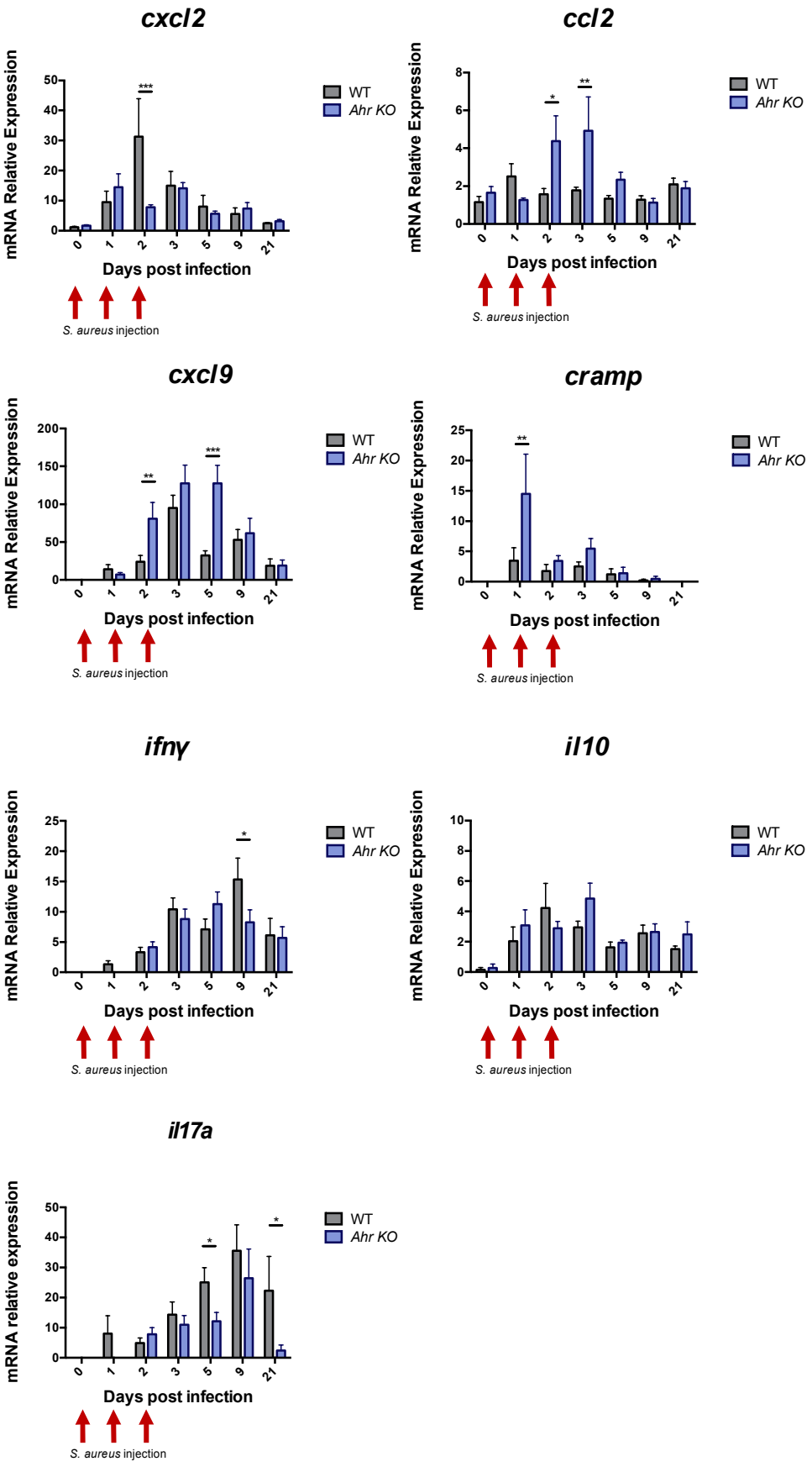
cxcl2
mRNA Relative Expression
WT
Ahr KO
***
Days post infection
S. aureus injection
ccl2
mRNA Relative Expression
WT
Ahr KO
*
**
Days post infection
S. aureus injection
cxcl9
mRNA Relative Expression
WT
Ahr KO
**
***
Days post infection
S. aureus injection
cramp
mRNA Relative Expression
WT
Ahr KO
**
Days post infection
S. aureus injection
ifnγ
mRNA Relative Expression
WT
Ahr KO
*
Days post infection
S. aureus injection
il10
mRNA Relative Expression
WT
Ahr KO
Days post infection
S. aureus injection
il17a
mRNA relative expression
WT
Ahr KO
*
*
Days post infection
S. aureus injection

**Figure 4.10: Chemokine, cytokine, and antimicrobial mRNA expression during a intradermal *S. aureus* infection.** Mice were administered $5x10^6$ CFUs of S8 intradermally on days 0, 1, and 2 (red arrows). RT-qPCR was used to analyze mRNA expression levels in the ear of WT and AHR KO mice on days 0 (n = 4), 1 (n = 5), 2 (n = 8), 3 (n = 8), 5 (n = 8), 9 (n = 5), and 21 (n = 5). All genes were normalized to B2m and TBP mRNA expression levels. The data shown are representative of two independent experiments. Error bars represent the SEM, $P<0.05$ = *, $P<0.01$ = **, and $P<0.001$ = ***.

## 4.3. Aim 3: Investigate whether AHR contributes to the generation of immunological memory to *S. aureus*

### *4.3.1.* AHR-deficient mice have proper CD4 T cell differentiation but decreased γδ T cell differentiation

AHR has been documented as an important transcription factor for the differentiation and development of many T cell lineages including $T_{reg}$ and $T_H17$ cells (10). Therefore, we wanted to investigate whether the differentiation of these cells during an *S. aureus* infection would be affected in AHR KO mice. WT and AHR KO mice were administered S8 intradermally at days 0, 1, and 2. To our surprise, the number of T cells in the lymph nodes of infected WT and AHR KO mice was identical on day 21 post infection (Figure 4.11 a). In addition, the proportion and absolute cell numbers of CD4, CD8, and γδ T cells were identical between the infected WT and AHR KO mice (Figure 4.11 b and c). When analyzing the CD4 T cell expression of lineage-specific transcription factors, we observed that the proportions of Foxp3, RORγt, GATA3 and T-bet-expressing T cells were similar in both WT and AHR KO mice (Figure 4.12 a). In addition, the largest CD4 differentiated population observed in both mouse strains was the $Foxp3^+$ $T_{regs}$. In contrast, the proportion and absolute number of $ROR\gamma t^+$ γδ T cell was drastically reduced in the AHR KO mice compared to the WT mice (Figure 4.12 b). Therefore, these data suggest that the CD4 T cell population activated in response to a *S. aureus* infection is not affected by the absence of AHR. However similar to the ear, lymph node $ROR\gamma t^+$ γδ T cells that develop in response to a *S. aureus* infection require the presence of AHR.

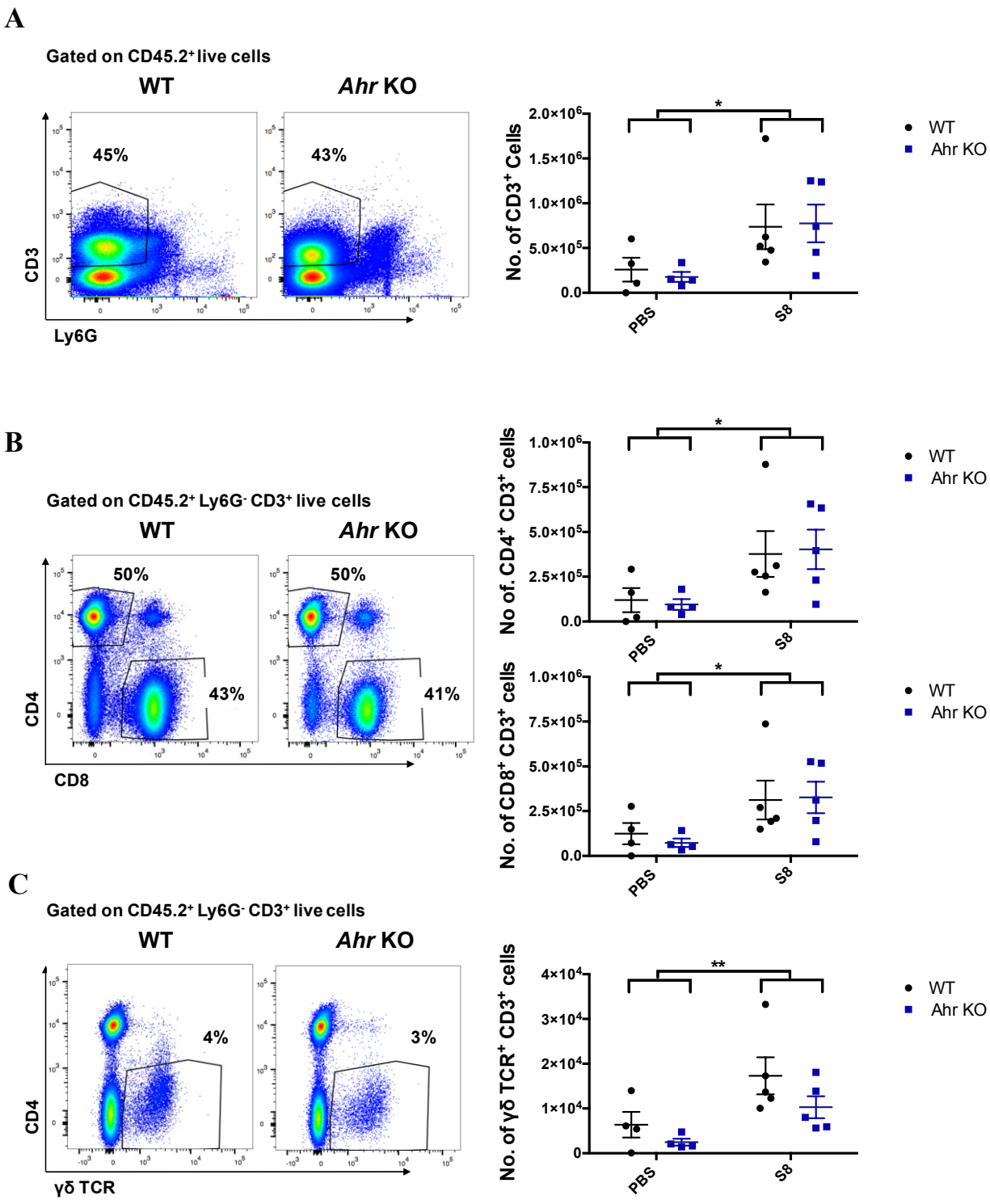
A
Gated on CD45.2+ live cells
WT
Ahr KO
45%
43%
CD3
Ly6G
No. of CD3+ Cells
2.0×10^6
1.5×10^6
1.0×10^6
5.0×10^5
0.0
*
PBS
S8
WT
Ahr KO
B
Gated on CD45.2+ Ly6G- CD3+ live cells
WT
Ahr KO
50%
50%
43%
41%
CD4
CD8
No of. CD4+ CD3+ cells
No. of CD8+ CD3+ cells
1.0×10^6
7.5×10^5
5.0×10^5
2.5×10^5
0.0
*
PBS
S8
WT
Ahr KO
C
Gated on CD45.2+ Ly6G- CD3+ live cells
WT
Ahr KO
4%
3%
CD4
γδ TCR
No. of γδ TCR+ CD3+ cells
4×10^4
3×10^4
2×10^4
1×10^4
0
**
PBS
S8
WT
Ahr KO

**Figure 4.11: CD4, CD8, and γδ T cells in the lymph nodes of *S. aureus* infected mice at day 21.** Mice were administered $5x10^6$ CFUs of S8 intradermally on days 0, 1, and 2. Flow cytometry was used to analyze the T cell populations present in the lymph nodes of S. aureus infected mice at day 21 (n = 5). A) Graphical representation of the $CD45.2^+$ $CD3^+$ $Ly6G^-$ population and the absolute numbers are summarized below. B) Graphical representation of the $CD4^+$ $CD8^-$ and $CD4^-$ $CD8^+$ T cell populations. The absolute numbers are represented on the right. C) Graphical representation of the $CD4^-$ γδ $TCR^+$ T cell population and the absolute numbers are presented on the right. Data are representative of two independent experiments. Error bars represent the SEM, $P<0.05$ = *, and $P<0.01$ = **.

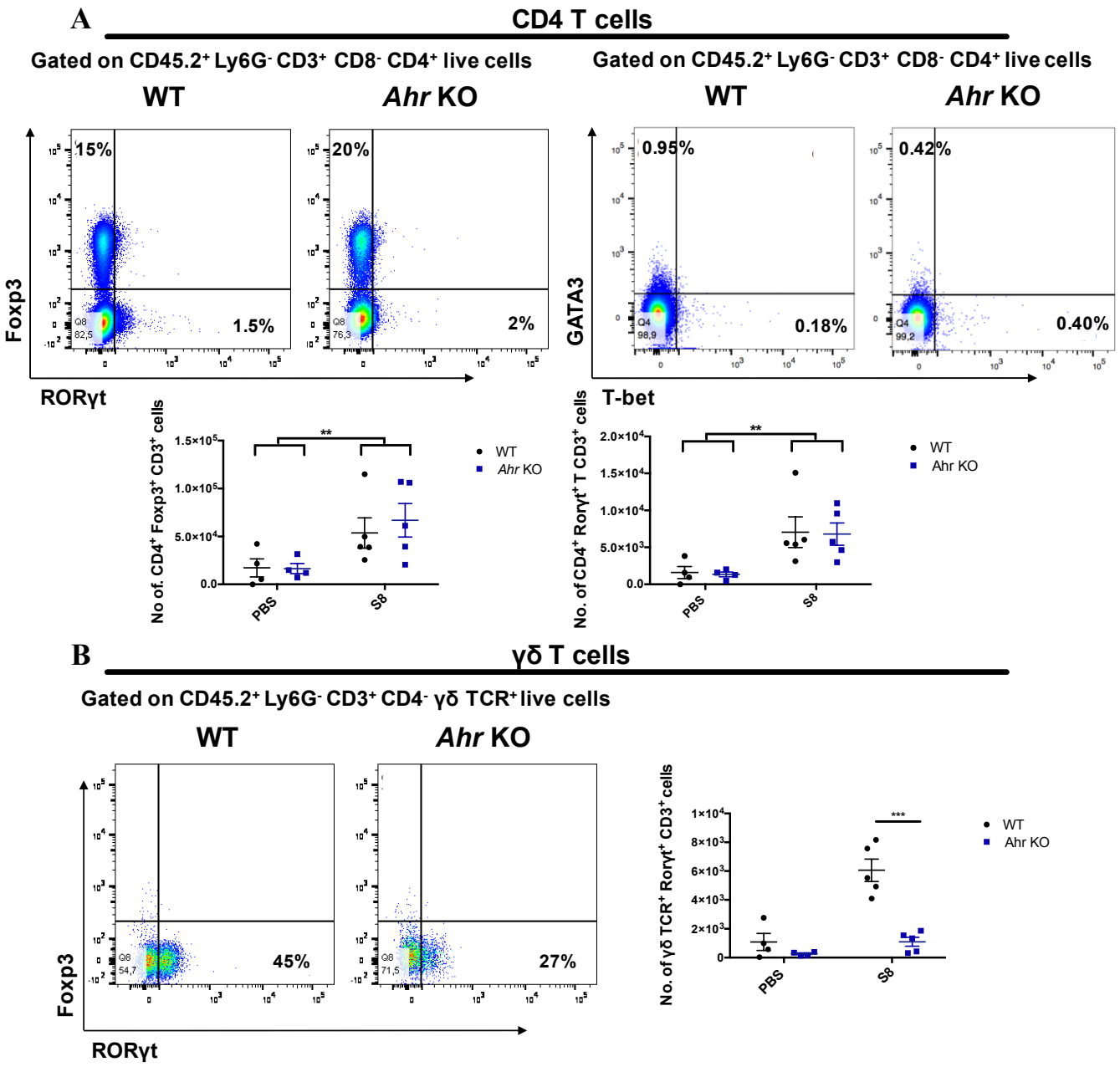
A
CD4 T cells
Gated on CD45.2+ Ly6G- CD3+ CD8- CD4+ live cells
WT
Ahr KO
15%
1.5%
20%
2%
Foxp3
RORγt
Gated on CD45.2+ Ly6G- CD3+ CD8- CD4+ live cells
WT
Ahr KO
0.95%
0.18%
0.42%
0.40%
GATA3
T-bet
No of. CD4+ Foxp3+ CD3+ cells
WT
Ahr KO
PBS
S8
No. of CD4+ Rorγt+ T CD3+ cells
B
γδ T cells
Gated on CD45.2+ Ly6G- CD3+ CD4- γδ TCR+ live cells
WT
Ahr KO
45%
27%
Foxp3
RORγt
No. of γδ TCR+ Rorγt+ CD3+ cells

**Figure 4.12: Lineage-specific transcription factor expression in CD4 and γδ T cells after a *S. aureus* infection.** Mice were administered $5x10^6$ CFUs of S8 intradermally on days 0, 1, and 2. Flow cytometry was used to analyze transcription factor expression by T cells in the lymph nodes of *S. aureus* infected mice at day 21 (n = 5). A) Graphical representation of $Foxp3^+$ and $ROR\gamma t^+$ CD4 T cells (left), $Gata3^+$ and T-$bet^+$ CD4 T cells (66), and the absolute numbers of $Foxp3^+$ CD4 T cells and $ROR\gamma t^+$ CD4 T cells (below). B) Graphical representation of $Foxp3^+$ and $ROR\gamma t^+$ γδ T cells (left) and absolute number of $ROR\gamma t^+$ γδ T cells (66). The data shown are representative of two independent experiments. Error bars represent the SEM, $P<0.05$ = *, $P<0.01$ = **, and $P<0.001$ = ***.

Recent studies have documented the development of memory Vγ4$^+$ IL-17$^+$ γδ T cells in response to lung *Bordetella Pertussis* infections (122) and intraperitoneal *S. aureus* infections (123). In order to investigate if the increased γδ T cells in the WT mice shared a similar phenotype, WT mice were administered 5x10$^6$ CFUs of S8 intradermally at day 0, 1, and 2 and γδ T cells were sorted from the ears and lymph nodes of WT mice at day 10. The sorted ear γδ T cells were pooled, and similarly the sorted lymph node γδ T cells were pooled. RT-qPCR was performed on the pooled cells. Preliminary results indicated high IL-17A mRNA expression (Figure 4.13 a) and high Vγ4 mRNA expression (Figure 4.13 b) in the sorted γδ T cell populations. However, the γδ T cells from the ear had more IL-17A and Vγ4 mRNA expression than the γδ T cells from the lymph nodes. The other Vγ chains were expressed at very low levels in the sorted cells. Lastly, Vγ4 mRNA expression was analyzed in the ears of mice from days 0, 1, 2, 3, 5, 9, and 21 after a S. aureus infection. The Vγ4 mRNA expression level was increased in WT mice on days 5 and 9 (Figure 4.13 d), mimicking the increase of IL-17$^+$ γδ T cells previously observed by flow cytometry (Figure. 4. 9 b).

Lastly, we performed a preliminary re-stimulation experiment in order to test the antigen specificity and IL-17A production by the sorted γδ T cells. γδ T cells from the ears and lymph nodes of infected WT mice were cultured with splenocytes from an uninfected mouse (as the source of APCs) in the presence of heat-killed S8 or heat-killed TB for 72 hours. The IL-17A accumulation in the supernatant was measured by ELISA. Data showed that the IL-17A production in response to S8 was doubled in the presence of the sorted γδ T cells (Figure 4.13 c). Therefore, these preliminary results suggest that the γδ T cells from WT mice infected with *S. aureus* display a similar phenotype to the memory γδ T cells recently described (122, 123).

A

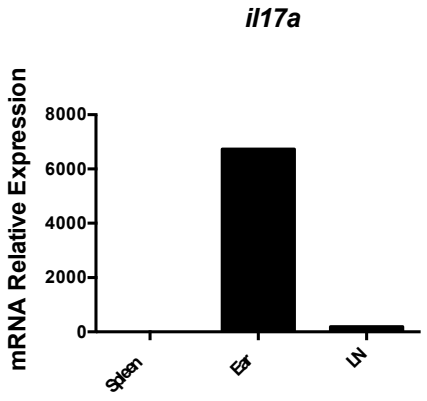
il17a
mRNA Relative Expression
8000
6000
4000
2000
0
Spleen
Ear
LN

B

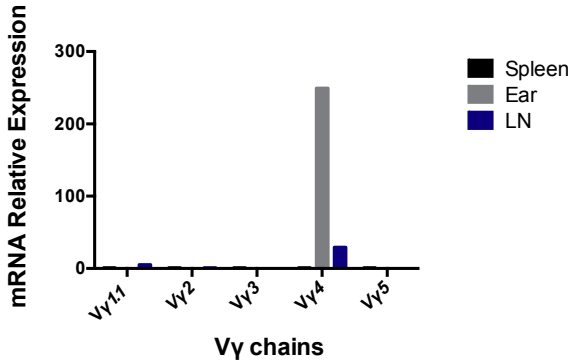
mRNA Relative Expression
300
200
100
0
Vγ1.1
Vγ2
Vγ3
Vγ4
Vγ5
Vγ chains
Spleen
Ear
LN

C

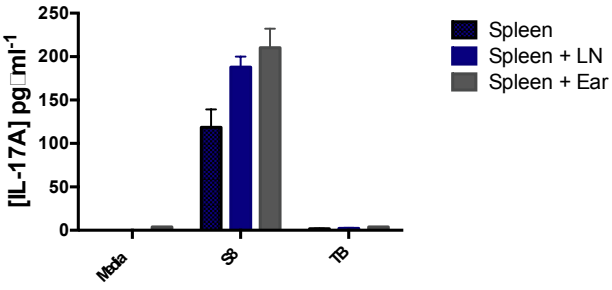
[IL-17A] pg□ml-1
250
200
150
100
50
0
Media
SB
TB
Spleen
Spleen + LN
Spleen + Ear

D

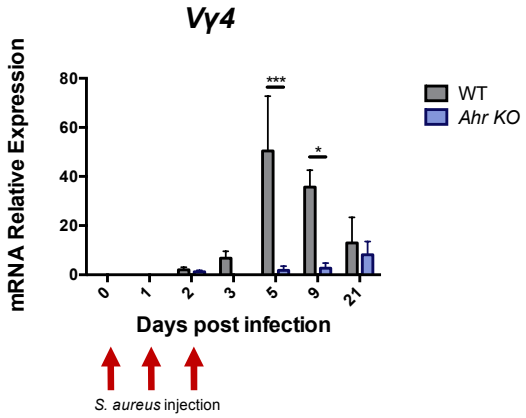
Vγ4
mRNA Relative Expression
80
60
40
20
0
***
*
0
1
2
3
5
9
21
Days post infection
S. aureus injection
WT
Ahr KO

**Figure 4.13: IL-17A production and Vγ4 chain expression by γδ T cells from *S. aureus* infected mice.** WT mice were administered S8 intradermally on days 0, 1, and 2. γδ T cells were sorted from both the ears and lymph nodes at day 10. As a control, spleen cells were harvested from a naïve mouse. A) RT-qPCR analysis of IL-17A mRNA expression by naïve spleen cells, and sorted γδ T cells from the ears and lymph nodes (LNs) of *S. aureus* infected mice. B) RT-qPCR analysis of Vγ1.1, Vγ2, Vγ3, Vγ4, Vγ5 mRNA expression by naïve spleen cells, and sorted γδ T cells from the ears and LNs of *S. aureus* infected mice. C) Sorted γδ T cells from the ears and lymph nodes of day 10 S8 infected mice were re-stimulated with media, $5x10^6$ CFUs of heat-killed S8, or $5x10^6$ CFUs heat-killed TB in the presence of naïve spleen cells (source of APCs) for 72 hours. IL-17A levels in the supernatants were measured by ELISA. The data shown are of a single independent experiment. The sorted γδ T cells were pooled together from 10 ears and 10 lymph nodes from 5 *S. aureus* infected mice. D) RT-qPCR analysis of Vγ4 mRNA expression in ears of WT and AHR KO mice on days 0 (n = 4), 1 (n = 5), 2 (n = 8), 3 (n = 8), 5 (n = 8), 9 (n = 5), and 21 (n = 5) post *S. aureus* infection (red arrows). All genes were normalized to B2m and TBP mRNA expression levels. Error bars represent the SEM of the technical triplicates.

4.3.2. Primed AHR-deficient mice behave as naïve WT mice upon a secondary infection

Our preliminary results indicate that the expanded γδ T cells in WT mice may be memory cells. Therefore, in order to test whether these cells could be protective against re-exposure to *S. aureus* we designed an *in vivo* secondary infection model (Figure 4.14 a). We expected that the γδ T cell expansion and bacterial clearance would occur faster in the primed WT mice. A subset of the WT and AHR KO mice were primed by the administration $5x10^6$ CFUs of S8 on days 0, 1, and 2. Ear thickness of the primed mice was measured on days 0, 1, 2, 3, 5, 9, 21, 28, and 35. Naïve and primed mice of both strains of mice were administered $5x10^6$ CFUs of S8 on days 40, 41, and 42 (Figure 4.14 a). Ear thickness of the primed and naïve mice was measured on days 40, 41, 42, 43, and 45. Regardless of priming, WT mice had more redness and ear crusting than the AHR KO mice on day 45 (Figure 4.14 b). After the primary *S. aureus* infection, WT mice had significantly higher ear thickness than AHR KO mice, as shown previously (Figure 4.5 f). Both strains of mice maintained a slightly increased ear thickness until the rechallenge at day 40. The ear swelling during the secondary infection was significantly higher in WT primed mice than in the AHR KO primed mice (Figure 4.14 c). Both strains of mice that were primed had higher ear swelling in the secondary infection than in the primary infection. Since AHR KO mice in each group (primed or naïve) had less swelling, the role of AHR appears to be independent of re-exposure to *S. aureus*.

The ears of these mice were harvested on days 43 and 45 in order to determine the bacterial burden by CFU counts and the T cell response by flow cytometry. The *S. aureus* CFUs were transiently higher in the primed mice compared to the naïve mice on day 43, however this difference disappeared by day 45 (Figure 4.15 a). There was no difference in the CFU counts between the WT and AHR KO mice in each group (primed and naïve).

As expected in a memory response, WT primed mice had increased T cell numbers (Figure 4.15 b), γδ T cell numbers, and IL-17A$^+$ γδ T cell numbers (Figure 4.15 d) at day 43 compared to the AHR KO primed mice and all the naïve mice. In fact, the AHR KO primed mice had similar CD3$^+$ T cell and γδ TCR$^+$ T cell numbers to the WT naïve mice. However, by day 45 the number of T cells and γδ T cells were the same between WT primed and WT naïve mice. Similarly, the number of T cells and γδ T cells were the same between AHR KO primed and AHR naïve mice at day 45, although the levels were much lower than in the WT groups. In all the mice, the γδ T cells expressed high levels of CD44, a T cell activation marker, and CD103, the ligand for E-cadherin on epithelial cells (Figure 4.15 e). In contrast, the CD4$^+$ T cells were relatively similar between all groups, except for a slightly increase in the IL-17A$^+$ CD4$^+$ T cell numbers in WT primed mice on day 45 (Figure 4.15 f). In all of the mice, only about about half of the CD4$^+$ T cells expressed CD44 and CD103 (Figure 4.15 e). These results indicate that the expanded γδ T cell pool responds to the infection but does not improve bacterial clearance upon a rechallenge.

The lymph nodes were harvested on day 43 and day 45 to test if the lymph node γδ T cell population would be reacting in a similar manner as the γδ T cell population in the ear. Cells were stained for lineage-specific transcription factors and analyzed by flow cytometry. A similar increase was seen in the CD3$^+$ T cells (Figure 4.16 a) and the RORγt$^+$ γδ T cells (Figure 4. 16 b) in WT primed mice on days 43 and 45. However in WT naïve mice, the T cells numbers did not increase to the same level as the WT primed mice on day 45. Instead, the WT naïve mice had low CD3$^+$ T cells and RORγt$^+$ γδ T cell numbers that matched the AHR KO primed mice on both days. There was no effect of priming on the CD4 and Foxp3$^+$ CD4 T cell populations. These data indicate

that *S. aureus* priming may lead to inflammation caused by IL-17A$^{+}$ γδ T cells during a secondary infection, and that the role of AHR during *S. aureus* infections is independent of priming.

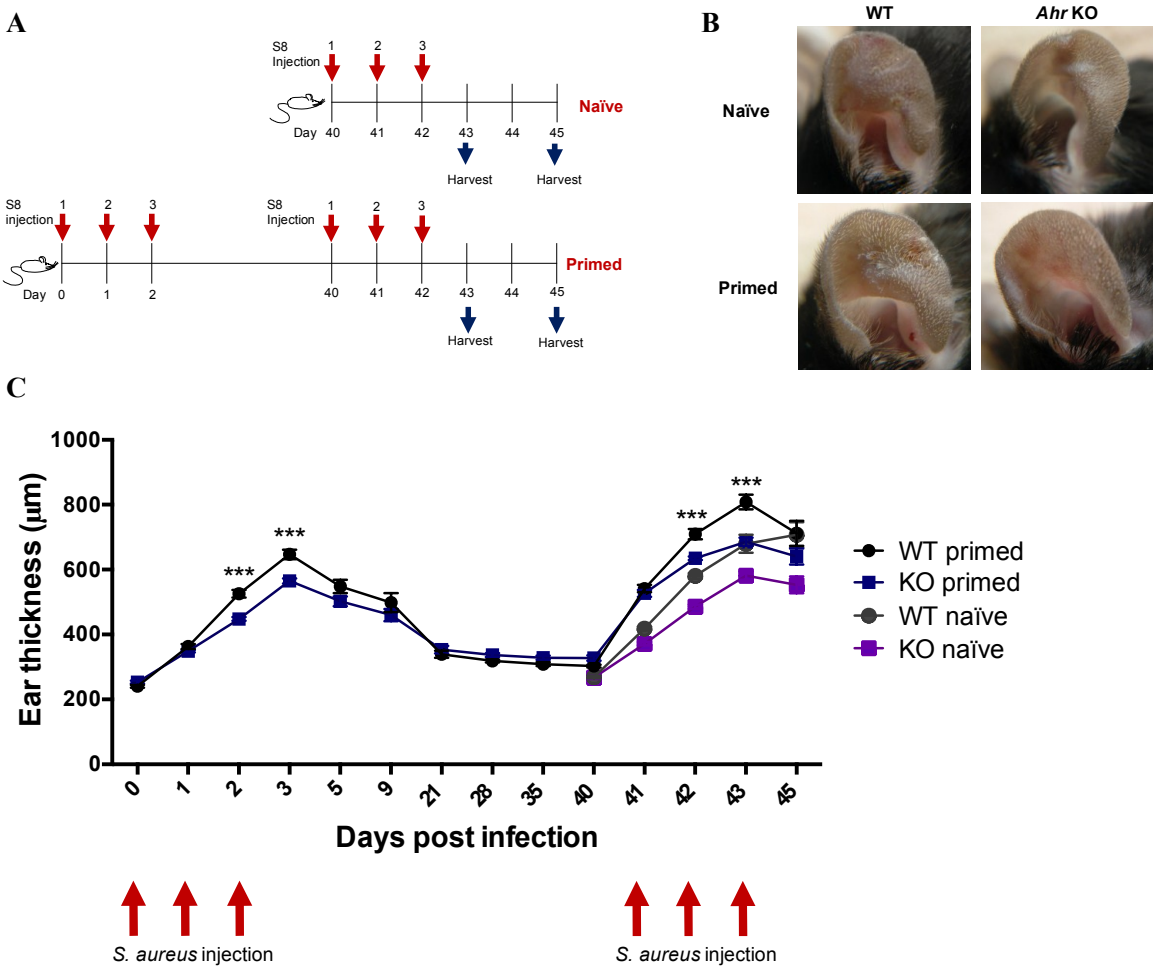


**Figure. 4.14: Ear thickness and morphology during a secondary *S. aureus* infection.** A) Timeline of the secondary *S. aureus* infection model. Mice were primed by administering $5x10^6$ CFUs of S8 intradermally on days 0, 1, and 2 (red arrows). Both primed and naïve mice were administered $5x10^6$ CFUs of S8 intradermally on days 40, 41, and 42 (red arrows). B) Ears of primed and naïve mice on day 45. C) Ear swelling of S8 primed mice was measured on days 0, 1, 2, 3, 5, 9, 21, 28 and 35 (n = 15). Days 21, 28, and 35 had n = 13 AHR KO mice due to the death of 2 mice from unrelated causes. Ear swelling of S8 primed and naïve mice was measured on days 40, 41, 42, 43, and 45 (n = 15 WT primed; n = 13 AHR KO primed; n = 15 WT naïve; n = 16 AHR KO naïve). The data shown is representative of a single independent experiment. Error bars represent the SEM, $P<0.001$ = ***.

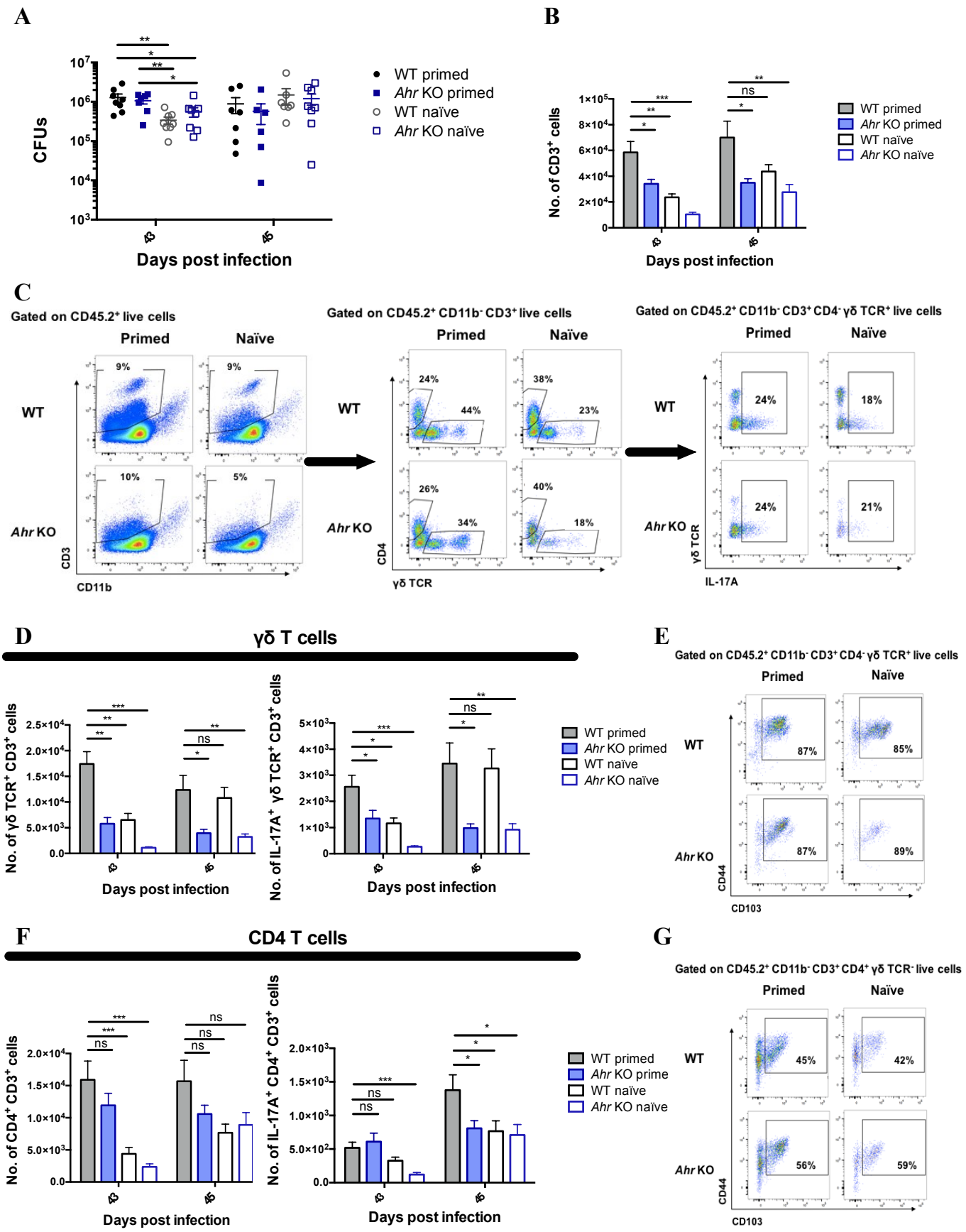
A
CFUs
Days post infection
WT primed
Ahr KO primed
WT naïve
Ahr KO naïve
B
No. of CD3+ cells
Days post infection
C
Gated on CD45.2+ live cells
Gated on CD45.2+ CD11b- CD3+ live cells
Gated on CD45.2+ CD11b- CD3+ CD4- γδ TCR+ live cells
Primed
Naïve
WT
Ahr KO
CD3
CD11b
CD4
γδ TCR
IL-17A
D
γδ T cells
No. of γδ TCR+ CD3+ cells
No. of IL-17A+ γδ TCR+ CD3+ cells
E
CD44
CD103
F
CD4 T cells
No. of CD4+ CD3+ cells
No. of IL-17A+ CD4+ CD3+ cells
G
Ahr KO prime

**Figure 4.15: Bacterial burden and cutaneous T cell expansion during a secondary *S. aureus* infection.** Mice were primed by administering $5x10^6$ CFUs of S8 intradermally on days 0, 1, and 2. Both primed and naïve mice were administered $5x10^6$ CFUs of S8 intradermally on days 40, 41, and 42. Flow cytometry was used to analyze the T cell populations in the ear on days 43 (n = 8 WT primed; n = 7 AHR KO primed; n = 8 WT naïve; and n = 8 AHR KO naïve), and 45 (n = 7 WT primed; n = 6 AHR KO primed; n = 7 WT naïve; n = 8 AHR KO naïve). A) *S. aureus* CFUs were cultured overnight on LB agar from ear supernatants from day 43 and 45. B) Absolute numbers of $CD45.2^+$ $CD3^+$ $CD11b^-$ cells at day 43 and 43. C) Graphical representation of the $CD45.2^+$ $CD3^+$ $CD11b^-$ population (left), $CD4^+$ and γδ $TCR^+$ T cell populations (middle), and IL-$17A^+$ γδ T cell population (right) at day 43. D) Absolute numbers of γδ $TCR^+$ and IL-$17A^+$ γδ $TCR^+$ populations. E) Graphical representation of the $CD44^+$ $CD103^+$ γδ $TCR^+$ T cell population at day 43. F) Absolute numbers of $CD4^+$ and IL-$17A^+$ $CD4^+$ T cell populations. G) Graphical representation of the $CD44^+$ $CD103^+$ $CD4^+$ T cell population at day 43. The data shown are representative of a single independent experiment. Error bars represent the SEM, $P<0.05$ = *, $P<0.01$ = **, and $P<0.001$ = ***.

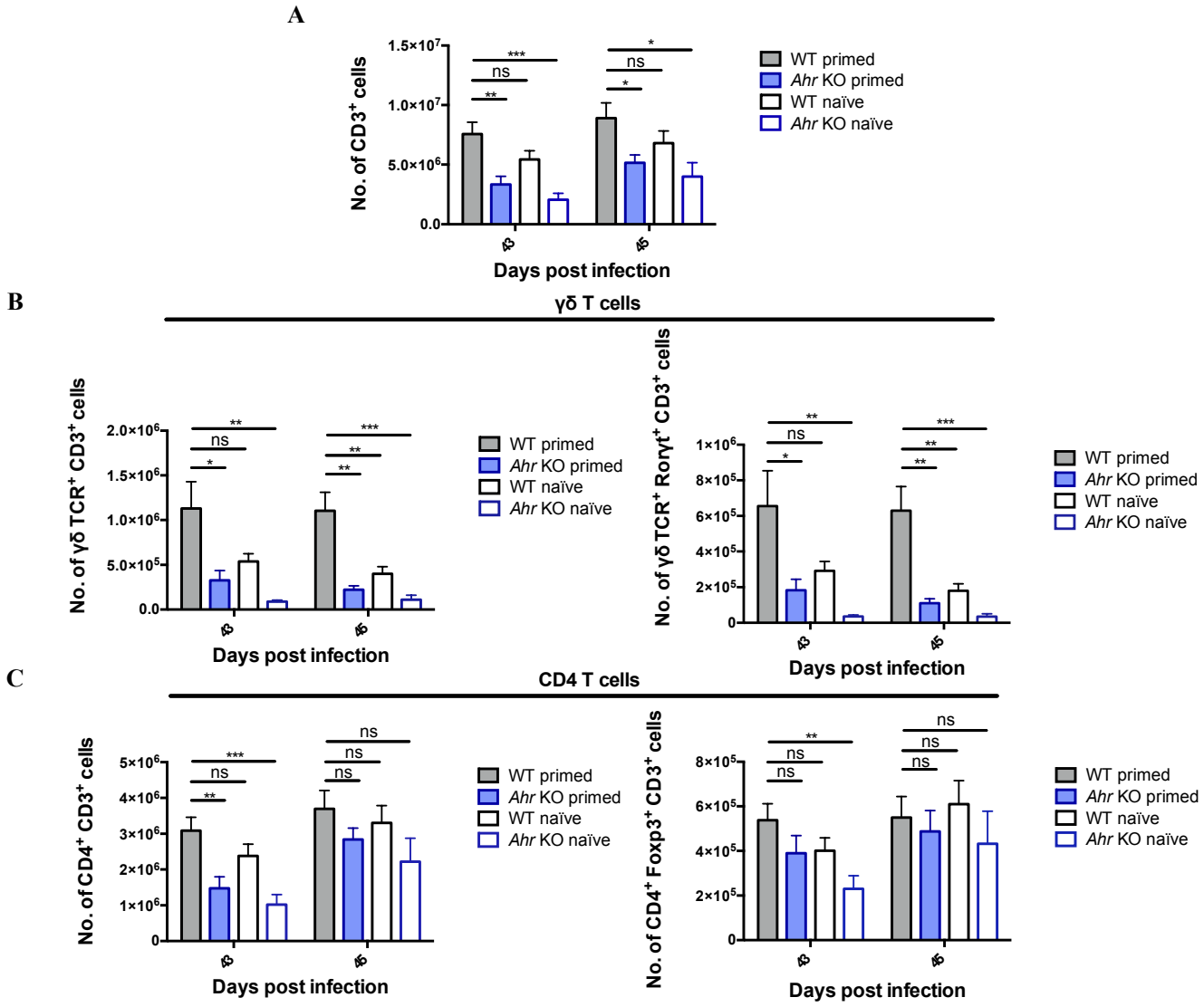


**Figure 4.16: Lineage-specific transcription factor expression in lymph node CD4 and γδ T cells after a secondary *S. aureus* infection.** Mice were primed by administering 5x10$^6$ CFUs of S8 intradermally on days 0, 1, and 2. Both primed and naïve mice were administered 5x10$^6$ CFUs of S8 intradermally on days 40, 41, and 42. Flow cytometry was used to analyze lineage-specific transcription factor expression by T cells in the lymph nodes of S. aureus infected mice on days 43 (n = 8 WT primed; n = 7 AHR KO primed; n = 8 WT naïve; and n = 8 AHR KO naïve), and 45 (n = 7 WT primed; n = 6 AHR KO primed; n = 7 WT naïve; n = 8 AHR KO naïve). A) Absolute number of CD45.2$^+$ CD3$^+$ CD11b$^-$ cells. B) Absolute number of γδ TCR$^+$ (left) and RORγt$^+$ γδ

$TCR^+$ cells (right). C) Absolute number of $CD4^+$ (left) and $Foxp3^+$ $CD4^+$ T cells (right). The data shown are representative of a single independent experiment. Error bars represent the SEM, $P<0.05$ = *, $P<0.01$ = **, and $P<0.001$ = ***.

## 4.4. Summary of results

In summary, the presence or absence of AHR does not impact the bacterial burden and is not required for clearing *S. aureus* cutaneous infections or for the colonization with *S. aureus*. After a single injection, *S. aureus* is cleared by day 21. In addition, after prolonged exposure *S. aureus* could still be detected at 21 days in half of the mice regardless of the background strain. However, the presence of AHR results in more acute inflammation, characterized by increased ear swelling and redness, during a *S. aureus* cutaneous infection. Therefore, AHR may be detrimental in the development of disease tolerance to *S. aureus*. Surprisingly, AHR-deficient mice have proper neutrophil recruitment to the site of infection despite their decreased γδ T cell population. In addition, an unexpected expansion and maintenance of cutaneous IL-17A$^+$ γδ T cells occurs at the later stages of infection, and this process is dependent on AHR. These γδ T cells are maintained at the site of infection up to 21 days. However, AHR-deficient mice can still produce IL-17A during infection, indicating that they might have developed a mechanism to compensate for the lack of IL-17A$^+$ γδ T cells. In the absence of AHR the development of adaptive CD4 T cells, such as the Foxp3$^+$ $T_{regs}$, in response to *S. aureus* is unaffected. Similar to the ear, the RORγt$^+$ γδ T cell population in the lymph nodes is dependent on AHR. Our preliminary data suggest that the expanded γδ T cells may be memory cells due to their rapid expansion upon *S. aureus* rechallenge. Yet, this γδ T cell pool did not confer increased killing of *S. aureus*. Additionally, primed mice that received a *S. aureus* rechallenge, had increased ear swelling and ear crusting. This suggests that priming to *S. aureus* may be additionally detrimental to disease tolerance. Lastly, the role of AHR is not affected by priming, since AHR KO mice maintain their phenotypic differences (decreased inflammation and decreased γδ T cells) compared to WT mice in identical treatment groups.

# 5. Discussion

*S. aureus* is a pathobiont that can cause a wide variety of human diseases (22) and can also colonize the human nostrils, skin, and other sites asymptomatically (4). In addition, *S. aureus* has been historically correlated with skin inflammatory diseases, such as AD (30). It has only been recently suggested that the inflammation in these skin conditions may be directly caused by *S. aureus* and the microbe's effect on the immune system (32). In addition, a recent publication illustrated how *S. aureus* vaccination can increase mortality upon *S. aureus* infection due to a heightened T cell-mediated immune response (77). Therefore, mechanisms of disease tolerance and avenues directed at limiting inflammation by dysregulated immune cells will be important in the future for both disease management and vaccine development. Since AHR has been implicated in the regulation of various T cell lineages, we expected that it would be required for both the protection against *S. aureus* infections, and for the induction of a disease tolerant state to *S. aureus*. The results presented in this thesis indicate that AHR is not required for clearing *S. aureus* during an infection but it may have a role in preventing the development of disease tolerance to *S. aureus,* in part, by its regulation of IL-17A producing γδ T cells.

## 5.1. The importance of neutrophils for *S. aureus* clearance

Our results illustrate that AHR-deficiency had no effect on the clearance or colonization of *S. aureus*. This can be explained by the observation that neutrophil recruitment to the site of infection occurred properly in the AHR KO mice. Future experiments should assess the recruited neutrophils for functional equivalence. It was unexpected that neutrophil recruitment would occur properly in

the AHR KO mice since they have a reduced cutaneous γδ T population. It has been previously reported that neutrophil recruitment is dependent on IL-17A production at 8 hours post *S. aureus* infection by the epidermal $V\gamma5^+$ γδ T cells (5). In this study, γδ T cell-deficient mice had decreased neutrophil recruitment and increased lesion sizes (5). Similarly, IL-22 production has been reported to peak at 6 hours post *S. aureus* infection, and is also produced by γδ T cells (124). This early IL-22 production has also been documented as a requirement for the recruitment of neutrophils (124). In our study, we observed a reduction of resident γδ T cells in AHR-deficient mice (Figure 4.6 b). A more dramatic decrease occurred in the γδ $TCR^{hi}$ population, which has been suggested to be the epidermal γδ T cells (119, 121). Complementary to this, epidermal γδ T cells have already been reported to be decreased in AHR-deficient mice (109).

Since the epidermal γδ T cells are reduced in AHR KO mice, there might be another cell type responsible for the recruitment of neutrophils. It has been suggested that perivascular macrophages are involved in the recruitment of neutrophils during dermal *S. aureus* infections by their expression of neutrophil chemoattractants, such as CXCL1 and CXCL2 (125). The macrophage population and CXCL2 mRNA expression in our model was not affected by AHR-deficiency, making this a population of interest for future studies. Interestingly, in other models of infection neutrophils have been proposed to produce both IL-17A (126) and IL-22 (112). However, this remains to be documented during a *S. aureus* cutaneous infection. Other cell populations that could also be compensating for the decreased γδ T cells are natural killer cells, and ILC3s. Another explanation could be that the small number of remaining dermal γδ T cells in the AHR KO mice compensate by producing more IL-17A early on during the infection. However, this cannot be determined from our results since our experiments did not look at cytokine production earlier than

24 hours after infection. The epidermal γδ T cell production of IL-17A is reported to peak at 8 hours and reach very low levels by 24 hours (5). Therefore, future experiments should investigate the cytokine and chemokine production prior to 24 hours post infection.

Lastly, it is important to mention the recent paradigm shift in the role of T cells during *S. aureus* infections. Historically, T and B cells were thought to be important in clearing many bacterial pathogens. However, the failures in developing an *S. aureus* vaccine brings to question whether adaptive T and B cells play a protective role in *S. aureus*. In fact, systemic *S. aureus* infections have been properly resolved in mice deficient in both T and B cells (127). Additionally, αβ T cell-deficient mice are able to clear *S. aureus* skin infections as efficiently as WT mice (5). In fact, our own preliminary experiments using RAG1 and AHR double knock out mice indicate that these mice can clear *S. aureus* skin infections just as well as WT mice (data not shown). Future experiments should confirm the mechanism by which neutrophils can be recruited independently from all types of T cells, and if these neutrophils can compensate by producing the $T_H17$ cytokines (IL-17A and IL-22) themselves.

5.2. Disease tolerance in the absence of AHR

In our studies, WT mice had increased *in vivo* signs of inflammation as suggested by increased ear swelling compared to AHR KO mice from days 2 to 9 post infection (Figure 4.5 f). However, the histological analysis of the ear's sections did not correlate with the ear swelling. There might be two explanations for this discrepancy. First, the histological processing might have removed some of the water in the tissues, making the histological edema scores suboptimal. Secondly, there might have not been enough histological samples sent to reach significant differences. 60% (3 out of 5)

of the WT mice had scored 3 on the lesion severity, while only 20% (1 out of 5) of the AHR KO mice had scored a 3. The ear swelling was typically measured on 8 to 40 mice (depending on the day), this large number of animals made the difference between WT and AHR KO mice very significant. Therefore, if more samples were scored each day during the infection perhaps the differences in the histological scoring would have been significant.

During the period of increased ear swelling in WT mice (days 2 to 9), there is also an AHR-dependent increase in the γδ T cell population (Figure 4.8 c). The IL-17A$^+$ γδ T cell production increases from day 3, reaching a maximum at day 5 and day 9 post infection. During a *S. aureus* rechallenge, primed WT mice have higher ear swelling and higher IL-17A$^+$ γδ T cell numbers compared to naïve WT and primed AHR KO mice. These results suggest that the expanded γδ T cells correlate with the increased inflammation observed in the mice.

The expanding γδ T cells observed in the WT mice after a *S. aureus* infection appear to be different from the protective epidermal γδ T cells reported by Cho, et al. (5). RT-qPCR of the whole ear and preliminary characterization of γδ T cells from WT mice indicate that there is an increase in IL-17A and Vγ4 mRNA expression during the later stages of infection (post day 3) (Figure 4.10 and 4.13 d). The IL-17A$^+$ Vγ4$^+$ γδ T cell population are thought to reside in the dermis (121) and are the cause of inflammation during psoriasis and dermatitis (119). These cells are additionally characterized by high expression of the CD44 marker, a sign of activation, and expression of Toll-like receptors such as TLR2 (11). Similarly, our results indicate that the γδ T cells within the ear of *S. aureus* infected mice express high levels of both CD44 and the skin homing receptor, CD103. This population is thought to be the same as the RORγt$^+$ γδ T cell

population that has the potential to migrate back and forth from the skin to draining lymph nodes (121). Their ability to be recruited to skin sites is thought to occur through their expression of skin homing receptors, including CD103 (128). Our results are in support of these recent studies, since a similar reduction in RORγt$^+$ γδ T cells is observed in the lymph nodes of AHR KO mice during *S. aureus* infection. Therefore, it appears that the expansion of these migratory and pro-inflammatory IL-17A$^+$ Vγ4$^+$ γδ T cells is dependent on AHR.

The observation of an expanded γδ T cell population in response to a *S. aureus* infection is interesting because psoriasis patients with phenotypically similar γδ T cells are reported to be at lower risk of infection or colonization by *S. aureus* (129). Whether initial bacterial exposure, such as a *S. aureus* infection, is the initiation event of inflammatory skin diseases such as psoriasis is currently being debated. Similarly, recent studies have reported that *S. aureus* colonization directly contributes to inflammation in dermatitis by an unknown mechanism (32). Future experiments, should investigate if *S. aureus*-induced expansion of IL-17A$^+$ γδ T cells can predispose the host to inflammatory skin diseases such as psoriasis. Furthermore, the expanded IL-17A$^+$ γδ T cell population should be tested for reactivity and specificity to other non-specific bacterial antigens.

Since IL-17A$^+$ Vγ4$^+$ γδ T cells appear responsible for murine inflammation during inflammatory skin diseases, targeting them may have therapeutic approaches. These findings additionally have potential implications in humans since dermal IL-17A$^+$ γδ T cell populations have been observed to be increased in the skin lesions of psoriasis patients (119). Our results suggest that inhibiting AHR could potentially prevent the development of these IL-17A$^+$ Vγ4$^+$ γδ T cells. Interestingly, human studies have identified that AHR expression is increased and that the

AHR pathway is activated in skin lesions of AD and psoriasis patients (13). Murine *in vitro* studies have demonstrated that both AHR activation by the high affinity AHR ligand, FITC, and TLR2 activation by pathogen products can result in an expansion of these γδ T cells (11). However, no one has documented this expansion to occur *in vivo* and to be maintained for as long as 21 days post cutaneous bacterial infection. In stark contrast, *in vivo* experiments have shown that AHR-deficient mice had increased inflammation during a model of psoriasis due to keratinocyte signaling and that systemic administration of FITC led to reduced IL-17A expression (14). These discrepancies may indicate a paradoxical role in AHR where its inhibition may be beneficial prior to the development of psoriasis by preventing the increase of resident dermal γδ T cells, but within the disease state AHR activation may be beneficial through an activation pathway in keratinocytes.

### 5.3. Primed innate immunity

Historically, the belief in the field of innate immunity has been that innate immune cells act rapidly, non-specifically, and cannot retain immunological memory. Typically, immunological memory was considered the role of T and B cells. Recently, it has been suggested that immune memory (or trained cells) can develop from APCs such as monocytes, and innate T cells such as γδ T cells (130). Pathogens can induce epigenetic modifications to either promote tolerance or train the innate immune cells (131). IL-$17^+$ V$\gamma4^+$ γδ T cells have been reported to expand in response to *B. pertussis* lung infections (122). These cells were shown to remain in the lung after a primary infection, and expand rapidly upon a secondary challenge to increase bacterial clearance (122). These cells are the same as the dermal γδ T cells involved in the inflammation of psoriasis. In fact, the dermal γδ T cells in psoriasis have also been claimed to be long-lived memory cells within the skin (128).

In the context of a *S. aureus* infection, memory IL-17$^+$ Vγ4$^+$ γδ T cells have only been documented to occur after *S. aureus*-induced peritonitis (123). These studies illustrated that prior *S. aureus* exposure leads to the development of protective memory IL-17$^+$ Vγ4$^+$ γδ T cells that help clear a secondary *S. aureus* infection faster (123). However, no one has reported the development of this population after a cutaneous *S. aureu*s infection. Our preliminary results indicate that a memory IL-17$^+$ CD44$^+$ CD103$^+$ Vγ4$^+$ γδ T cell population developed after priming with *S. aureus*. Additionally, these cells rapidly expand in the primed WT mice during a secondary *S. aureus* infection. However, unlike the peritonitis experiments, the bacterial burden in our preliminary rechallenge experiment was not affected by the increased presence of γδ T cells in the primed mice. Therefore, this raises the question of whether these cells are protective in the skin or if they are pathogenic and are a byproduct of a cutaneous infection.

5.4. Differences in immunity based on the site of infection and host

Cutaneous *S. aureus* infections often predispose individuals to bacteremia and systemic infections. Similarly, individuals colonized by *S. aureus* are at greater risk for *S. aureus* bacteremia, especially with their own colonizing strain (34, 35). However, the cutaneous immune response to *S. aureus* is unique and different from systemic immune responses during sepsis or *S. aureus* bacteremia (53). For example, both $T_H1$ cells (70) and antibodies (33) are known to be involved during systemic *S. aureus* infections but not during cutaneous infections. Our results suggest that AHR is not required for the clearance of cutaneous *S. aureus* infections, but may be detrimental to the development of disease tolerance. However, we cannot predict whether AHR would be important in the survival of the host during systemic *S. aureus* infections. Although AHR is not directly

involved in the development of antibodies and $T_H1$ immunity, it has been shown that AHR promotes $T_H17$ differentiation by inhibiting Stat1 phosphorylation and ultimately $T_H1$ differentiation (96). In the absence of AHR, it is possible that the development of $T_H1$ immune cells in response to systemic *S. aureus* infections would be increased. Therefore, future experiments should investigate the role of AHR in systemic *S. aureus* infections.

One major challenge in studying *S. aureus* infections *in vivo* is that mice have an intrinsic high resistance to severe *S. aureus* infections. In order to obtain a dermonecrosis lesion, $10^7$ CFUs of *S. aureus* need to be administered (132, 133). To compare, data suggest that as few as $10^4$ CFUs are needed to establish a *S. aureus* skin infection in humans (132, 134). In our experiments we administered $5x10^6$ CFUs of *S. aureus* to our mice for 1 or 3 days, a dose significantly higher than the amount required for an infection in humans. Once the infection was established, the mice were able to start efficiently clearing the infection within a few days. Additionally, there are many differences between the human and murine immune responses to *S. aureus*. To name one, humans do not have the epidermal γδ T cells that are thought to be required for the early production of IL-17A (5). Therefore, many results may differ between murine models and human *S. aureus* cutaneous infections.

There are numerous limitations to studying AHR *in vivo*. One of the limitations is that AHR has a wide range of different ligands, with several of them remaining to be discovered. Natural and/or endogenous ligands were not accounted for in our experiments, and therefore our results might not accurately represent the functional roles of AHR during natural human exposure to *S. aureus* where additional endogenous AHR ligands are present. In addition, AHR is expressed

ubiquitously in cells throughout the body, so AHR deficiency may have impacted other cell populations that are not accounted for in our experiments. Future studies should use selective AHR deletion by Cre-lox recombination in specific cell populations, such as in γδ $TCR^+$ T cells.

Furthermore, several differences exist between the mouse AHR and human AHR. Mouse AHR and human AHR have been found to have different ligand selectivity and affinities (87). This implies that AHR might regulate *S. aureus* infections differently in mice and in humans simply because of differences in ligand binding. Other differences include cytoplasmic complex stability (135), recruitment of coactivators (136), and regulation of gene expression (137). Therefore, repetition of these experiments in transgenic mice that express the human AHR instead of the mouse AHR would prove confirmation of our findings with the human AHR.

Lastly, many studies have acknowledged the important role of the microbiota in diseases and immunity. For example, human skin infections and their outcomes can be influenced by the skin microbiota (40). On the other hand, skin infections can also influence the skin microbial community (40). In addition, temporal shifts in the microbiota have been correlated with inflammatory flares of AD patients (31). Furthermore, microbiota tryptophan products have been discovered to activate AHR and influence the immune cells of the skin (98). The microbiota has been shown to be important for $CD4^+$ T cell production of IL-17A and IL-22 against *S. aureus* (138). When culturing *S. aureus* CFUs we also detected the presence of a colonizing bacteria in both the PBS and *S. aureus* treated groups. We have replicated our experiments with WT and AHR KO co-housed mice in order to try to keep the microbiota consistent between these two strains of mice. During these experiments, our results were consistent and the microbiota colonization

pattern was equal between the two mouse strains. However, we did not characterize the microbiota that was present or its potential role on AHR. Therefore, future studies should consider the potential involvement of the microbiota in both human and murine studies.

## 5.5. Conclusion and future directions

The role of AHR in *S. aureus* cutaneous infections has been undocumented up until now. Since AHR is important for the development and function of many T lymphocytes, we hypothesized that the AHR pathway would be necessary for both the protection against *S. aureus* and the establishment of a disease tolerant state to *S. aureus*. Our data shows that the AHR pathway is not required for *S. aureus* clearance. Additionally, AHR-deficient mice have intact neutrophil recruitment to the cutaneous site of infection suggesting that a proper neutrophil response may be sufficient to clear staphylococcal cutaneous infections even with decreased numbers of T cells. Furthermore, *S. aureus* infection induces an AHR-dependent expansion of IL-17A$^+$ γδ T cells that remain at the site of infection for at least 21 days. The γδ T cell pool in WT mice after a primary *S. aureus* infection does not lead to increased bacterial killing during a secondary *S. aureus* infection. Future experiments will further test the memory potential of these cells with adaptive transfer experiments. Lastly, AHR inhibition may facilitate disease tolerance to *S. aureus*, and this suggests that differential AHR expression in humans may provide an explanation to why some individuals are transient and chronic asymptomatic carriers of this microbe. Future experiments should test AHR-deficiency during systemic *S. aureus* infections, and *S. aureus* carriage states to further elucidate the potential role of AHR in disease tolerance.

## 6. References


1. Miller, L. S., and J. S. Cho. 2011. Immunity against Staphylococcus aureus cutaneous infections. *Nat Rev Immunol* 11: 505-518.
2. Lowy, F. D. 1998. Staphylococcus aureus infections. *N Engl J Med* 339: 520-532.
3. Klevens, R. M., M. A. Morrison, J. Nadle, S. Petit, K. Gershman, S. Ray, L. H. Harrison, R. Lynfield, G. Dumyati, J. M. Townes, A. S. Craig, E. R. Zell, G. E. Fosheim, L. K. McDougal, R. B. Carey, and S. K. Fridkin. 2007. Invasive methicillin-resistant Staphylococcus aureus infections in the United States. *Jama* 298: 1763-1771.
4. Brown, A. F., J. M. Leech, T. R. Rogers, and R. M. McLoughlin. 2014. Staphylococcus aureus Colonization: Modulation of Host Immune Response and Impact on Human Vaccine Design. *Front Immunol* 4: 507.
5. Cho, J. S., E. M. Pietras, N. C. Garcia, R. I. Ramos, D. M. Farzam, H. R. Monroe, J. E. Magorien, A. Blauvelt, J. K. Kolls, A. L. Cheung, G. Cheng, R. L. Modlin, and L. S. Miller. 2010. IL-17 is essential for host defense against cutaneous Staphylococcus aureus infection in mice. *J Clin Invest* 120: 1762-1773.
6. Montgomery, C. P., M. Daniels, F. Zhao, M. L. Alegre, A. S. Chong, and R. S. Daum. 2014. Protective immunity against recurrent Staphylococcus aureus skin infection requires antibody and interleukin-17A. *Infect Immun* 82: 2125-2134.
7. Carretero, M., S. Guerrero-Aspizua, N. Illera, V. Galvez, M. Navarro, F. Garcia-Garcia, J. Dopazo, J. L. Jorcano, F. Larcher, and M. Del Rio. 2015. Differential Features Between Chronic Skin Inflammatory Diseases Revealed in Skin-Humanized Psoriasis and Atopic Dermatitis Mouse Models. *J Invest Dermatol*.

8. Peres, A. G., and J. Madrenas. 2017. in submision.

9. Julliard, W., J. H. Fechner, and J. D. Mezrich. 2014. The aryl hydrocarbon receptor meets immunology: friend or foe? A little of both. *Front Immunol* 5: 458.

10. Quintana, F. J., A. S. Basso, A. H. Iglesias, T. Korn, M. F. Farez, E. Bettelli, M. Caccamo, M. Oukka, and H. L. Weiner. 2008. Control of T(reg) and T(H)17 cell differentiation by the aryl hydrocarbon receptor. *Nature* 453: 65-71.

11. Martin, B., K. Hirota, D. J. Cua, B. Stockinger, and M. Veldhoen. 2009. Interleukin-17-producing gammadelta T cells selectively expand in response to pathogen products and environmental signals. *Immunity* 31: 321-330.

12. Veldhoen, M., K. Hirota, A. M. Westendorf, J. Buer, L. Dumoutier, J. C. Renauld, and B. Stockinger. 2008. The aryl hydrocarbon receptor links TH17-cell-mediated autoimmunity to environmental toxins. *Nature* 453: 106-109.

13. Kim, H. O., J. H. Kim, B. Y. Chung, M. G. Choi, and C. W. Park. 2014. Increased expression of the aryl hydrocarbon receptor in patients with chronic inflammatory skin diseases. *Exp Dermatol* 23: 278-281.

14. Di Meglio, P., J. H. Duarte, H. Ahlfors, N. D. Owens, Y. Li, F. Villanova, I. Tosi, K. Hirota, F. O. Nestle, U. Mrowietz, M. J. Gilchrist, and B. Stockinger. 2014. Activation of the aryl hydrocarbon receptor dampens the severity of inflammatory skin conditions. *Immunity* 40: 989-1001.

15. Hao, N., and M. L. Whitelaw. 2013. The emerging roles of AhR in physiology and immunity. *Biochem Pharmacol* 86: 561-570.

16. Quintana, F. J., G. Murugaiyan, M. F. Farez, M. Mitsdoerffer, A. M. Tukpah, E. J. Burns, and H. L. Weiner. 2010. An endogenous aryl hydrocarbon receptor ligand acts on

dendritic cells and T cells to suppress experimental autoimmune encephalomyelitis. *Proc Natl Acad Sci U S A* 107: 20768-20773.

17. Gagliani, N., M. C. Vesely, A. Iseppon, L. Brockmann, H. Xu, N. W. Palm, M. R. de Zoete, P. Licona-Limon, R. S. Paiva, T. Ching, C. Weaver, X. Zi, X. Pan, R. Fan, L. X. Garmire, M. J. Cotton, Y. Drier, B. Bernstein, J. Geginat, B. Stockinger, E. Esplugues, S. Huber, and R. A. Flavell. 2015. Th17 cells transdifferentiate into regulatory T cells during resolution of inflammation. *Nature* 523: 221-225.

18. 1984. Classics in infectious diseases. "On abscesses". Alexander Ogston (1844-1929). *Rev Infect Dis* 6: 122-128.

19. Liu, G. Y., A. Essex, J. T. Buchanan, V. Datta, H. M. Hoffman, J. F. Bastian, J. Fierer, and V. Nizet. 2005. Staphylococcus aureus golden pigment impairs neutrophil killing and promotes virulence through its antioxidant activity. *J Exp Med* 202: 209-215.

20. Masalha, M., I. Borovok, R. Schreiber, Y. Aharonowitz, and G. Cohen. 2001. Analysis of transcription of the Staphylococcus aureus aerobic class Ib and anaerobic class III ribonucleotide reductase genes in response to oxygen. *J Bacteriol* 183: 7260-7272.

21. Kenneth Ryan, C. G. R. 2004. *Sherris Medical Microbiology*.

22. Tong, S. Y., J. S. Davis, E. Eichenberger, T. L. Holland, and V. G. Fowler, Jr. 2015. Staphylococcus aureus infections: epidemiology, pathophysiology, clinical manifestations, and management. *Clin Microbiol Rev* 28: 603-661.

23. DeLeo, F. R., and H. F. Chambers. 2009. Reemergence of antibiotic-resistant Staphylococcus aureus in the genomics era. *J Clin Invest* 119: 2464-2474.

24. MP, J. 1961. “Celbenin” -resistant Staphylococci. *British Medical Journal* 1: 124-125.

25. Hiramatsu, K., N. Aritaka, H. Hanaki, S. Kawasaki, Y. Hosoda, S. Hori, Y. Fukuchi, and I. Kobayashi. 1997. Dissemination in Japanese hospitals of strains of Staphylococcus aureus heterogeneously resistant to vancomycin. *Lancet* 350: 1670-1673.

26. Hiramatsu, K., H. Hanaki, T. Ino, K. Yabuta, T. Oguri, and F. C. Tenover. 1997. Methicillin-resistant Staphylococcus aureus clinical strain with reduced vancomycin susceptibility. *J Antimicrob Chemother* 40: 135-136.

27. Herold, B. C., L. C. Immergluck, M. C. Maranan, D. S. Lauderdale, R. E. Gaskin, S. Boyle-Vavra, C. D. Leitch, and R. S. Daum. 1998. Community-acquired methicillin-resistant Staphylococcus aureus in children with no identified predisposing risk. *Jama* 279: 593-598.

28. Udo, E. E., J. W. Pearman, and W. B. Grubb. 1993. Genetic analysis of community isolates of methicillin-resistant Staphylococcus aureus in Western Australia. *J Hosp Infect* 25: 97-108.

29. 1999. Four pediatric deaths from community-acquired methicillin-resistant Staphylococcus aureus - Minnesota and North Dakota, 1997-1999. *MMWR Morb Mortal Wkly Rep* 48: 707-710.

30. Leyden, J. J., R. R. Marples, and A. M. Kligman. 1974. Staphylococcus aureus in the lesions of atopic dermatitis. *Br J Dermatol* 90: 525-530.

31. Kong, H. H., J. Oh, C. Deming, S. Conlan, E. A. Grice, M. A. Beatson, E. Nomicos, E. C. Polley, H. D. Komarow, P. R. Murray, M. L. Turner, and J. A. Segre. 2012. Temporal shifts in the skin microbiome associated with disease flares and treatment in children with atopic dermatitis. *Genome Res* 22: 850-859.

32. Kobayashi, T., M. Glatz, K. Horiuchi, H. Kawasaki, H. Akiyama, D. H. Kaplan, H. H. Kong, M. Amagai, and K. Nagao. 2015. Dysbiosis and Staphylococcus aureus Colonization Drives Inflammation in Atopic Dermatitis. *Immunity* 42: 756-766.

33. Stentzel, S., N. Sundaramoorthy, S. Michalik, M. Nordengrun, S. Schulz, J. Kolata, P. Kloppot, S. Engelmann, L. Steil, M. Hecker, F. Schmidt, U. Volker, M. C. Roghmann, and B. M. Broker. 2015. Specific serum IgG at diagnosis of Staphylococcus aureus bloodstream invasion is correlated with disease progression. *J Proteomics* 128: 1-7.

34. von Eiff, C., K. Becker, K. Machka, H. Stammer, and G. Peters. 2001. Nasal carriage as a source of Staphylococcus aureus bacteremia. Study Group. *N Engl J Med* 344: 11-16.

35. Wertheim, H. F., M. C. Vos, A. Ott, A. van Belkum, A. Voss, J. A. Kluytmans, P. H. van Keulen, C. M. Vandenbroucke-Grauls, M. H. Meester, and H. A. Verbrugh. 2004. Risk and outcome of nosocomial Staphylococcus aureus bacteraemia in nasal carriers versus non-carriers. *Lancet* 364: 703-705.

36. Grice, E. A., and J. A. Segre. 2011. The skin microbiome. *Nat Rev Microbiol* 9: 244-253.

37. Otto, M. 2010. Staphylococcus colonization of the skin and antimicrobial peptides. *Expert Rev Dermatol* 5: 183-195.

38. Gallo, R. L., K. J. Kim, M. Bernfield, C. A. Kozak, M. Zanetti, L. Merluzzi, and R. Gennaro. 1997. Identification of CRAMP, a cathelin-related antimicrobial peptide expressed in the embryonic and adult mouse. *J Biol Chem* 272: 13088-13093.

39. Rosenthal, M., D. Goldberg, A. Aiello, E. Larson, and B. Foxman. 2011. Skin microbiota: microbial community structure and its potential association with health and disease. *Infect Genet Evol* 11: 839-848.

40. van Rensburg, J. J., H. Lin, X. Gao, E. Toh, K. R. Fortney, S. Ellinger, B. Zwickl, D. M. Janowicz, B. P. Katz, D. E. Nelson, Q. Dong, and S. M. Spinola. 2015. The Human Skin Microbiome Associates with the Outcome of and Is Influenced by Bacterial Infection. *MBio* 6: e01315-01315.

41. Cogen, A. L., V. Nizet, and R. L. Gallo. 2008. Skin microbiota: a source of disease or defence? *Br J Dermatol* 158: 442-455.

42. Frank, D. N., L. M. Feazel, M. T. Bessesen, C. S. Price, E. N. Janoff, and N. R. Pace. 2010. The human nasal microbiota and Staphylococcus aureus carriage. *PLoS One* 5: e10598.

43. Otto, M., H. Echner, W. Voelter, and F. Gotz. 2001. Pheromone cross-inhibition between Staphylococcus aureus and Staphylococcus epidermidis. *Infect Immun* 69: 1957-1960.

44. Otto, M., R. Sussmuth, C. Vuong, G. Jung, and F. Gotz. 1999. Inhibition of virulence factor expression in Staphylococcus aureus by the Staphylococcus epidermidis agr pheromone and derivatives. *FEBS Lett* 450: 257-262.

45. Cogen, A. L., K. Yamasaki, K. M. Sanchez, R. A. Dorschner, Y. Lai, D. T. MacLeod, J. W. Torpey, M. Otto, V. Nizet, J. E. Kim, and R. L. Gallo. 2010. Selective antimicrobial action is provided by phenol-soluble modulins derived from Staphylococcus epidermidis, a normal resident of the skin. *J Invest Dermatol* 130: 192-200.

46. Cogen, A. L., K. Yamasaki, J. Muto, K. M. Sanchez, L. Crotty Alexander, J. Tanios, Y. Lai, J. E. Kim, V. Nizet, and R. L. Gallo. 2010. Staphylococcus epidermidis antimicrobial delta-toxin (phenol-soluble modulin-gamma) cooperates with host antimicrobial peptides to kill group A Streptococcus. *PLoS One* 5: e8557.

47. Takeuchi, O., and S. Akira. 2010. Pattern recognition receptors and inflammation. *Cell* 140: 805-820.

48. Schroder, K., and J. Tschopp. 2010. The inflammasomes. *Cell* 140: 821-832.

49. von Bernuth, H., C. Picard, Z. Jin, R. Pankla, H. Xiao, C. L. Ku, M. Chrabieh, I. B. Mustapha, P. Ghandil, Y. Camcioglu, J. Vasconcelos, N. Sirvent, M. Guedes, A. B. Vitor, M. J. Herrero-Mata, J. I. Arostegui, C. Rodrigo, L. Alsina, E. Ruiz-Ortiz, M. Juan, C. Fortuny, J. Yague, J. Anton, M. Pascal, H. H. Chang, L. Janniere, Y. Rose, B. Z. Garty, H. Chapel, A. Issekutz, L. Marodi, C. Rodriguez-Gallego, J. Banchereau, L. Abel, X. Li, D. Chaussabel, A. Puel, and J. L. Casanova. 2008. Pyogenic bacterial infections in humans with MyD88 deficiency. *Science* 321: 691-696.

50. Ku, C. L., H. von Bernuth, C. Picard, S. Y. Zhang, H. H. Chang, K. Yang, M. Chrabieh, A. C. Issekutz, C. K. Cunningham, J. Gallin, S. M. Holland, C. Roifman, S. Ehl, J. Smart, M. Tang, F. J. Barrat, O. Levy, D. McDonald, N. K. Day-Good, R. Miller, H. Takada, T. Hara, S. Al-Hajjar, A. Al-Ghonaium, D. Speert, D. Sanlaville, X. Li, F. Geissmann, E. Vivier, L. Marodi, B. Z. Garty, H. Chapel, C. Rodriguez-Gallego, X. Bossuyt, L. Abel, A. Puel, and J. L. Casanova. 2007. Selective predisposition to bacterial infections in IRAK-4-deficient children: IRAK-4-dependent TLRs are otherwise redundant in protective immunity. *J Exp Med* 204: 2407-2422.

51. Picard, C., A. Puel, M. Bonnet, C. L. Ku, J. Bustamante, K. Yang, C. Soudais, S. Dupuis, J. Feinberg, C. Fieschi, C. Elbim, R. Hitchcock, D. Lammas, G. Davies, A. Al-Ghonaium, H. Al-Rayes, S. Al-Jumaah, S. Al-Hajjar, I. Z. Al-Mohsen, H. H. Frayha, R. Rucker, T. R. Hawn, A. Aderem, H. Tufenkeji, S. Haraguchi, N. K. Day, R. A. Good, M.

A. Gougerot-Pocidalo, A. Ozinsky, and J. L. Casanova. 2003. Pyogenic bacterial infections in humans with IRAK-4 deficiency. *Science* 299: 2076-2079.

52. Takeuchi, O., K. Hoshino, and S. Akira. 2000. Cutting edge: TLR2-deficient and MyD88-deficient mice are highly susceptible to Staphylococcus aureus infection. *J Immunol* 165: 5392-5396.

53. Miller, L. S., R. M. O'Connell, M. A. Gutierrez, E. M. Pietras, A. Shahangian, C. E. Gross, A. Thirumala, A. L. Cheung, G. Cheng, and R. L. Modlin. 2006. MyD88 mediates neutrophil recruitment initiated by IL-1R but not TLR2 activation in immunity against Staphylococcus aureus. *Immunity* 24: 79-91.

54. Hruz, P., A. S. Zinkernagel, G. Jenikova, G. J. Botwin, J. P. Hugot, M. Karin, V. Nizet, and L. Eckmann. 2009. NOD2 contributes to cutaneous defense against Staphylococcus aureus through alpha-toxin-dependent innate immune activation. *Proc Natl Acad Sci U S A* 106: 12873-12878.

55. Archer, N. K., J. M. Harro, and M. E. Shirtliff. 2013. Clearance of Staphylococcus aureus nasal carriage is T cell dependent and mediated through interleukin-17A expression and neutrophil influx. *Infect Immun* 81: 2070-2075.

56. Andrews, T., and K. E. Sullivan. 2003. Infections in patients with inherited defects in phagocytic function. *Clin Microbiol Rev* 16: 597-621.

57. Molne, L., M. Verdrengh, and A. Tarkowski. 2000. Role of neutrophil leukocytes in cutaneous infection caused by Staphylococcus aureus. *Infect Immun* 68: 6162-6167.

58. Olaru, F., and L. E. Jensen. 2010. Staphylococcus aureus stimulates neutrophil targeting chemokine expression in keratinocytes through an autocrine IL-1alpha signaling loop. *J Invest Dermatol* 130: 1866-1876.

59. Greenlee-Wacker, M. C., K. M. Rigby, S. D. Kobayashi, A. R. Porter, F. R. DeLeo, and W. M. Nauseef. 2014. Phagocytosis of Staphylococcus aureus by human neutrophils prevents macrophage efferocytosis and induces programmed necrosis. *J Immunol* 192: 4709-4717.

60. Brinkmann, V., U. Reichard, C. Goosmann, B. Fauler, Y. Uhlemann, D. S. Weiss, Y. Weinrauch, and A. Zychlinsky. 2004. Neutrophil extracellular traps kill bacteria. *Science* 303: 1532-1535.

61. McLoughlin, R. M., J. C. Lee, D. L. Kasper, and A. O. Tzianabos. 2008. IFN-gamma regulated chemokine production determines the outcome of Staphylococcus aureus infection. *J Immunol* 181: 1323-1332.

62. Milner, J. D., J. M. Brenchley, A. Laurence, A. F. Freeman, B. J. Hill, K. M. Elias, Y. Kanno, C. Spalding, H. Z. Elloumi, M. L. Paulson, J. Davis, A. Hsu, A. I. Asher, J. O'Shea, S. M. Holland, W. E. Paul, and D. C. Douek. 2008. Impaired T(H)17 cell differentiation in subjects with autosomal dominant hyper-IgE syndrome. *Nature* 452: 773-776.

63. Minegishi, Y., M. Saito, M. Nagasawa, H. Takada, T. Hara, S. Tsuchiya, K. Agematsu, M. Yamada, N. Kawamura, T. Ariga, I. Tsuge, and H. Karasuyama. 2009. Molecular explanation for the contradiction between systemic Th17 defect and localized bacterial infection in hyper-IgE syndrome. *J Exp Med* 206: 1291-1301.

64. Ishigame, H., S. Kakuta, T. Nagai, M. Kadoki, A. Nambu, Y. Komiyama, N. Fujikado, Y. Tanahashi, A. Akitsu, H. Kotaki, K. Sudo, S. Nakae, C. Sasakawa, and Y. Iwakura. 2009. Differential roles of interleukin-17A and -17F in host defense against mucoepithelial bacterial infection and allergic responses. *Immunity* 30: 108-119.

65. Soltesz, B., B. Toth, A. K. Sarkadi, M. Erdos, and L. Marodi. 2015. The Evolving View of IL-17-Mediated Immunity in Defense Against Mucocutaneous Candidiasis in Humans. *Int Rev Immunol* 34: 348-363.

66. Okada, S., J. G. Markle, E. K. Deenick, F. Mele, D. Averbuch, M. Lagos, M. Alzahrani, S. Al-Muhsen, R. Halwani, C. S. Ma, N. Wong, C. Soudais, L. A. Henderson, H. Marzouqa, J. Shamma, M. Gonzalez, R. Martinez-Barricarte, C. Okada, D. T. Avery, D. Latorre, C. Deswarte, F. Jabot-Hanin, E. Torrado, J. Fountain, A. Belkadi, Y. Itan, B. Boisson, M. Migaud, C. S. Arlehamn, A. Sette, S. Breton, J. McCluskey, J. Rossjohn, J. P. de Villartay, D. Moshous, S. Hambleton, S. Latour, P. D. Arkwright, C. Picard, O. Lantz, D. Engelhard, M. Kobayashi, L. Abel, A. M. Cooper, L. D. Notarangelo, S. Boisson-Dupuis, A. Puel, F. Sallusto, J. Bustamante, S. G. Tangye, and J. L. Casanova. 2015. IMMUNODEFICIENCIES. Impairment of immunity to Candida and Mycobacterium in humans with bi-allelic RORC mutations. *Science* 349: 606-613.

67. Niebuhr, M., H. Scharonow, M. Gathmann, D. Mamerow, and T. Werfel. 2010. Staphylococcal exotoxins are strong inducers of IL-22: A potential role in atopic dermatitis. *J Allergy Clin Immunol* 126: 1176-1183.e1174.

68. Moriwaki, Y., K. Takada, T. Nagasaki, N. Kubo, T. Ishii, K. Kose, T. Kageyama, S. Tsuji, K. Kawashima, and H. Misawa. 2015. IL-22/STAT3-Induced Increases in SLURP1 Expression within Psoriatic Lesions Exerts Antimicrobial Effects against Staphylococcus aureus. *PLoS One* 10: e0140750.

69. Mulcahy, M. E., J. M. Leech, J. C. Renauld, K. H. Mills, and R. M. McLoughlin. 2016. Interleukin-22 regulates antimicrobial peptide expression and keratinocyte differentiation to control Staphylococcus aureus colonization of the nasal mucosa. *Mucosal Immunol*.

70. Brown, A. F., A. G. Murphy, S. J. Lalor, J. M. Leech, K. M. O'Keeffe, M. Mac Aogain, D. P. O'Halloran, K. A. Lacey, M. Tavakol, C. H. Hearnden, D. Fitzgerald-Hughes, H. Humphreys, J. P. Fennell, W. J. van Wamel, T. J. Foster, J. A. Geoghegan, E. C. Lavelle, T. R. Rogers, and R. M. McLoughlin. 2015. Memory Th1 Cells Are Protective in Invasive Staphylococcus aureus Infection. *PLoS Pathog* 11: e1005226.

71. Leijh, P. C., M. T. van den Barselaar, M. R. Daha, and R. van Furth. 1981. Participation of immunoglobulins and complement components in the intracellular killing of Staphylococcus aureus and Escherichia coli by human granulocytes. *Infect Immun* 33: 714-724.

72. Lee, J. C. 1996. The prospects for developing a vaccine against Staphylococcus aureus. *Trends Microbiol* 4: 162-166.

73. Fowler, V. G., Jr., and R. A. Proctor. 2014. Where does a Staphylococcus aureus vaccine stand? *Clin Microbiol Infect* 20 Suppl 5: 66-75.

74. Joshi, A., G. Pancari, L. Cope, E. P. Bowman, D. Cua, R. A. Proctor, and T. McNeely. 2012. Immunization with Staphylococcus aureus iron regulated surface determinant B (IsdB) confers protection via Th17/IL17 pathway in a murine sepsis model. *Hum Vaccin Immunother* 8: 336-346.

75. Kuklin, N. A., D. J. Clark, S. Secore, J. Cook, L. D. Cope, T. McNeely, L. Noble, M. J. Brown, J. K. Zorman, X. M. Wang, G. Pancari, H. Fan, K. Isett, B. Burgess, J. Bryan, M. Brownlow, H. George, M. Meinz, M. E. Liddell, R. Kelly, L. Schultz, D. Montgomery, J. Onishi, M. Losada, M. Martin, T. Ebert, C. Y. Tan, T. L. Schofield, E. Nagy, A. Meineke, J. G. Joyce, M. B. Kurtz, M. J. Caulfield, K. U. Jansen, W. McClements, and A. S. Anderson. 2006. A novel Staphylococcus aureus vaccine: iron surface determinant

B induces rapid antibody responses in rhesus macaques and specific increased survival in a murine S. aureus sepsis model. *Infect Immun* 74: 2215-2223.

76. Fowler, V. G., K. B. Allen, E. D. Moreira, M. Moustafa, F. Isgro, H. W. Boucher, G. R. Corey, Y. Carmeli, R. Betts, J. S. Hartzel, I. S. Chan, T. B. McNeely, N. A. Kartsonis, D. Guris, M. T. Onorato, S. S. Smugar, M. J. DiNubile, and A. Sobanjo-ter Meulen. 2013. Effect of an investigational vaccine for preventing Staphylococcus aureus infections after cardiothoracic surgery: a randomized trial. *Jama* 309: 1368-1378.

77. Karauzum, H., C. C. Haudenschild, I. N. Moore, M. Mahmoudieh, D. L. Barber, and S. K. Datta. 2017. Vaccination induces CD4 T cell-mediated mortality during Staphylococcus aureus bacteremia. *J Infect Dis*.

78. Medzhitov, R., D. S. Schneider, and M. P. Soares. 2012. Disease tolerance as a defense strategy. *Science* 335: 936-941.

79. Raberg, L., D. Sim, and A. F. Read. 2007. Disentangling genetic variation for resistance and tolerance to infectious diseases in animals. *Science* 318: 812-814.

80. Soares, M. P., L. Teixeira, and L. F. Moita. 2017. Disease tolerance and immunity in host protection against infection. *Nat Rev Immunol* 17: 83-96.

81. Chau, T. A., M. L. McCully, W. Brintnell, G. An, K. J. Kasper, E. D. Vines, P. Kubes, S. M. Haeryfar, J. K. McCormick, E. Cairns, D. E. Heinrichs, and J. Madrenas. 2009. Toll-like receptor 2 ligands on the staphylococcal cell wall downregulate superantigen-induced T cell activation and prevent toxic shock syndrome. *Nat Med* 15: 641-648.

82. Frodermann, V., T. A. Chau, S. Sayedyahossein, J. M. Toth, D. E. Heinrichs, and J. Madrenas. 2011. A modulatory interleukin-10 response to staphylococcal peptidoglycan

prevents Th1/Th17 adaptive immunity to Staphylococcus aureus. *J Infect Dis* 204: 253-262.

83. Peres, A. G., C. Stegen, J. Li, A. Q. Xu, B. Levast, M. G. Surette, B. Cousineau, M. Desrosiers, and J. Madrenas. 2015. Uncoupling of pro- and anti-inflammatory properties of Staphylococcus aureus. *Infect Immun* 83: 1587-1597.

84. Li, Z., B. Levast, and J. Madrenas. 2017. Staphylococcus aureus Downregulates IP-10 Production and Prevents Th1 Cell Recruitment. *J Immunol* 198: 1865-1874.

85. Burbach, K. M., A. Poland, and C. A. Bradfield. 1992. Cloning of the Ah-receptor cDNA reveals a distinctive ligand-activated transcription factor. *Proc Natl Acad Sci U S A* 89: 8185-8189.

86. Ema, M., K. Sogawa, N. Watanabe, Y. Chujoh, N. Matsushita, O. Gotoh, Y. Funae, and Y. Fujii-Kuriyama. 1992. cDNA cloning and structure of mouse putative Ah receptor. *Biochem Biophys Res Commun* 184: 246-253.

87. Flaveny, C. A., I. A. Murray, C. R. Chiaro, and G. H. Perdew. 2009. Ligand selectivity and gene regulation by the human aryl hydrocarbon receptor in transgenic mice. *Mol Pharmacol* 75: 1412-1420.

88. Opitz, C. A., U. M. Litzenburger, F. Sahm, M. Ott, I. Tritschler, S. Trump, T. Schumacher, L. Jestaedt, D. Schrenk, M. Weller, M. Jugold, G. J. Guillemin, C. L. Miller, C. Lutz, B. Radlwimmer, I. Lehmann, A. von Deimling, W. Wick, and M. Platten. 2011. An endogenous tumour-promoting ligand of the human aryl hydrocarbon receptor. *Nature* 478: 197-203.

89. Gonzalez, F. J., and P. Fernandez-Salguero. 1998. The aryl hydrocarbon receptor: studies using the AHR-null mice. *Drug Metab Dispos* 26: 1194-1198.

90. Abbott, B. D., J. E. Schmid, J. A. Pitt, A. R. Buckalew, C. R. Wood, G. A. Held, and J. J. Diliberto. 1999. Adverse reproductive outcomes in the transgenic Ah receptor-deficient mouse. *Toxicol Appl Pharmacol* 155: 62-70.

91. Schmidt, J. V., G. H. Su, J. K. Reddy, M. C. Simon, and C. A. Bradfield. 1996. Characterization of a murine Ahr null allele: involvement of the Ah receptor in hepatic growth and development. *Proc Natl Acad Sci U S A* 93: 6731-6736.

92. Kim, D. W., L. Gazourian, S. A. Quadri, R. Romieu-Mourez, D. H. Sherr, and G. E. Sonenshein. 2000. The RelA NF-kappaB subunit and the aryl hydrocarbon receptor (AhR) cooperate to transactivate the c-myc promoter in mammary cells. *Oncogene* 19: 5498-5506.

93. Lahvis, G. P., and C. A. Bradfield. 1998. Ahr null alleles: distinctive or different? *Biochem Pharmacol* 56: 781-787.

94. Bessede, A., M. Gargaro, M. T. Pallotta, D. Matino, G. Servillo, C. Brunacci, S. Bicciato, E. M. Mazza, A. Macchiarulo, C. Vacca, R. Iannitti, L. Tissi, C. Volpi, M. L. Belladonna, C. Orabona, R. Bianchi, T. V. Lanz, M. Platten, M. A. Della Fazia, D. Piobbico, T. Zelante, H. Funakoshi, T. Nakamura, D. Gilot, M. S. Denison, G. J. Guillemin, J. B. DuHadaway, G. C. Prendergast, R. Metz, M. Geffard, L. Boon, M. Pirro, A. Iorio, B. Veyret, L. Romani, U. Grohmann, F. Fallarino, and P. Puccetti. 2014. Aryl hydrocarbon receptor control of a disease tolerance defence pathway. *Nature* 511: 184-190.

95. Sekine, H., J. Mimura, M. Oshima, H. Okawa, J. Kanno, K. Igarashi, F. J. Gonzalez, T. Ikuta, K. Kawajiri, and Y. Fujii-Kuriyama. 2009. Hypersensitivity of aryl hydrocarbon receptor-deficient mice to lipopolysaccharide-induced septic shock. *Mol Cell Biol* 29: 6391-6400.

96. Kimura, A., T. Naka, T. Nakahama, I. Chinen, K. Masuda, K. Nohara, Y. Fujii-Kuriyama, and T. Kishimoto. 2009. Aryl hydrocarbon receptor in combination with Stat1 regulates LPS-induced inflammatory responses. *J Exp Med* 206: 2027-2035.

97. Moura-Alves, P., K. Fae, E. Houthuys, A. Dorhoi, A. Kreuchwig, J. Furkert, N. Barison, A. Diehl, A. Munder, P. Constant, T. Skrahina, U. Guhlich-Bornhof, M. Klemm, A. B. Koehler, S. Bandermann, C. Goosmann, H. J. Mollenkopf, R. Hurwitz, V. Brinkmann, S. Fillatreau, M. Daffe, B. Tummler, M. Kolbe, H. Oschkinat, G. Krause, and S. H. Kaufmann. 2014. AhR sensing of bacterial pigments regulates antibacterial defence. *Nature* 512: 387-392.

98. Zelante, T., R. G. Iannitti, C. Cunha, A. De Luca, G. Giovannini, G. Pieraccini, R. Zecchi, C. D'Angelo, C. Massi-Benedetti, F. Fallarino, A. Carvalho, P. Puccetti, and L. Romani. 2013. Tryptophan catabolites from microbiota engage aryl hydrocarbon receptor and balance mucosal reactivity via interleukin-22. *Immunity* 39: 372-385.

99. Fernandez-Salguero, P., T. Pineau, D. M. Hilbert, T. McPhail, S. S. Lee, S. Kimura, D. W. Nebert, S. Rudikoff, J. M. Ward, and F. J. Gonzalez. 1995. Immune system impairment and hepatic fibrosis in mice lacking the dioxin-binding Ah receptor. *Science* 268: 722-726.

100. Bellemore, S. M., E. Nikoopour, J. A. Schwartz, O. Krougly, E. Lee-Chan, and B. Singh. 2015. Preventative role of interleukin-17 producing regulatory T helper type 17 (T 17) cells in type 1 diabetes in non-obese diabetic mice. *Clin Exp Immunol*.

101. Mascanfroni, I. D., M. C. Takenaka, A. Yeste, B. Patel, Y. Wu, J. E. Kenison, S. Siddiqui, A. S. Basso, L. E. Otterbein, D. M. Pardoll, F. Pan, A. Priel, C. B. Clish, S. C.

Robson, and F. J. Quintana. 2015. Metabolic control of type 1 regulatory T cell differentiation by AHR and HIF1-alpha. *Nat Med* 21: 638-646.

102. Takami, M., K. Fujimaki, M. I. Nishimura, and M. Iwashima. 2015. Cutting Edge: AhR Is a Molecular Target of Calcitriol in Human T Cells. *J Immunol* 195: 2520-2523.

103. Stockinger, B., P. Di Meglio, M. Gialitakis, and J. H. Duarte. 2014. The aryl hydrocarbon receptor: multitasking in the immune system. *Annu Rev Immunol* 32: 403-432.

104. Durant, L., W. T. Watford, H. L. Ramos, A. Laurence, G. Vahedi, L. Wei, H. Takahashi, H. W. Sun, Y. Kanno, F. Powrie, and J. J. O'Shea. 2010. Diverse targets of the transcription factor STAT3 contribute to T cell pathogenicity and homeostasis. *Immunity* 32: 605-615.

105. Kimura, A., T. Naka, K. Nohara, Y. Fujii-Kuriyama, and T. Kishimoto. 2008. Aryl hydrocarbon receptor regulates Stat1 activation and participates in the development of Th17 cells. *Proc Natl Acad Sci U S A* 105: 9721-9726.

106. Ramirez, J. M., N. C. Brembilla, O. Sorg, R. Chicheportiche, T. Matthes, J. M. Dayer, J. H. Saurat, E. Roosnek, and C. Chizzolini. 2010. Activation of the aryl hydrocarbon receptor reveals distinct requirements for IL-22 and IL-17 production by human T helper cells. *Eur J Immunol* 40: 2450-2459.

107. Singh, N. P., U. P. Singh, B. Singh, R. L. Price, M. Nagarkatti, and P. S. Nagarkatti. 2011. Activation of aryl hydrocarbon receptor (AhR) leads to reciprocal epigenetic regulation of FoxP3 and IL-17 expression and amelioration of experimental colitis. *PLoS One* 6: e23522.

108. Qiu, J., J. J. Heller, X. Guo, Z. M. Chen, K. Fish, Y. X. Fu, and L. Zhou. 2012. The aryl hydrocarbon receptor regulates gut immunity through modulation of innate lymphoid cells. *Immunity* 36: 92-104.

109. Kadow, S., B. Jux, S. P. Zahner, B. Wingerath, S. Chmill, B. E. Clausen, J. Hengstler, and C. Esser. 2011. Aryl hydrocarbon receptor is critical for homeostasis of invariant gammadelta T cells in the murine epidermis. *J Immunol* 187: 3104-3110.

110. Ebihara, T., C. Song, S. H. Ryu, B. Plougastel-Douglas, L. Yang, D. Levanon, Y. Groner, M. D. Bern, T. S. Stappenbeck, M. Colonna, T. Egawa, and W. M. Yokoyama. 2015. Runx3 specifies lineage commitment of innate lymphoid cells. *Nat Immunol* 16: 1124-1133.

111. Guo, H., and D. J. Topham. 2010. Interleukin-22 (IL-22) production by pulmonary Natural Killer cells and the potential role of IL-22 during primary influenza virus infection. *J Virol* 84: 7750-7759.

112. Zindl, C. L., J. F. Lai, Y. K. Lee, C. L. Maynard, S. N. Harbour, W. Ouyang, D. D. Chaplin, and C. T. Weaver. 2013. IL-22-producing neutrophils contribute to antimicrobial defense and restitution of colonic epithelial integrity during colitis. *Proc Natl Acad Sci U S A* 110: 12768-12773.

113. Lee, Y. S., H. Yang, J. Y. Yang, Y. Kim, S. H. Lee, J. H. Kim, Y. J. Jang, B. A. Vallance, and M. N. Kweon. 2015. Interleukin-1 (IL-1) signaling in intestinal stromal cells controls KC/ CXCL1 secretion, which correlates with recruitment of IL-22- secreting neutrophils at early stages of Citrobacter rodentium infection. *Infect Immun* 83: 3257-3267.

114. Forlow, S. B., J. R. Schurr, J. K. Kolls, G. J. Bagby, P. O. Schwarzenberger, and K. Ley. 2001. Increased granulopoiesis through interleukin-17 and granulocyte colony-stimulating factor in leukocyte adhesion molecule-deficient mice. *Blood* 98: 3309-3314.

115. Imai, Y., N. Ayithan, X. Wu, Y. Yuan, L. Wang, and S. T. Hwang. 2015. Cutting Edge: PD-1 Regulates Imiquimod-Induced Psoriasiform Dermatitis through Inhibition of IL-17A Expression by Innate gammadelta-Low T Cells. *J Immunol* 195: 421-425.

116. Teske, S., A. A. Bohn, J. P. Hogaboam, and B. P. Lawrence. 2008. Aryl hydrocarbon receptor targets pathways extrinsic to bone marrow cells to enhance neutrophil recruitment during influenza virus infection. *Toxicol Sci* 102: 89-99.

117. de Souza, A. R., M. Zago, D. H. Eidelman, Q. Hamid, and C. J. Baglole. 2014. Aryl hydrocarbon receptor (AhR) attenuation of subchronic cigarette smoke-induced pulmonary neutrophilia is associated with retention of nuclear RelB and suppression of intercellular adhesion molecule-1 (ICAM-1). *Toxicol Sci* 140: 204-223.

118. Wheeler, J. L., K. C. Martin, and B. P. Lawrence. 2013. Novel cellular targets of AhR underlie alterations in neutrophilic inflammation and inducible nitric oxide synthase expression during influenza virus infection. *J Immunol* 190: 659-668.

119. Cai, Y., X. Shen, C. Ding, C. Qi, K. Li, X. Li, V. R. Jala, H. G. Zhang, T. Wang, J. Zheng, and J. Yan. 2011. Pivotal role of dermal IL-17-producing gammadelta T cells in skin inflammation. *Immunity* 35: 596-610.

120. Li, Z., A. G. Peres, A. C. Damian, and J. Madrenas. 2015. Immunomodulation and Disease Tolerance to Staphylococcus aureus. *Pathogens* 4: 793-815.

121. Gray, E. E., K. Suzuki, and J. G. Cyster. 2011. Cutting edge: Identification of a motile IL-17-producing gammadelta T cell population in the dermis. *J Immunol* 186: 6091-6095.

122. Misiak, A., M. M. Wilk, M. Raverdeau, and K. H. Mills. 2017. IL-17-Producing Innate and Pathogen-Specific Tissue Resident Memory gammadelta T Cells Expand in the Lungs of Bordetella pertussis-Infected Mice. *J Immunol* 198: 363-374.

123. Murphy, A. G., K. M. O'Keeffe, S. J. Lalor, B. M. Maher, K. H. Mills, and R. M. McLoughlin. 2014. Staphylococcus aureus infection of mice expands a population of memory gammadelta T cells that are protective against subsequent infection. *J Immunol* 192: 3697-3708.

124. Malhotra, N., J. Yoon, J. M. Leyva-Castillo, C. Galand, N. Archer, L. S. Miller, and R. S. Geha. 2016. IL-22 derived from gammadelta T cells restricts Staphylococcus aureus infection of mechanically injured skin. *J Allergy Clin Immunol* 138: 1098-1107.e1093.

125. Abtin, A., R. Jain, A. J. Mitchell, B. Roediger, A. J. Brzoska, S. Tikoo, Q. Cheng, L. G. Ng, L. L. Cavanagh, U. H. von Andrian, M. J. Hickey, N. Firth, and W. Weninger. 2014. Perivascular macrophages mediate neutrophil recruitment during bacterial skin infection. *Nat Immunol* 15: 45-53.

126. Werner, J. L., M. A. Gessner, L. M. Lilly, M. P. Nelson, A. E. Metz, D. Horn, C. W. Dunaway, J. Deshane, D. D. Chaplin, C. T. Weaver, G. D. Brown, and C. Steele. 2011. Neutrophils produce interleukin 17A (IL-17A) in a dectin-1- and IL-23-dependent manner during invasive fungal infection. *Infect Immun* 79: 3966-3977.

127. Schmaler, M., N. J. Jann, F. Ferracin, and R. Landmann. 2011. T and B cells are not required for clearing Staphylococcus aureus in systemic infection despite a strong TLR2-MyD88-dependent T cell activation. *J Immunol* 186: 443-452.

128. Hartwig, T., S. Pantelyushin, A. L. Croxford, P. Kulig, and B. Becher. 2015. Dermal IL-17-producing gammadelta T cells establish long-lived memory in the skin. *Eur J Immunol* 45: 3022-3033.

129. Elfatoiki, F. Z., M. El Azhari, A. El Kettani, Z. Serhier, M. B. Othmani, M. Timinouni, H. Benchikhi, S. Chiheb, and H. Fellah. 2016. Psoriasis and staphylococcus aureus skin colonization in Moroccan patients. *Pan Afr Med J* 23: 33.

130. Netea, M. G., E. Latz, K. H. Mills, and L. A. O'Neill. 2015. Innate immune memory: a paradigm shift in understanding host defense. *Nat Immunol* 16: 675-679.

131. Mehta, S., and K. L. Jeffrey. 2015. Beyond receptors and signaling: epigenetic factors in the regulation of innate immunity. *Immunol Cell Biol* 93: 233-244.

132. Tseng, C. W., J. C. Biancotti, B. L. Berg, D. Gate, S. L. Kolar, S. Muller, M. D. Rodriguez, K. Rezai-Zadeh, X. Fan, D. O. Beenhouwer, T. Town, and G. Y. Liu. 2015. Increased Susceptibility of Humanized NSG Mice to Panton-Valentine Leukocidin and Staphylococcus aureus Skin Infection. *PLoS Pathog* 11: e1005292.

133. Bunce, C., L. Wheeler, G. Reed, J. Musser, and N. Barg. 1992. Murine model of cutaneous infection with gram-positive cocci. *Infect Immun* 60: 2636-2640.

134. Elek, S. D. 1956. Experimental staphylococcal infections in the skin of man. *Ann N Y Acad Sci* 65: 85-90.

135. Manchester, D. K., S. K. Gordon, C. L. Golas, E. A. Roberts, and A. B. Okey. 1987. Ah receptor in human placenta: stabilization by molybdate and characterization of binding of 2,3,7,8-tetrachlorodibenzo-p-dioxin, 3-methylcholanthrene, and benzo(a)pyrene. *Cancer Res* 47: 4861-4868.

136. Flaveny, C., R. K. Reen, A. Kusnadi, and G. H. Perdew. 2008. The mouse and human Ah receptor differ in recognition of LXXLL motifs. *Arch Biochem Biophys* 471: 215-223.

137. Flaveny, C. A., I. A. Murray, and G. H. Perdew. 2010. Differential gene regulation by the human and mouse aryl hydrocarbon receptor. *Toxicol Sci* 114: 217-225.

138. Zaidi, T., T. Zaidi, C. Cywes-Bentley, R. Lu, G. P. Priebe, and G. B. Pier. 2014. Microbiota-driven immune cellular maturation is essential for antibody-mediated adaptive immunity to Staphylococcus aureus infection in the eye. *Infect Immun* 82: 3483-3491.